Universidade de Aveiro Departamento de Biologia
2011

Joana Brás Pereira

Synthesis and antibacterial activity of cationic phthalocyanines

Universidade de Aveiro Departamento de Biologia
Ano 2011

Joana Brás Pereira

Síntese e atividade antibacteriana de ftalocianinas catiónicas.

Synthesis and antibacterial activity of cationic phthalocyanines

Dissertação apresentada à Universidade de Aveiro para cumprimento dos requisitos necessários à obtenção do grau de Mestre em Biologia Molecular e Celular, realizada sob orientação do Doutor João Paulo Costa Tomé, investigador auxiliar do Departamento de Química da Universidade de Aveiro e co-orientação da Professora Doutora Maria Adelaide de Pinho Almeida, professora auxiliar do Departamento de Biologia da Universidade de Aveiro.

Aos meus pais e à minha irmã

The most beautiful thing we can experience is the mysterious.
It is the source of all true art and all science.
He to whom this emotion is a stranger, who can no longer pause to wonder and stand rapt in awe, is as good as dead: his eyes are closed.

Albert Einstein

o júri

Presidente

Doutora Laura Cristina da Silva Carreto
Investigadora Auxiliar do Departamento de Biologia da Universidade de Aveiro.

Vogais

Prof. Doutora Olga Maria Fernandes Pereira Coutinho
Professora Associada do Departamento de Biologia da Universidade do Minho

Doutor João Paulo Costa Tomé (Orientador)
Investigador Auxiliar do Departamento de Química da Universidade de Aveiro

Prof. Doutora Maria Adelaide de Pinho Almeida (Co-orientadora)
Professora Auxiliar do Departamento de Biologia da Universidade de Aveiro

agradecimentos

Ao Doutor João Tomé, orientador da dissertação, por todo o incentivo, pela paciência, pelas críticas construtivas e por me ter apresentado a um novo desafio.

À Professora Doutora Adelaide Almeida, co-orientadora da dissertação, pela confiança, pelo apoio e pelo seu rigor científico.

Ao Professor José Cavaleiro, pela oportunidade que me deu.

À Professora Doutora Ângela Cunha, pelas sugestões e disponibilidade.

À Professora Doutora Amparo Faustino, pela disponibilidade, pela ajuda e todas as sugestões.

À Eliana Carvalho, pela ajuda disponibilizada.

Aos colegas do laboratório de Química Orgânica, por toda a ajuda, simpatia e conhecimento transmitido.

Aos colegas do laboratório de Microbiologia Ambiental e Aplicada, por toda ajuda e simpatia.

À Clara Gomes, que está comigo desde o início deste desafio, por toda a amizade e apoio.

À Dora, ao Flávio, ao João, ao Leandro, ao Sérgio, à Sónia e à Diana do laboratório de Química Orgânica, pela amizade e pelos risos partilhados.

À Ana Luísa, pela amizade, pela paciência e por todo o apoio.

Aos meus pais e à minha irmã, porque sem eles nada fazia sentido.

À Universidade de Aveiro, pelo financiamento do QOPNA e CESAM.

À FCT (Lisboa) e FEDER, pelo financiamento do QOPNA e CESAM.

Ao Projeto PTDC/QUI/65228/2006 pelo financiamento parcial do trabalho experimental.

keywords

Antimicrobial photodynamic therapy, cationic phthalocyanines, bioluminescent *E. coli*, uptake

abstract

Antimicrobial photodynamic therapy (aPDT) was described more than 100 years ago, but its potential as an alternative to combating microorganisms, was only recognized when antibiotic resistance became an important public health issue. aPDT refers to the action of 3 non-toxic elements: a photosensitizer, light and molecular oxygen that, when combined, results in the production of singlet oxygen ($^1O_2$) and/or free radicals which are cytotoxic to target cells.

The aim of this work was to synthetize, evaluate and compare the photoinactivation efficiency of new cationic phthalocyanines (Pcs) derivatives. Three new derivatives, tetra and octa-thio-pyridinium Pcs, **17**, **18** and **19**, were tested against Gram-negative bacteria. A recombinant bioluminescent *Escherichia coli* strain was used to assess, in real time, the photoinactivation efficiency of these cationic Pcs, under white and red light. After a pre-incubation period with 20 μmol L^{-1} of PS in the dark, the pure bacterial suspensions were irradiated with white light (400-800 nm) or red light (620-750 nm) at a fluence rate of 150 mW cm^{-2}, for 30 minutes. Dark and light controls were performed in all experiments. The cellular localization, uptake, $^1O_2$, photophysical and photochemical tests such as photostability, solubility and fluorescence quantum yields were also determined, in order to evaluate the potential of these new Pcs as antibacterial agents.

Pc **18** was the most effective photosensitizer, causing a 5 logs reduction in bioluminescence after 30 minutes of irradiation under white or red lights. The photoinactivation efficiency of the Pc **19** was similar (5 logs reduction in bioluminescence) to that of **18** when irradiated with white light, but the efficiency of inactivation was reduced (2.1 logs reduction in bioluminescence) under red light. Pc **17** was the least effective PS, causing only 2.1 log bioluminescence reduction under white light and 1 log decrease under red light.

The three new cationic thio-pyridinium phthalocyanines with different physico-chemical properties have different photoinactivation efficiencies to inactivate a gram negative bacterium. Several factors such as aggregation, $^1O_2$ generation, number of thio-pyridinium groups, cellular uptake/localization and irradiation conditions could cause the different efficiency observed.

The high photodynamic efficiency of compound **18** under red light is of special interest for clinical applications, since red light is the most preferable for treatment of microbial infections, because it penetrates deeper into infected human tissues.

palavras-chave

Terapia fotodinâmica antimicrobiana, ftalocianinas catiónicas, *E. coli* bioluminescente, uptake celular

resumo

A terapia fotodinâmica antimicrobiana (aPDT) foi descrita pela primeira vez há mais de 100 anos, mas o seu potencial como alternativa no combate de microrganismos apenas foi reconhecido devido à resistência a antibióticos, que se revelou um grave problema de saúde pública. aPDT refere-se à acção de três componentes não tóxicos: um fotossensibilizador (PS), uma fonte de luz e oxigénio molecular que, em conjunto, levam à geração de oxigénio singuleto ($^1O_2$) e/ou radicais livres, que são citotóxicos para as células alvo.

O objectivo deste trabalho foi sintetizar, avaliar e comparar a eficiência da fotoinativação de novos derivados catiónicos de ftalocianinas (Pcs). Três novos derivados, ftalocianinas tetra e octa-tio-piridil, **17**, **18** e **19**, foram testadas numa bactéria Gram-negativa. Foi utilizada uma estirpe de *Escherichia coli* recombinante bioluminescente para determinar, em tempo real, a eficácia da fotoinativação das ftalocianinas catiónicas, sob luz branca e luz vermelha. Após um período de pré-incubação no escuro com 20 µmol L^{-1}de PS, as suspensões bacterianas puras foram irradiadas com luz branca (400-800 nm) ou luz vermelha (620-750 nm) sob 150 mW cm^{-2}, durante 30 minutos. Foram realizados em todos os ensaios controlos claro (irradiação da suspensão bacteriana sem PS) e escuro (suspensão bacteriana com PS, sem irradiação). Foram também determinados a localização subcelular, uptake, $^1O_2$, testes fotofísicos e fotoquímicos tal como a fotoestabilidade, solubilidade e determinação do rendimento quântico de fluorescência para avaliar o potencial das novas ftalocianinas como agentes antibacterianos.

O derivado **18** foi o PS mais eficiente, causando uma redução de 5 logs na bioluminescência após 30 minutos de irradiação com luz branca ou com luz vermelha. A fotoinativação provocada pela Pc **19** foi semelhante (5 logs de decréscimo na bioluminescência) à da **18**, quando irradiada com luz branca, mas a eficiência da inactivação reduziu (2.1 logs decréscimo na bioluminescência) sob luz vermelha. A Pc **17** foi o PS menos eficiente, causando apenas 2.1 logs de decréscimo na bioluminescência sob luz branca e diminuição de 1 log sob luz vermelha.

As três novas ftalocianinas tio-piridil com diferentes propriedades físico-químicas, revelam uma eficiência diferente na fotoinativação de uma bactéria Gram-negativa. Vários factores tais como agregação, geração de $^1O_2$, número de grupos tio-piridil, bem como as condições de irradiação, uptake /localização celular podem estar na causa das diferenças verificadas na fotoinativação.

A elevada eficiência fotodinâmica do composto **18** na presença da luz vermelha é de especial interesse para aplicações clínicas, uma vez que a luz vermelha é a mais adequada para o tratamento de infecções microbianas, pois penetra mais profundamente em tecidos humanos infectados.

Table of contents

List of Acronyms and Abbreviations

$^1O_2$	Singlet oxygen
°C	Degree Celsius
µm	Micrometer
ALA	Aminolevulinic acid
aPDT	Antimicrobial photodynamic therapy
BPD	Benzoporphyrin derivative
CFU	Colony forming units
Da	Dalton
DEA	Diethylamine
DHE	Hematoporphyrin ether
DMSO	Dimethyl sulfoxide
DNA	Deoxyribonucleic acid
Eq	Equivalents
$FMNH_2$	Reduced form of flavin mononucleotide
H_2O	Water
H_2O_2	Hydrogen peroxide
HpD	Hematoporphyrin derivative
Hp	Hematoporphyrin
K_2CO_3	Potassium carbonate
LEDS	Light emitting diode
m-THPC	Hydroxyphenylchlorin
mmol	Milimol
NEt_3	Triethylamine
NMR	Nuclear magnetic resonance
Pc	Phthalocyanine
PDT	Photodynamic therapy
PS	Photosensitizer
r.t.	Room temperature

ROS	Reactive oxygen species
TLC	Thin layer chromatography
W	Watt
$ZnPcF_{16}$	Hexadecafluorophthalocyaninatozinc(II)
MeOH	Methanol
ppm	Parts-per-million
$ZnCl_2$	Zinc Chloride
DMAE	Dimethylaminoethanol
CH_3I	Methyl iodide
MHz	Mega hertz
$CDCl_3$	Deuterated chloroform
DMSO-d_6	Deuterated DMSO
TMS	Tetramethylsilane
J	Coupling constant (in Hz)
Hz	Hertz
UV-Vis	Ultraviolet-visible spectroscopy
m.p.	Melting point
E. coli	*Escherichia coli*
µM	Micromolar
TSA	Tryptic soy agar
rpm	Revolutions per minutes
µL	Microliter
LB	Luria Broth
PBS	Phosphate buffered saline
br	Broad
s	singlet
CH_2Cl_2	Dichloromethane
M	Multiplet
dd	Double doublet
d	Doublet

Abs.	Absorbance
DPBF	3-diphenylisobenzofuran
ZnPc	Phthalocyaninatozinc(II)
Φ_F	Fluorescence quantum yield
g	Centrifugal force
SDS	Sodium Dodecyl Sulfate
RLU	Relative light units
SOD	Superoxide dismutase
$O_2^{-\cdot}$	Superoxide anions
$^3O_2\sum_g$-	Ground state (triplet) molecular oxygen
$O_2^{\cdot}$	Superoxide radicals
$OH^{-\cdot}$	Hydroxyl radicals
$OH^{\cdot}$	Hydroxyl radical
OH^-	Hydroxide ion
NO^-	Nitric oxide
$OONO^-$	Peroxynitrite

Thesis outline

The aims of this thesis are to synthetize new cationic phthalocyanines, from a commercial template and from phthalonitriles, and to evaluate their potential as photosensitizers in aPDT. A recombinant bioluminescent *Escherichia coli* strain was used to assess, in real time, the photoinactivation efficiency of these cationic phthalocyanines, under white and red lights.

In chapter I, introductory concepts about antimicrobial photodynamic therapy and phthalocyanines are presented.

Chapter II defines the several approaches used to synthetize cationic phthalocyanines, as well as the characterization by NMR and mass spectrometry techniques of the three new compounds used in Chapter III.

Chapter III describes the effect of the cationic phthalocyanines presented in chapter II, on the viability of a representative strain of Gram-negative bacteria. The photodynamic inactivation kinetics were assessed under white and red light irradiation. Cellular localization and uptake are also presented. Aggregation, spectroscopic, photophysical and photochemical properties studies, performed under the same conditions used in aPDT studies, are also described.

The main conclusions are presented in chapter IV.

Chapter I

Introduction

1.1 PHOTODYNAMIC THERAPY

Already in ancient history light played an important role in therapy. Named heliotherapy (after Helios - the sun God) by the Greeks, it began as sun worship rituals and used for treatment of psoriasis by the Egyptians, evolving through the centuries and claiming its place as an accepted scientific treatment (1).

The combination of light with chemical compounds starts in ancient India and China through the use of psoralens to treat vitiligo (2) but it was only in the late 1800s that the first clinic, offering light therapy to treat smallpox and tuberculosis, opened by Niels Finsen, who was awarded a Nobel Prize for his work on phototherapy (1). Light treatments became world-renowned and several hospitals offered this therapy.

In the early 1900s, Raab, working for Professor Herman von Tappeiner, used the combination of acridine orange and light to destroy living organisms (paramecium), these results combined with other works by Prime and Jesionek, stated that light combined with sensitizing agents (photosensitizers, PSs) and oxygen, had the ability to destroy cells. It was von Tappeiner and Jodlbauer who identified oxygen has an indispensable component in photosensitizing reactions and coined the phrase “photodynamic action” or “photodynamic effect”, depending on the translation (3).

Meyer-Betz was the first to study the effect of a first generation photosensitizer, hematoporphyrin, in humans, by self-injecting himself with a substantial dose, followed by intentional light exposure, creating the first intentional porphyrin based photodynamic therapy (PDT) reaction. This caused an edema and hyperpigmentation, which persisted for 2 months (Figure 1.1) (4).

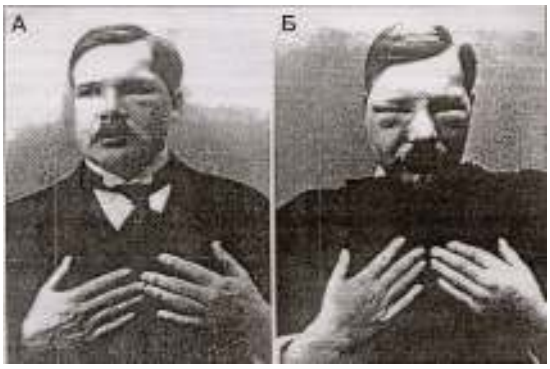

Figure 1.1 - Meyer-Betz before (A) and after (B) injecting hematoporphyrin followed by light exposure.

Regardless of all these significant findings and worldwide recognition of light therapy, PDT did not succeed to become a self-sustaining clinical entity.

The interest in PDT for clinical applications, as we know it, began around 1960 when R. L. Lipson and S. Schwartz used the hematoporphyrin derivate to try to fluoresce human tumors for diagnostic purposes and unintentionally caused tumor cells destruction (5).

Since its discovery, photodynamic therapy and all aspects involved, from mechanisms of action, photosensitizers to possible applications have been thoroughly studied. Briefly, photodynamic therapy occurs when a non-toxic drug or dye is selectively activated by an appropriate wavelength of light, resulting in the production of several reactive oxygen species (ROS), amongst them singlet oxygen ($^1O_2$) as the primary photochemical product. So, three components are required for PDT: a photosensitizer (PS), oxygen and a light source (2). Nowadays PDT is a worldwide treatment, approved in all continents.

1.1.1 Photosensitizers

A PDT photosensitizer is a compound that has the ability of absorbing light of a specific wavelength and transforms it into energy to induce reactions in non-absorbing molecules, resulting in cell damage (6).

The ideal Ps should include the following characteristics:

- be chemically pure, of known and constant composition;
- have minimal dark toxicity and only be cytotoxic in presence of light;

- have selective accumulation in target tissue;
- rapid excretion from the body, resulting in minimal toxicity;
- be non-mutagenic in host;
- be photo and chemically stable;
- have short time interval between administration and maximal accumulation in target tissues;
- have high photochemical reactivity, with high triplet – state yields, long triplet – state lifetime, being able to effectively produce singlet oxygen and other reactive oxygen species;
- have a high extinction coefficient at longer wavelength (600 – 800 nm) where penetration into tissue is maximal, while the photons still maintain the ability to produce singlet oxygen (7,8). It should be also soluble, with minimal aggregation, in biological environments and have a straightforward, clean, and easy of scaling – up synthesis (9).

Mentioning porphyrin based PSs is mandatory, in PDT history. In 1841, Scherer obtained a precipitate after blood heating with sulphuric acid, washed it freeing it form iron, and treated with alcohol. The precipitate was named hematoporphyrin three decades after its discovery. Also, porphyrins were discovered in urine, as uroporphyrins, of patients with porphyria. Patients with this disease had sun sensitivity due to endogenous photosensitizers production (1). It was the discovery of porphyrins as photosensitizing agents.

Through the 1950s-60s, a synthesis method was optimized to give birth to a more refined and highly active form of hematoporphyrin named Hematoporphyrin Derivate (HpD). Hematoporphyrin (Hp) and HpD were called first generation photosensitizers. Photofrin®, a purified mixture of HpD, was the first Ps to be studied in detail. However, being a mixture, it was very difficult to determine its chemical structure and to identify its components (10). Adding to the difficult characterization, Photofrin® also had a lack of reasonably-sized absorption band superior to 650 nm (for deepen tissue penetration), caused severe cutaneous photosensitivity since it was retained by cutaneous tissues up to weeks (11).

In order to overcome first generation sensitizer disadvantages, second generation PSs were developed. These new sensitizers include 1,5-aminolevulinic acid (ALA) and porphyrin derivatives, such as chlorins (Chlorin e6 and derivatives), benzoporphyrin derivative (BPD), meta (Tetra) hydroxyphenylchlorin (m-THPC), phthalocyanines, texaphyrins and bacteriochlorophyll. They also include non–porphyrinic sensitizers, quinones, xanthenes, cyanins and some cationic dyes (12).

Photosensitizers can be originated from several broad families and be categorized by direct chemical structure. The three major photosensitizer families under investigation or in clinical use are outlined in table 1.1.

Table 1.1 - Major photosensitizer families under investigation or in clinical use.

Porphyrin platform	HpD, HpD-based
	BPD
	ALA
	Texaphyrins
Chlorophyll platform	Chlorins
	Bacteriochlorins
Phthalocyanine platform	Photosense
	Pc4
	CGP 55847

Design strategies for new photosensitizers are directed toward specificity. The new third generation photosensitizers consist in modification of available drugs with antibody conjugates, biologic conjugates, built in photobleaching capacity, among others, in an attempt to achieve the concept of ideal photosensitizer (13).

1.1.2 Oxygen

In 1978 researcher's in Moan's group recognized the importance of $^1O_2$ in several chemical and biological processes, such as, phototherapy of cancer, photodynamic

inactivation of viruses and cells and dye-sensitized photooxidation of lipids, proteins and nucleic acids. Highly reactive $^1O_2$ was found to play a vital role as toxic reagent during the process of PDT (10).

Studies concerning $^1O_2$ formation in PDT, using Hp, HpD (Photofrin I) and di-hematoporphyrin ether (DHE, Photofrin II) showed that the state of the photosensitizer aggregation influences the photochemical yield of $^1O_2$. Hp tends to aggregate when its concentration is increased, HpD and DHE are mixtures of porphyrins in different states of aggregation. When comparing the yield of $^1O_2$ formed by those photosensitizers, Moan's group found that photoexcitation of HpD and DHE resulted in lowers yields than photoexcitation of Hp. So, the fluorescence quantum yield and the singlet oxygen quantum yield produced by an aggregated Ps is remarkably lower than those of the monomeric form (14).

Further work from its team using cancer cells, lead to the conclusion that the inactivation efficiency is tightly dependent of the oxygen concentration since photoinactivation of cells decreased with decreasing oxygen concentration. In fact, hypoxic tumor cells showed resistance to PDT, so they suggested an increase of O_2 administration to the air breathed by patients during PDT, in order to increase tumor oxygenation (15).

Other experiments by Moan and Boye indicated that $^1O_2$ generated outside the cell wall cannot penetrate this wall. Through the observation of *Escherichia coli* and human cells, they found that the $^1O_2$ generated outside these cells did not introduce DNA strand break as long as the Ps is outside the cells (16,17). The diffused distance of $^1O_2$ was estimated to be lower than 0.05 µm during its short lifetime, from the site of origin before reacting with several cellular targets (18). Therefore, PDT damage through $^1O_2$ occurs close to the localization of photosensitizers during light exposure, which means that the subcellular localization of photosensitizing molecules is extremely important, since it determines the site or primary damage and its impact.

1.1.3 Light

The sun was the original light source in light therapy. Although very powerful (1000 W cm^{-2}) and with a wide multi-spectrum, it was not convenient or ideal. The need for indoor treatment, selective wavelength and ability to focus the light to the region of interest, lead to the development of other lights sources. It started with arc lamps that generated much heat and could be dangerous, evolving to slide projectors generally with filters to control wavelength. A great development came with the employment of lasers, which allowed the use of very precise wavelengths and highly focused beams. Non-laser light sources, such as light emitting diodes (LEDS) have a high impact on PDT, since they are less expensive, small, lightweight and highly flexible. They allow the use of high levels of light and wavelength that activate commercially available sensitizers. Reliable optical fibers are also very important for clinically successful PDT. They are able to fit into endoscopes or through biopsy needles, allowing the light sources to be used in a greater array of clinical cases (19).

The wavelength range between 600 and 800 nm was determined as the practical "therapeutic window" for clinical PDT (6). Light penetration in tissue at 630 nm is about 1-3 mm depth, while at 700-850 nm is twice the depth. Therefore, longer wavelength light with increased penetration depths encourages the development of photosensitizers which absorbs preferentially at those wavelengths, such as phthalocyanines, naphthalocyanines and bacteriochlorins (11). In order to obtain a maximal yield of $^1O_2$ at maximal depth, the chosen wavelength has to match the absorption spectra of the chosen Ps.

A process called "photobleaching" can occur as a result of a reaction between the excited Ps and the ROS produced upon illumination. This event leads to loss of absorbance and photosensitizing ability (20).

Light dose delivered influences PDT success. The unit usually used to measure the total energy delivered is the joule and is determined by watt (W) multiplied by time. The number of photons in a joule depends upon the wavelength of the light. The delivered rate of light, fluence rate, influences treatment time so it must be considered in PDT.

Fluence rate, in W/area, depends on the light source used. The higher the rate delivered by light, the higher is the probability of heating the molecules and its surroundings (6).

1.2 PHOTOCHEMISTRY

The photodynamic process is initiated when the photosensitizer absorbs photons from light and after excitation can suffers simultaneous or sequential decays, resulting in intramolecular energy transfer reactions. The ground state PS has two electrons with opposite spins (singlet state) in the lowest energy molecular orbital. When the photons are absorbed, one of the electrons jumps into a high-energy orbital, keeping its spin (first excited singlet state). This specie has a very short lifetime (nanoseconds) and can lose its energy, relaxing to the ground state by emitting a fluorescent photon or by internal conversion, releasing heat (20). The fluorescence ability can be used to quantify the amount of Ps in cell and tissue, allowing measuring the pharmacokinetics and distribution of the Ps in living animals and patients, and also as imaging agents in cancer diagnosis (21-23).

The excited singlet state can also undergo through a process known as intersystem crossing, leading to as inversion of the excited electron spin, forming a relatively long lived (microseconds) excited triplet state that has parallel electron spins (20). From the excited triplet state, the Ps can relax back to ground state through emission of a phosphorescent photon or by energy transference to another molecule. The long lifetime of the PS triplet state is explained by the fact that the loss of energy by emission of light (phosphorescence) is a “spin – forbidden” process, as the PS would go directly from a triplet to a single state. In the presence of oxygen, the chromophore reacts with ground state molecular oxygen, leading to the formation of singlet oxygen (20). The photochemical reactions described are represented in the simplified Jablonski diagram (Fig.1.2).

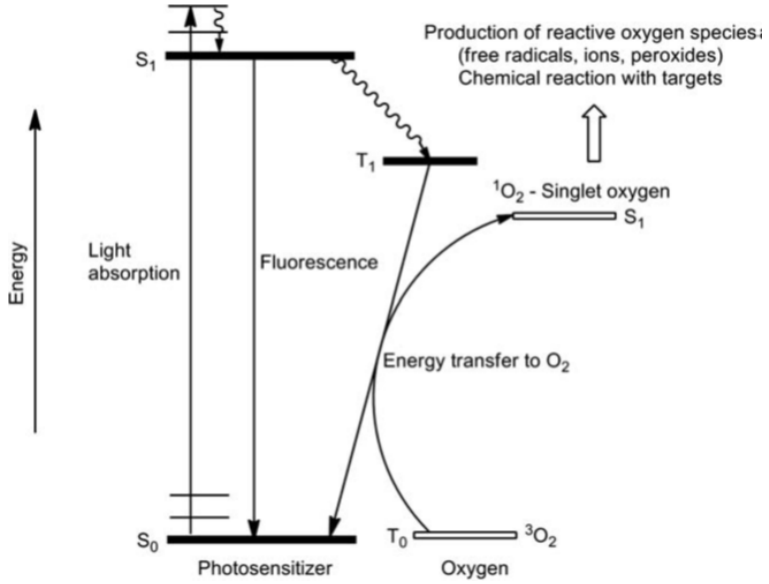

Figure 1.2 - Simplified Jablonski diagram. S_0: singlet ground state photosensitizer **;** S_1: short-lived singlet excited state photosensitizer; T_1: long-lived triplet state photosensitizer; T_0: ground state molecular oxygen (Kejík *et al.*, 2011).

1.2.1 Type I photooxigenation process

There are two main classes of energy transfer reactions involving oxygen, Type I and Type II. Type I photoreactions are characterized by a dependence on the target-substrate concentration. In anoxic conditions the excited PS can react directly with a substrate, such as the cell membrane or a molecule, producing an oxidized substrate and a reduced PS, by electron exchange (i). These anionic and cationic radicals may later react with oxygen to produce reactive oxygen species. The reduced PS, in hypoxic environments and after reacting with ground state molecular oxygen ($^3O_2$), may produce superoxide anions ($O_2^{-\cdot}$) (ii). These anions may also be produced by the reaction of the excited PS with superoxide radicals ($O_2^{\cdot}$) (iii) (24).

Superoxide is not very reactive in biological systems, but can react with itself forming hydrogen peroxide (H_2O_2) and oxygen, a reaction that can be catalyzed by the enzyme superoxide dismutase (SOD), through a reaction called “dismutation” (iv) (24).

H_2O_2 is important in biological systems once it can pass effortlessly through cell membranes and cannot be excluded form cells, since is necessary for the function of several enzymes. Once damage caused by H_2O_2 is not restricted to one cellular compartment, hydrogen peroxide is considerably relevant in producing cellular damage.

Superoxide can also form the highly reactive hydroxyl radicals ($OH^{-\cdot}$), by acting as a reducing agent through donation of one electron in order to reduce metal ions (such as ferric iron or Fe^{3+}), that act as the catalyst to convert H_2O_2 into their hydroxyl radical ($OH^{\cdot}$). This processed is called the Fenton reaction (v) and is important in biological processes because most cells have iron, copper or other metals, which can catalyze this reaction. The reduced metal (ferrous iron or Fe^{2+}) then catalyzes the breaking of oxygen – oxygen bond of H_2O_2 to produce a hydroxyl radical and a hydroxide ion (OH^-) (vi) (24,25).

Superoxide can react with $OH^{\cdot}$ to form singlet oxygen (vii), or with nitric oxide (NO^-, also a radical) to produce peroxynitrite ($OONO^-$)(viii), another highly reactive oxidizing molecule (24). $OH^{\cdot}$ can also pass effortlessly through membranes and cannot be kept out of cells, just like H_2O_2. $OH^{\cdot}$ can add to an organic (carbon containing) substrate, for instance a fatty acid which could form a hydroxylated adduct that is itself a radical. It also can oxidize the organic substrate by "stealing" or abstracting an electron from it. The resulting oxidized substrate is itself a radical that can react with other molecules in a chain reaction, which is common in oxidative damage of fatty acids and other lipids (20,25)

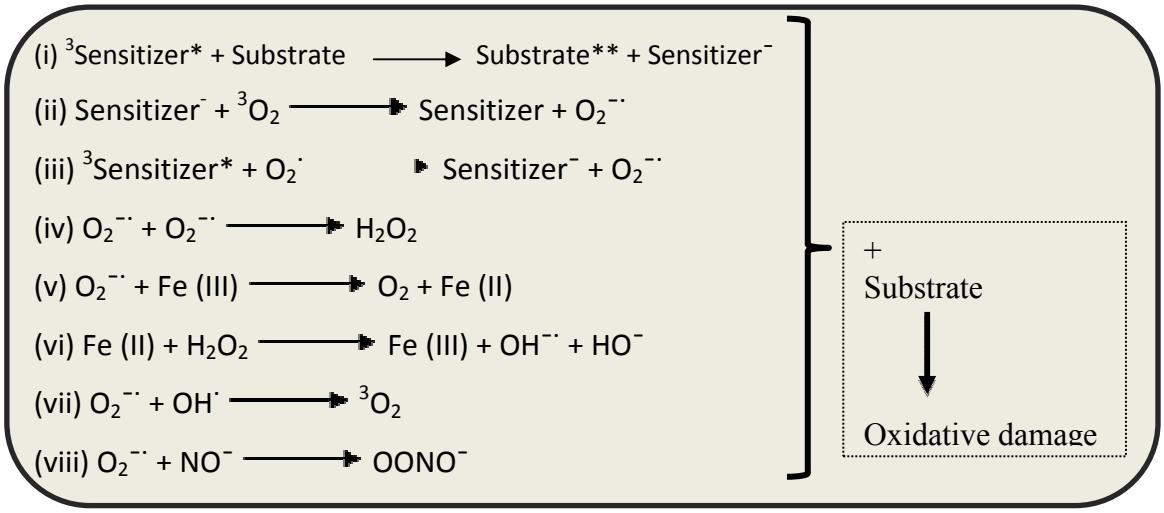

1.2.2 Type II photooxigenation process

A Type II reaction is characterized by dependence on the oxygen concentration. In this pathway, the triplet state PS can transfer its energy directly to molecular oxygen to

form excited singlet oxygen ($^1O_2$) that can participate in lipid and protein membrane oxidation or induce DNA damage (20,26).

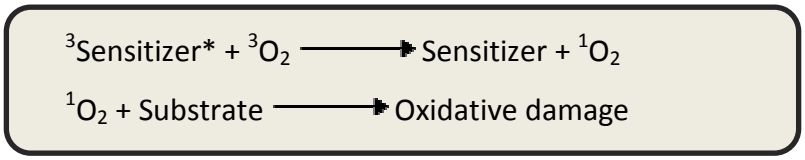

Despite the association of this reaction with singlet oxygen production, some other compounds, such as nitric oxide and vitamin A, have triplet-ground states and can also be involved (27).

Both Type I and Type II pathways can occur simultaneously, the ratio between these two processes depends on the type of PS used, the concentration of oxygen and substrate. Type II reactions are reported to be prevalent during PDT, while Type I could be dominant under hypoxic conditions and in the presence of high concentrations of photosensitizer (27).

Most photosensitization reactions are attributed to the action of Type I and Type II mechanisms, but there are also two types of reactions caused by the PS triplet state, that does not involves oxygen but can also cause cellular damage, Type III and Type IV reactions.

1.2.3 Type III photodynamic mechanism

In these reactions a covalent photobinding between the PS and one macromolecule is formed, leading to the formation of stable photo products independent of oxygen that could induce cells damage (25).

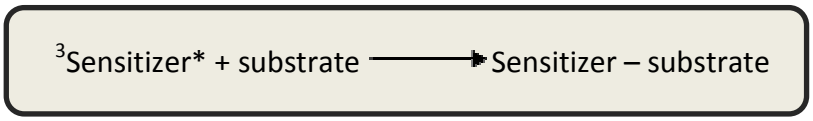

1.2.4 Type IV photodynamic mechanism

The photosensitizer can also suffer a decomposition, resulting in photoproducts that can act either as toxin or as a new photosensitizer (28).

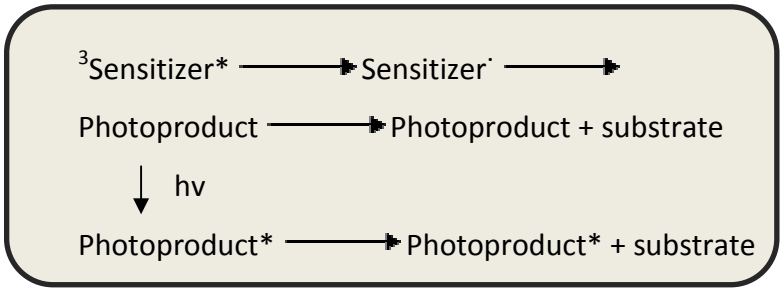

The Figure 1.3 resumes all photochemical reactions that can lead to cell damage.

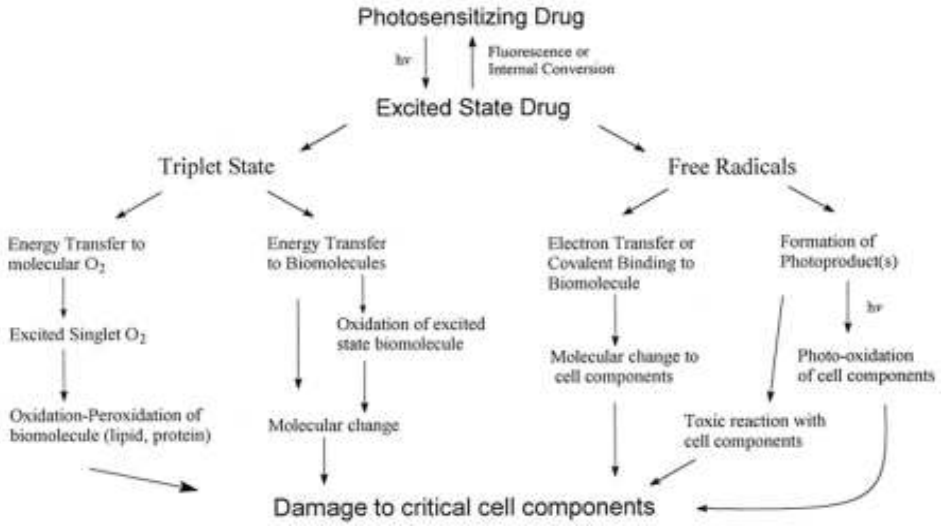

Figure 1.3 - Photochemical reactions that can lead to cell damage (Moore, 1998).

1.3 PHOTODYNAMIC THERAPY APPLICATIONS

Although the first successful PDT experiments were in microorganisms, it was the clinical success on a wide diversity of tumors that gained the interest of clinicians, allowing its growth, not only in oncology but several other areas.

1.3.1 Oncology applications

The visible tumor destruction, sparing the normal tissue, with rapid vascular and cytotoxic reactions and mobile, reliable light sources, gave the impetus to study PDT in several tumors. Skin is the simplest target for PDT, due to its accessibility. Photofrin® and

ALA action proved to be beneficial in several skin diseases such as Kaposi sarcoma, basal cell, squamous cell carcinoma (29-31) and metastasis lesions originated from breast, gynecological and gastrointestinal tumors (32). Like skin, head and neck tumors offer easy access, either by superficial or interstitial illumination. It includes face, oral cavity (tongue, jaw), nasopharynx, larynx and neck tumors. Porphyrin photosensitizer derivatives also showed promising results in gastrointestinal track (33), lungs (34), genitourinary and prostate (35,36), brain (37), as well as hematological diseases (leukemia and lymphoma)(38,39).

1.3.2 Antimicrobial applications

The antimicrobial activity of PDT, although well known, only became of interest when microorganisms started developing antibiotic resistance. Photomicrobial action is now well documented for a wide range of microorganisms *in vitro* and *in vivo*. Antibiotic PDT includes infectious diseases treatment (40,41), decontamination / pathogen inactivation of blood products for transfusion (riboflavin, methylene blue, amotosalen) (42-44), acne treatment (ALA) (45), wastewater treatment (porphyrins derivates) (46) and insecticides (ALA)(47).

1.3.3 Other applications

Other PDT applications grew out from the intensive investigation regarding PDT and oncology. Verteporfin is used in ophthalmology to slow lesions caused by age – related macular degeneration (48). It can also help in arthritis and autoimmune disorders (49). ALA and lutetium texaphyrin are beneficial in atherosclerosis, inhibiting the built-up of plaques (50,51). Again, ALA has a good impact in endometriosis cases (52).

Photosensitizers, due to their fluorescence ability, can also be used in diagnosis. Fluorescent tumor marking is a highly effective tool. Lower concentrations of PS are required and, in addition, the method is very sensitive to changes in tissue caused by the presence of malignant or dysplastic cells (21-23).

The use of photosensitizers can also facilitate the delivery of other therapeutic agents, by causing cell wall disarrangement, or to increase intracellular release rates of cytotoxic molecules from molecules taken by endocytosis, by the opening of vesicles or otherwise liberation of drugs via the action of singlet oxygen (53).

Thus, PDT is an economic, fast, simple and effective method that offers a wide range of applications in multidimensional areas regarding health.

1.4 ANTIMICROBIAL PHOTODYNAMIC THERAPY

It was during the XX century, facing the urgent treatment need for infectious diseases, that the antibiotics were discovered and improved. At the time they were seen as a miraculous drug but, a century later, they helped the emerging of a major healthcare issue: bacterial antibiotic resistance. The misuse and abuse of antibiotics in medicine, its widespread use in livestock feedstuff, the longer survival of patients with severe illness and at risk for infections, lack of use of effective preventive infection control measures, among others, lead to bacterial activation of adaptation mechanisms, originating resistant and multi-resistant species, on which antibiotics have no effect. Adding to this, global traveling allowed in a large scale the frequent transmission of microorganisms (40). Bacteria replication is very fast, so a mutation that allows its survival in the presence of a killing agent, such as an antibiotic drug, will rapidly become predominant.

Basically, bacteria resistance to antibiotics has it base at the genetic level. Most cases of bacterial resistance are originated by changes in the genetic information, either via a mutation or introduction of new genetic information. These changes results in alteration of one or more biological mechanisms of the affected bacteria, such as destruction of the antibacterial agent before it has an effect, acquisition of efflux pumps that expel the antibacterial agent before reaching the target site, alteration of bacterial cell wall by eliminating the binding site for antimicrobial agent, or by downregulation of porin genes that causes limit access of the agents to the intracellular target site, ultimately leading to resistance to therapeutic agents. Thus, there is the need of new effective and affordable approaches, not susceptible to resistance and extensively applicable (54).

Antimicrobial photodynamic therapy (aPDT) was described more than 100 years ago by Raab, referring to the lethal effect of acridine and visible light on *Paramecium caudatum*, but the potential of this finding was not fully researched due to the discovery of antibiotics and poor response of some pathogens, namely Gram-negative bacteria and protozoa in the cystic stage, to some of the most common photosensitizers, such as porphyrins used in tumor therapy, xanthenes or acridine dyes (40). But several data show that PDT could be a possible alternative to combating microorganisms, presenting several advantageous aspects (7,8):

-prospect to broaden PDT protocols which lead to an extensive reduction in pathogen population with very limited damage to the host tissue;

-wide spectrum of action, since one photosensitizer can act on fungi, yeasts, bacteria, parasitic protozoa and virus;

-apparent inexistence of photoresistant strains after multiple treatments;

-efficacy independent of the antibiotic resistance type of the given microbial strain;

-lack of mutagenicity;

-use of affordable light sources for activation of the photosensitizer;

-possibility of formulations allowing a ready and specific delivery of the photosensitizer to the infected area

aPDT can be used in a wide range of fields, such as dermatology (impetigo, acne vulgaris, wound infections) (55), dentistry (oral biofilms, dental and mucosal infections) (56), gastroenterology (*Helicobacter pylori* in stomach) (57), transfusion medicine (blood and platelet concentrate decontamination) (58), wastewater treatment and tropical microorganisms inactivation (leishmaniasis, malaria) (59,60), among others.

1.5 PHOTOSENSITIZERS IN aPDT

To achieve maximum efficacy, a photosensitizer in aPDT should have several specific characteristics (40), such as:

- a high quantum yield for the generation of both the long-lived triplet state and the cytotoxic oxygen species;

- preferential affinity to microbial cells;

- wide range of action to efficiently act on infections with a heterogeneous flora of pathogens;

- a process of cell inactivation minimizing the chance of inducing the selection of resistant strains or promoting the development of mutagenic processes;

- possibility to select a therapeutic window that allows an extensive killing of microorganisms that induce disease, with minimal damage to the host tissue in the surroundings of the infection, without resistance development to the treatment.

Nowadays a broad range of photosensitizers are being studied to evaluate their effectiveness in the inactivation of microorganisms. Some of them include methylene blue, a well-known photosensitizer in this field, being used for over a century against bacteriophages and viruses, among others (61). Several assays with macrocycle photosensitizers (porphyrins and phthalocyanines) also show efficient photodynamic inactivation of viruses and bacteria, both Gram-positive and Gram-negative.

Phthalocyanines (Pcs) usually show high yields of singlet oxygen production, greater than that of standard photosensitizers, such as methylene blue (62).

This wide variety of photosensitizers that can be effectively use for microorganisms photoinactivation, allows an enhancement of microorganisms specificity, also the difference of susceptibility of human and microorganisms cells, due to differences in cell size, making lethal conditions to microorganisms, less toxic to human cells, indicates that aPDT is a technique with great potential to be included in clinical practices (62).

1.6 PHOTOINACTIVATION OF BACTERIAL CELL

Bacterial cell photoinactivation is achieved by the accumulation of significant quantities of a photosensitizer on the citoplasmatic membrane or in the cell causing irreversible damages through the generation of cytotoxic species. The efficiency and mechanism of this process is influenced by cellular structure and organization differences, affecting the interaction of photosensitizers with cell constituents (67).

It was Christian Gram that classified bacteria as Gram-positive or Gram-negative when, in 1880, developed a staining technique, the Gram staining. The difference in staining is due to structural differences on bacteria outer cell membrane of the wall (63). Gram-positive bacteria cell wall is 15 – 80 nm thickness, it contains up to 100 peptidoglycan layers, with no significant quantity of lipids or proteins. Although it has more layers of peptidoglycan, much thicker than in gram-negative ones. Gram-positive bacteria wall presents a rather high degree of porosity, once several macromolecules in the range of 30 to 57 kDa can easily diffuse to the inner plasma membrane. Gram-negative bacteria wall architecture has an additional membrane layer, external to the peptidoglycan layer, that presents an asymmetric lipid structure composed by strongly negatively charged lipopolysaccharides, phospholipids, lipoproteins and proteins with porin function (fig. 1.4) (55). Only relatively hydrophilic compounds with a molecular weight lower than 600-700 Da can diffuse through the porin channels, making the outer membrane a very effective permeability barrier that confers resistance against host cellular and humoral defence factors (40). Thus, the susceptibility to aPDT between Gram-negative and Gram-positive is due to their outer membrane.

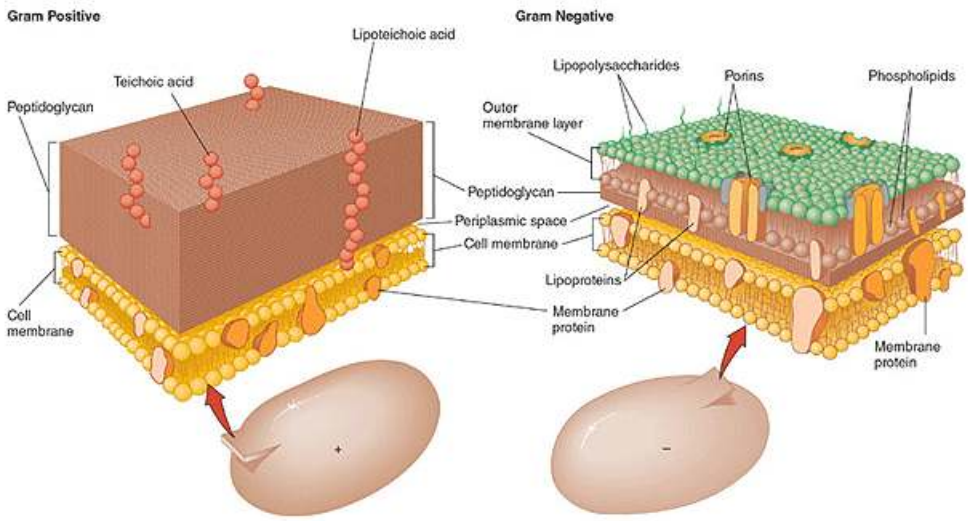

Figure 1.4 - Schematic representation of Gram-positive and gram-negative bacteria cell wall (Betsy, Keogh, 2005).

Due to their permeability, gram-positive bacteria can be readily photoinactivated by anionic and neutral photosensitizers that bind and easily diffuse trough the membrane of the cell. Gram-negative bacteria showed no susceptibility to these photosensitizers. Several studies showed that adding biological or chemical molecules such as peptide polymyxin or Tris-EDTA, enhances photosensitization of Gram-negative bacteria, altering the original consistence of the outer membrane, causing a higher permeability and facilitating the diffusion of the PS to the cytoplasmic membrane (64). Although this method allowed a higher susceptibility to PDT by Gram-negative bacteria, it would be preferable if a photosensitizer could have such effect without adding a disrupting agent. Merchat *et al.* (65), with cationic porphyrins, and Minnock *et al.* (66), with cationic phthalocyanines, provided the solution. These cationic PSs show to be effective in photoinactivating Gram-negative bacteria. Also non-cationic photosensitizers, such as chlorins, can promote efficient photoinactivation as long as they are covalently bound to a polylysine oligomer positively charged (67). A possible explanation for the cationic PS uptake by Gram-negative bacteria is the interaction of the divalent cation binding sites on the surface of lipopolysaccharides with the cationic PS, once these molecules have an affinity for those sites 2-4 orders of magnitude higher than the divalent cations. The bulkiness of the displacing polycations causes a deformity of outer membrane structure, leading to a permeabilization of the outer membrane to several molecules. At the same time, the uptake of the polycations themselves is enhanced. This mechanism is known as “self-promoted uptake pathway” (68).

After the translocation of the photosensitizer to the inner plasma membrane, the photoactivation of the macromolecule promote the generation of cytotoxic species, as mentioned before, oxidizing specific targets in the microenvironment surrounding the sensitizer, leading to deterioration of cell functions and metabolism, resulting in inhibition of cell growth and consequently cell death (69).

Two basic mechanisms were proposed to explain the lethal damage caused to bacteria by aPDT: DNA damage and damage to the cytoplasmic membrane, causing the release of cellular contents or inactivation of membrane transport systems and enzymes. Evidence shows that treatment of bacteria with several PS and light leads to DNA

damage. Breaks in both single and double-stranded DNA, and the disappearance of the plasmid super-coiled fraction have been detected in both Gram-positive and Gram-negative bacteria after the photodynamic process with a wide range of PS structural types. Some findings suggest that photosensitizers that can more easily intercalate into double-stranded DNA readily can cause more damage. Guanine residues seem to be more easily oxidized. However several authors have concluded that, although DNA damage occurs, it may not be the main cause of cell death, as shown by *D. radiodurans*, bacterium known by their very efficient DNA repair mechanism, that is easily killed by aPDT (41). Other factors such as alteration of cytoplasmic membrane proteins, shown by Valduga *et al.* (70) and Bertoloni *et al.* (71), disturbance of cell wall synthesis, the appearance of a multilamelar structure near the septum of dividing cells, along with loss of potassium ions from the cell, reported by Nitzan *et al.* (72) can promote bacteria cell death.

Typical type I reactions, e.g. at the bacterial cytoplasm, involves the abstraction of allylic hydrogens from unsaturated molecules such as phospholipids. The radical species thus formed may undergo reaction with oxygen to yield the lipid hydroperoxidase. Lipid peroxidation is detrimental to membrane integrity, causing loss of fluidity and increased ion permeability. Other cell wall / membrane targets include aminolipids and peptides; hence inactivation of membrane enzymes and receptors is also possible. In the type II mechanism, the short life of singlet oxygen ensures a localized response, causing the singlet oxygen formed to react rapidly with its environment – cell wall, nucleic acids, peptides, etc. Type II processes are generally accepted as the major pathways in photooxidative microbial cell damage. In DNA damage, there is also a difference in selectivity between type I and type II processes. Type I is mediated through hydroxyl radical attack at the sugar moiety, while type II is an attack of singlet oxygen at the guanine base (62).

The photosensitivity of bacteria is also affected by its physiological state. Cells in the logarithmic phase of growth are pronouncedly more susceptible to photodynamic inactivation than the corresponding cells in the stationary phase (40).

1.7 RAPID METHODS TO MONITOR BACTERIA PHOTOINACTIVATION

Conventional methods to follow the bacterial photoinactivation process frequently involve animal sacrifice, removal of the infected tissue, homogenization, serial dilution, plating and colony counting. These processes use a large number of animals, are time consuming due to overnight incubation as counting of colony - forming units (CFU) and often are not statistically reliable (58). Thus, faster methods are in demand to study potential PS *in vitro*, and have been essential to accelerate the development of aPDT. The bacterial bioluminescence method could be the response to this issue, once is considered to be a rapid, sensitive and cost–effective option. It also allows only living or viable cells detection and does not need exogenous administration of substrates to obtain light emission (73-75).

Bioluminescence is the process of visible light emission by living organisms through the intervention of an enzyme catalyst. Evidence show that inhibition of cellular activity results in a decrease in the respiration rate and consequentially a decrease in the bioluminescence rate, so light emission is directly dependent on the metabolic activity of the organism (76,77). The bioluminescence phenomena has been observed in several different organisms including bacteria, fungi, fish, insects, algae and squid, in marine, freshwater and terrestrial environments (78).

Luciferases are enzymes that catalyze the bacterial luminescent reaction, they consist on an oxygenase, where the fatty aldehydes are the substrate that produces the correspondent fatty acid. The light emission reaction involves the oxidation of reduced riboflavin phosphate ($FMNH_2$) and a long fatty aldehyde chain with the emission of blue – green light (fig. 1.5) (79,80).

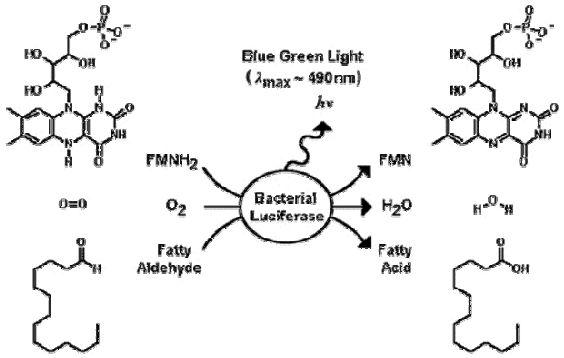

Figure 1.5 - Bacterial luciferase catalyzed reaction. (Lin and Meighen, 2004)

In both marine and terrestrial bioluminescent bacteria, a five genes operon (*lux*CDABE) encodes the biosynthetic and luciferase enzymes (for the synthesis of the aldehyde substrate) fundamental for light production. *lux*A and *lux*B genes encode the alpha and beta subunits of the luciferase, with *lux*C, *lux*D and *lux*E genes encoding proteins for aldehyde production (81).

The emission of light by most luminescent bacteria is highly dependent on the extent of cellular growth. Through the initial stages of growth at low cell density, the *lux* genes are not expressed and luminescence in a cell culture will actually decrease with growth, mainly due to a limitation in the substrates for the luminescent reaction. During mid to late logarithmic growth, depending on the species and the nutrient composition of growth medium, light emission will increase dramatically. The increase in luminescence is originated by activation of expression of the genes in the *lux* operon including the *lux*CDABE genes. Only these genes are essential for the biosynthetic production of light, although a number of additional *lux* genes in bioluminescent bacteria have been identified (80). In marine bioluminescent bacteria, light emission occurs preferentially at temperature below 30 °C (82).

Light output is noncumulative, reflecting with highly sensibility actual metabolic rate, it can be measured directly, continuously and non–destructively in high–throughput screening of continuous–culture models, making it useful for monitoring real time effects of antimicrobials on bacteria metabolism (75,83,84). A strong correlation between bioluminescence and viable count can be observed (75,85).

The development of recombinant DNA technology allowed the selection of the phenomenon of bacteria bioluminescence and its application within any bacterial species from several rather different perspectives. It offers a real-time, non-invasive reporter for measuring gene expression, a sensitive marker for bacteria detection and a measure of intracellular biochemical functions, such as a holistic determinant of cellular viability (86).

1.8 PHTHALOCYANINES

Phthalocyanines were accidentally discovered in 1907 by Braun and Tcherniac after examining the results of a chemistry study on o–cyanobenzamide, that when heated, a trace amount of a blue substance was obtained. This compound was undoubtedly metal–free phthalocyanine (Pc). However, the importance of this observation was not fully recognized. In 1927 de Diesbach and co–workers found that a blue product was obtained in moderate yields when 1,2–dibromobenzene was treated with copper (I) cyanidein boiling quinolone for eight hours. This was probably the first synthesis of copper Pc, but they were unable to propose a structure. A year later, in the manufacture of a phthalimide from the reaction of phthalic anhydride with ammonia in a glass–lined reactor by Dandridge, Drescher and Thomas of Scottish Dyes, a blue impurity was observed. This impurity proved to be iron Pc, being the source or iron the reactor wall that became exposed due to a flaw in glass lining (87,88).

After this discovery, the color manufacturing industry quickly recognized the unique properties of the compounds and started to explore their commercial potential. In 1929, Dandridge, Drescher and Thomas patented the compounds that now are known as phthalocyanines. The name derivate from the Greek terms for naphtha (rock oil) and for cyanine (dark blue) and was given by Linstead, whom extensive work confirmed the structure and contained the experimental details to the preparation of Pcs from phthalonitrile (89).

Phthalocyanines are planar aromatic macrocycles consisting of four isoindole units connected by four nitrogen atoms, forming altogether an internal 16-membered ring, presenting an 18–electron aromatic cloud delocalized over an arrangement of alternated carbon and nitrogen atoms (Fig. 1.6).

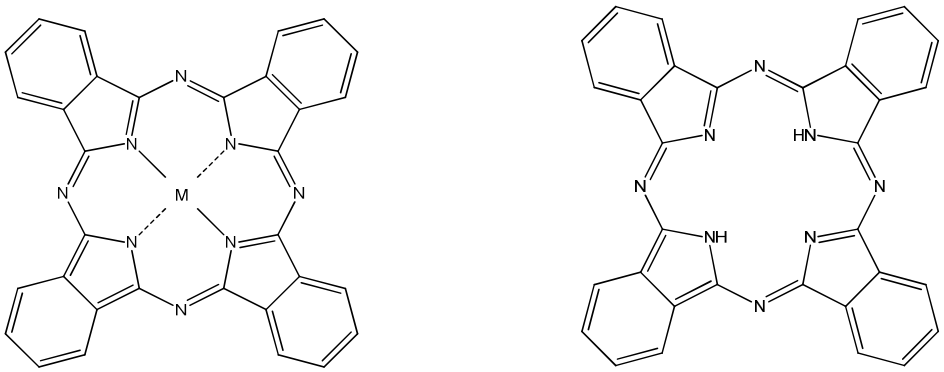

Figure 1.6 - Structures of metal and metal-free phthalocyanines

The numerous properties given by the electronic delocalization allows the use of these compounds in several fields of science and technology, due to the acquired versatility and thermal and chemical stability (90).

Pcs can have a metal-free core, metal-free phthalocyanine, or a metal replacing the hydrogen atoms of the central cavity, metallophthalocyanine (Fig. 1.6). Almost every metal and some metalloids can replace the hydrogen atoms, in a total of more than 70 elements (91). A diversity of substituents can be incorporated at the periphery of the macrocycle and at the axial positions, allowing fine-tuning of the physical properties

Also, several modifications can be made over the phthalocyanine ring originating the so-called Pc analogues. The most common structural changes that leads to Pc related compounds are the extension of the π-system, the formal substitution of some of the isoindole moieties by another (hetero) aromatic ring and the variation in the number of isoindole units (91).

Figure 1.7 represents the nomenclature usually used by IUPAC. All atoms, with the exception of the ones merging the pyrrole and benzene rings, are numbered (92).

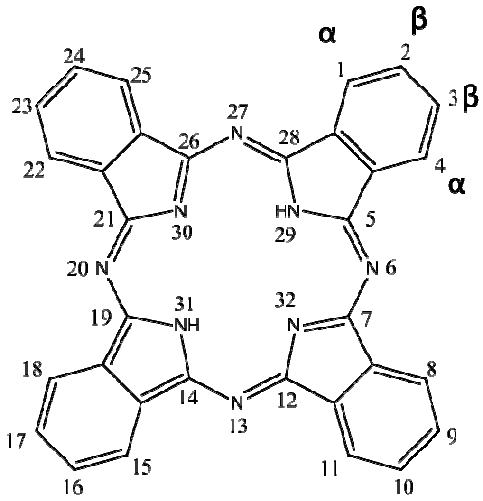

Figure 1.7 - Phthalocyanine numbered atoms, used by IUPAC

1.8.1 Phthalocyanines Spectra

The extensively conjugated aromatic chromophoric system of phthalocyanines generates intense bands in their absorption spectra. The strongest absorption band in most phthalocyanines usually lies in in the visible region at wavelengths between 650–670 nm, the Q–band, while the weaker band is near 340 nm, the Soret or B band (Fig. 1.8). This preferential absorption in the red light region confers the characteristically blue color of the Pcs (93). An introduction of a metal ion inside the cavity will originate a slight blue shit in the Q – Band, due to a reduction of the electron density, being a bigger blue shift directly related to the higher metal ion electromagnetic field.

Besides the central metal, the positions of the absorption bands in Pcs (specially the Q–bands) are affected by axial substitutions, solvents, peripheral and non-peripheral substitution, aggregation and extension of the conjugation. Metallation increases the symmetry to D4h, maintaining the planarity of the molecule. Metal–free Pcs presents D2h symmetry. Lowering the symmetry leads to a splitting of the Q–band, that is the reason why a clear split of the Q–band is observer in metal–free phthalocyanines (94).

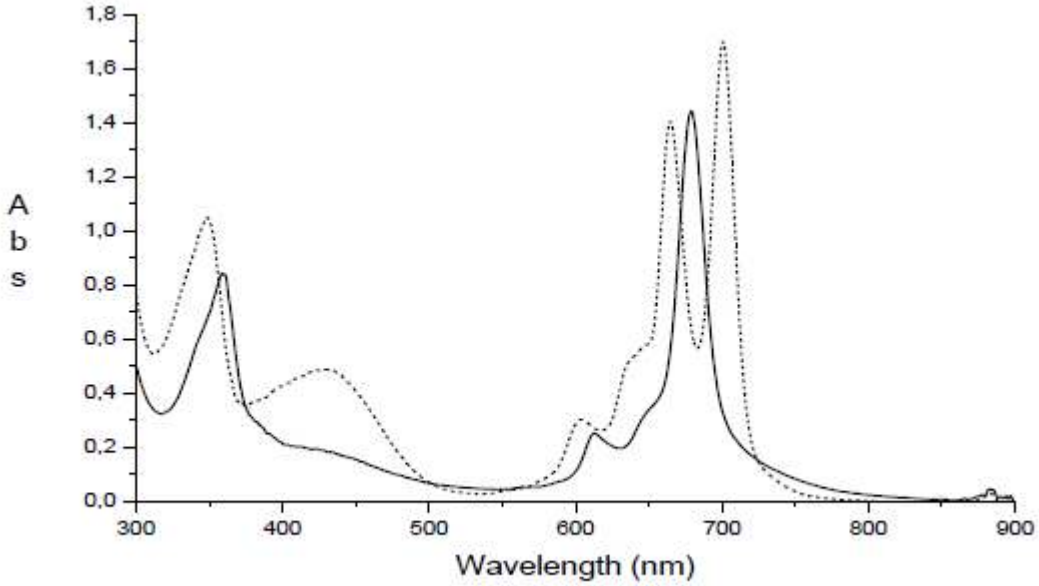

Figure 1.8 - Absorption spectra of a metal free (dashed line) and a metallophthalocyanine (solid line). (Carvalho E., Master thesis, University of Aveiro, 2009)

1.8.2 Phthalocyanines Aggregation

Phthalocyanines have great potential due to their unique electronic spectra, high degree of aromaticity, singular chemical structure and versatility, but it has a great disadvantage, the extreme insolubility of their unsubstituted derivatives. This characteristic is a result of the extreme hydrophobicity of the aromatic core and planarity of the macrocycle, that leads to a tendency to stack (π-π stacking) upon themselves progressing from monomer to dimer and higher order complexes and is driven by enhanced van der Waals' attractive forces between phthalocyanine rings.

In the aggregated state, the electronic structure of the phthalocyanine rings is discomposed, leading to an alteration of the ground and excited state properties. Aggregation in phthalocyanines is characterized by a broadening of the Q-band with a corresponding blue- (H-aggregate) or red-shift (J-aggregate) in their wavelength values or by splitting of the Q-band. This issue can be overcome by bulky or long chain peripheral beta–substitution, by alpha–peripheral substitution, by axial substitution and metal ion effects (blocking the coplanar association of the rings) (95).

The peripheral group substitution, besides enhancing the solubility of the macrocycle in water and organic solvents, also allows tuning the properties and be used as anchoring or bridging groups for formation of controlled supramolecular assemblies and similar applications (95).

1.8.3 Phthalocyanines Synthesis

Although the Pc macrocycle can be modified by changing the central atom and/or its axial coordination, or by changing the meso–atoms, the most advantageous is its peripheral modification. The term “periphery” refers to all substituents on the benzene rings. The α–substituents are the ones located at positions 1, 4, 8, 11, 15, 18, 22 and 25 of the macrocycle. The β–substituents are those located at positions 2, 3, 9, 10, 16, 17, 23 and 24 (Fig. 1.7) (96).

Two basic methods are used to introduce peripheral substituents into the Pc ring: the direct substitution on an already existing phthalocyanine or condensation of substituted precursors. The alteration of a preexisting Pc employs rough reaction conditions and leads to complex isomeric mixtures and several degrees of substitution, due to the sixteen available positions for substitution. The characterization, purification and isolation of these mixtures are very difficult.

A much more clean and easier to control reaction is obtained with the condensation of substituted precursors. Despite the fact that the unsymmetrically precursors can result in constitutional isomers, the number of substituents and their relative position is known. This is the favored method to the macrocycle functionalization.

Phthalocyanine precursors are aromatic ortho–carboxylic acid derivatives, such as phthalic acids, phthalic anhydrides, phthalimides, diiminoisoindolines, o–cyanobenzamides and phthalonitriles. For the purpose of this dissertation, the focus will be on these last compounds and synthesis of metal – phthalocyanines.

Phthalonitriles generate Pcs complexes in good yields with most metals (being silver and mercury the exception), involving often simple reactions in which the phthalonitrile is heated in the presence of a metal ion source as a melt of reagents or in an appropriate high boiling solvent, making them the most preferred of the precursors.

They can be synthetized or substituents can be introduced in a preexisting phthalonitrile. Reactions with phthalonitriles are clearer and give yields typically in the range of 30 – 50%, in some cases up to 90%, than other precursors (92).

Phthalocyanines results from phthalonitriles via a metal template assisted cyclotetramerization reaction. The mechanism of this reaction is still uncomprehended, conventionally is presumed that four phthalonitrile units mesh with the metal ion, leading to the formation of the macrocycle through a template effect. There are other theories involving the mechanism of Pcs, where the solvent, an alcohol, plays an important part in the reaction, but this is not relevant to the work done in this dissertation (92).

Phthalocyanines can be symmetrically or unsymmetrically substituted. We will target on symmetrically the tetra- and octa–substituted forms, although they can also be hexadeca-substituted (Fig. 1.9).

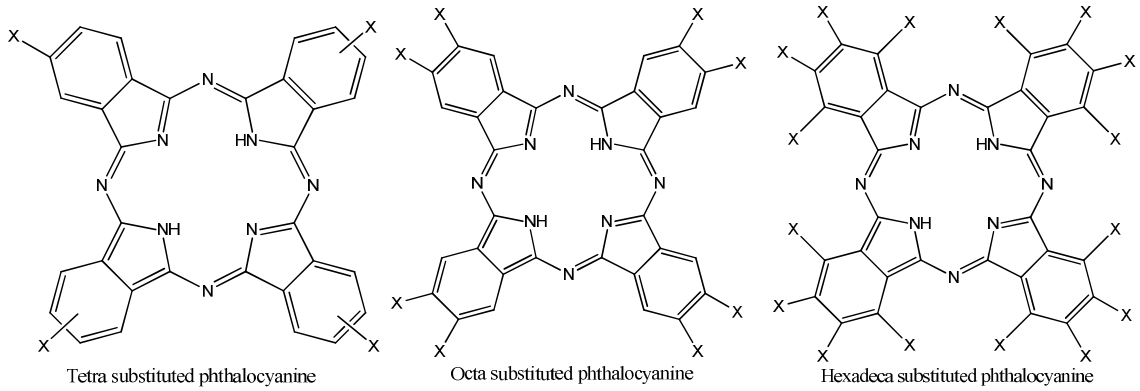

Figure 1.9 - Structures of tetra-, octa- and hexadeca-substituted phthalocyanines.

Tetra–substituted phthalocyanines, from mono–substituted phthalonitriles, leads to a mixture of constitutional isomers. Matching to the substituted positions on the precursor, two types of tetra-substituted phthalocyanines can be obtained. beta–tetra-substituted Pcs are synthetized from 4-substituted phthalonitriles, while alpha–substituted phthalocyanines results from 3–substituted phthalonitriles.

The mixture of isomers obtained from the 4–substituted precursors occurs in the statistical mixture of 12,5 % C_{4h}, 25 % C_{2v}, 50 % C_s and 12,5 % D_{2h} isomer (Fig. 1.10). The isomers of alpha–substituted phthalocyanines depends on the central metal ion and the structure of peripheral substituents (92).

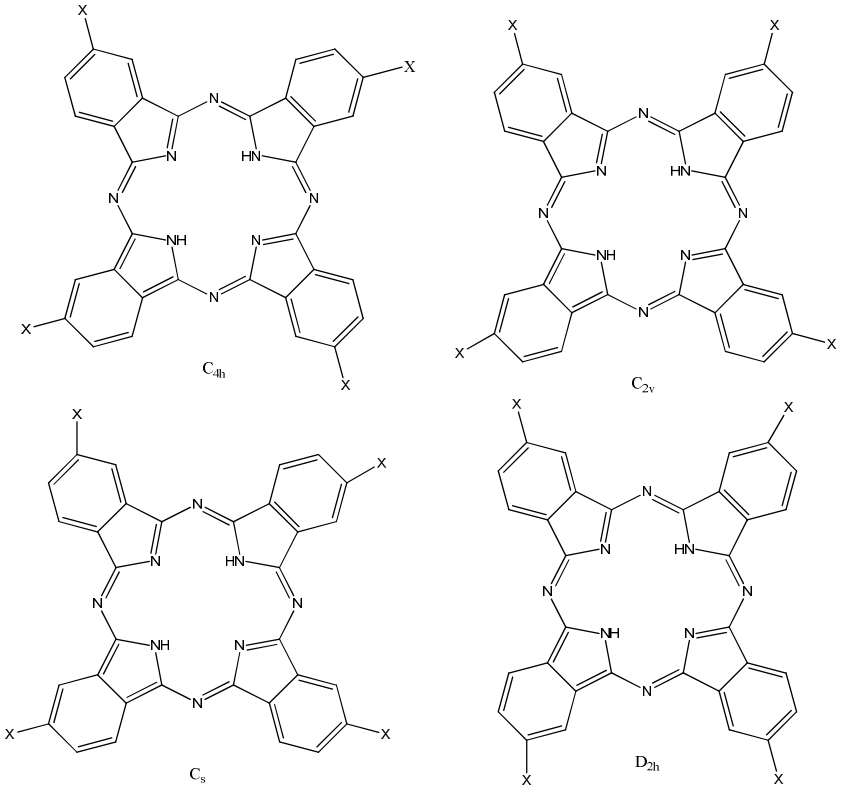

Figure 1.10 - The four isomers possible for a tetrasubstituted phthalocyanine.

Octasubstituted compounds with symmetric nature contains two substituents in each of the isoindole units, either at peripheral (2, 3, 9, 10, 16, 17, 23, 24) or nonperipheral (1, 4, 8, 11, 15, 18, 22, 25) positions. The former is formed by cyclotetramerization of 4,5-disubstituted phthalonitrile derivatives, whereas the latter is formed by condensation of the 3,6-disubstituted phthalonitrile derivatives.

Tetra-substituted phthalocyanines have usually higher solubility than the corresponding octa-substituted ones due to the formation of constitutional isomers and the high dipole moment that results from the unsymmetrical arrangement of the substituents (97).

1.8.4 Applications

Since their serendipity discover in 1928, these synthetic analogues of the porphyrins have been the extensively studied in many different fields. The application of phthalocyanines in the industry began due to their characteristically dark green–blue

color, as dyestuffs for textiles, paints and inks (98). Phthalocyanines have many interesting properties, not related to their color, that allows a wide range of applications such as catalysts for oxidation (99), lubricating greases (100), molecular electronic devices (94), optical recording materials (101), in nuclear reactors (87) and as photosensitizers (102), to name a few.

The interest in phthalocyanines as photosensitizers came from the need of compounds that absorb strongly in the red. Red light is most commonly used in PDT to obtain the maximum depth of light penetration in mammalian tissue, and some sensitizers, such as porphyrins, absorb poorly in that region.

1.8.5 Phthalocyanines in aPDT

The recognition of phthalocyanines as potential photosensitizers for PDT dates back to 1985, after Ben-Hur and Rosenthal demonstrated that chloroaluminium phthalocyanine can photosensitize mammalian cells (103). More than 400 publications describing synthesis of new Pcs tailored for PDT were published in the followed decade.

Intense absorption bands in the red region, usually at longer wavelengths than those of HpD, protoporphyrin IX, among other, combined with a somewhat straight forward synthesis, absence of dark toxicity, tumor localizing properties, made the phthalocyanines an attractive class in terms of potential photosensitizers for PDT. Not surprisingly, they are second only in popularity to the porphyrin class in this respect (104,105).

In figure 1.11 is presented some examples of phthalocyanine applications in PDT (106).

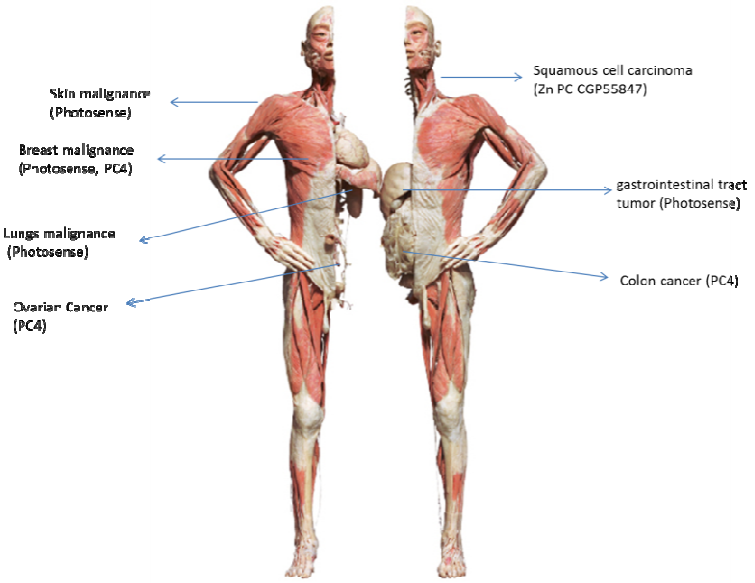

Figure 1.4 - Examples of Pc applications in PDT.

There is a considerable literature associated with phthalocyanines in the fields of photodynamic inactivation. This was mostly due to the significant investigations undertaken by Ben-Hur and co-workers in the 1990s into the use of silicon phthalocyanines in blood product decontamination protocols (107,108). Nevertheless, much work has also been reported afterwards by Jori and co-workers regarding peripherally rather than axially functionalized derivatives, especially those of cationic nature (55,109).

Besides successful inactivation of HIV (107,108) phthalocyanines proved to be efficient photosensitizing agents regarding blood-borne pathogens involved in tropical diseases, such as *Plasmodium falciparum* (110) and *Trypanosoma cruzi* (111), such activity is important in blood product decontamination protocols in many non-temperate parts of the world.

Several groups have synthesized derivatives targeted at conventional bacterial (66,112) and fungi (113), intended for clinical uses (114) (i.e. periodontitis). Testing of anionic, cationic and neutral zinc phthalocyanines against both Gram-positive and Gram-negative bacteria once again confirmed that the positively charged phthalocyanine had higher efficiency (115,116).

Correspondingly to other classes of photosensitizer, the recognition of the photosensitizer charge/Gram-class activity pattern has led to a substantial increase in the synthesis of (broad-spectrum) cationic derivatives.

Chapter II – Synthesis Of Phthalocyanine Derivates

2.1 GENERAL CONSIDERATIONS

Second-generation photosensitizers like phthalocyanines gained, in recent years, an enormous interest mainly due to their singlet oxygen generation capabilities, absorption in higher wavelengths (> 670 nm) and well recognized chemistry. However, phthalocyanine molecules have the tendency to aggregate, causing insolubility problems which dramatically affect their photochemical properties (117), by reducing lifetimes of the PS excited states, possibly due to conversion of electronic energy into vibrational motion, decreasing drastically molecular interaction with $^3O_2$ and the ability to absorb photons to activate the PS (118). The aggregation issues can be overcome through the use of adequate substituents in the peripheral positions of the macrocycle core (117,119). Derivatization of phthalocyanines can also adjust other properties (120), like their interaction with cells and tissues, leading to different photobiological effects (121).

It was mentioned in chapter I that Gram-positive and Gram-negative bacteria have different susceptibility to the photodynamic effect and that this constrains can be surpassed with cationic PSs (65,66). In that way, the initial working plan for this dissertation was the functionalization of the commercial available hexadecafluorophthalocyaninatozinc(II) (**$ZnPcF_{16}$**), with thio-pyridyl groups and further coupling to polylysine, followed by cationization (Scheme 2.1). Zinc phthalocyanine complexes have been studied as efficient drugs in microbial photodynamic inactivation (109,116). The introduction of zinc, a diamagnetic metal ion, provides useful properties in a photosensitizer, such as long triplet lifetime and a relatively high triplet quantum yield (26). Thiol-substituted phthalocyanine complexes are also known to absorb light at higher wavelengths (> 700 nm) and show interesting photochemical and spectroscopic properties compared to non-substituted analogs (122,123). Several studies have been shown that polylysine PS conjugates can be more effective against Gram-negative bacteria than the PS individually (124,125).

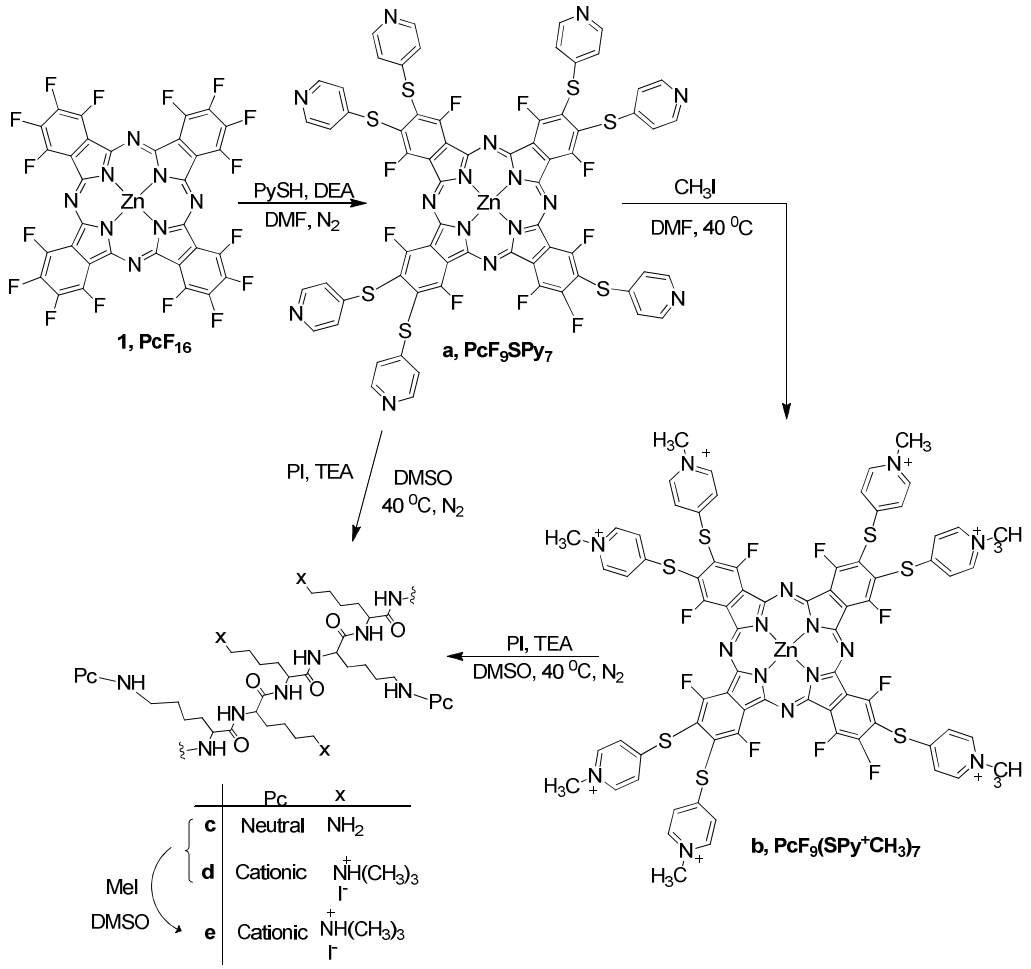

Scheme 2.1

Initially several coupling studies of **ZnPcF$_{16}$** with lysine and glycine methyl ester, have been attempted in order to determine the best conditions to be used in these coupling reactions. The direct use of poly lysine would be more expensive and difficult to follow the reactions, by TLC. The idea was to get optimized the reaction conditions before start using polylysine.

2.2 COUPLING CONDITIONS STUDIES

In a first attempt of coupling an amino acid to **ZnPcF$_{16}$**, we started with glycine methyl ester in 1:1, in DMF using NEt_3 as base, under nitrogen atmosphere at room temperature, hoping to synthesize **2** (Scheme 2.2). After stirring for two hours, the TLC revealed that the starting material didn't react. The temperature was increased to 50 °C

and the reaction mixture remained in these conditions for another 24 hours. However again, no evolution was observed and K_2CO_3 was added to the reaction. After another 24 hours, the reaction TLC was inconclusive, but we decided to finish the reaction. The solvent was evaporated and the product was analyzed through mass spectrometry. The mass spectrum result only showed the peak corresponding to **$ZnPcF_{16}$**.

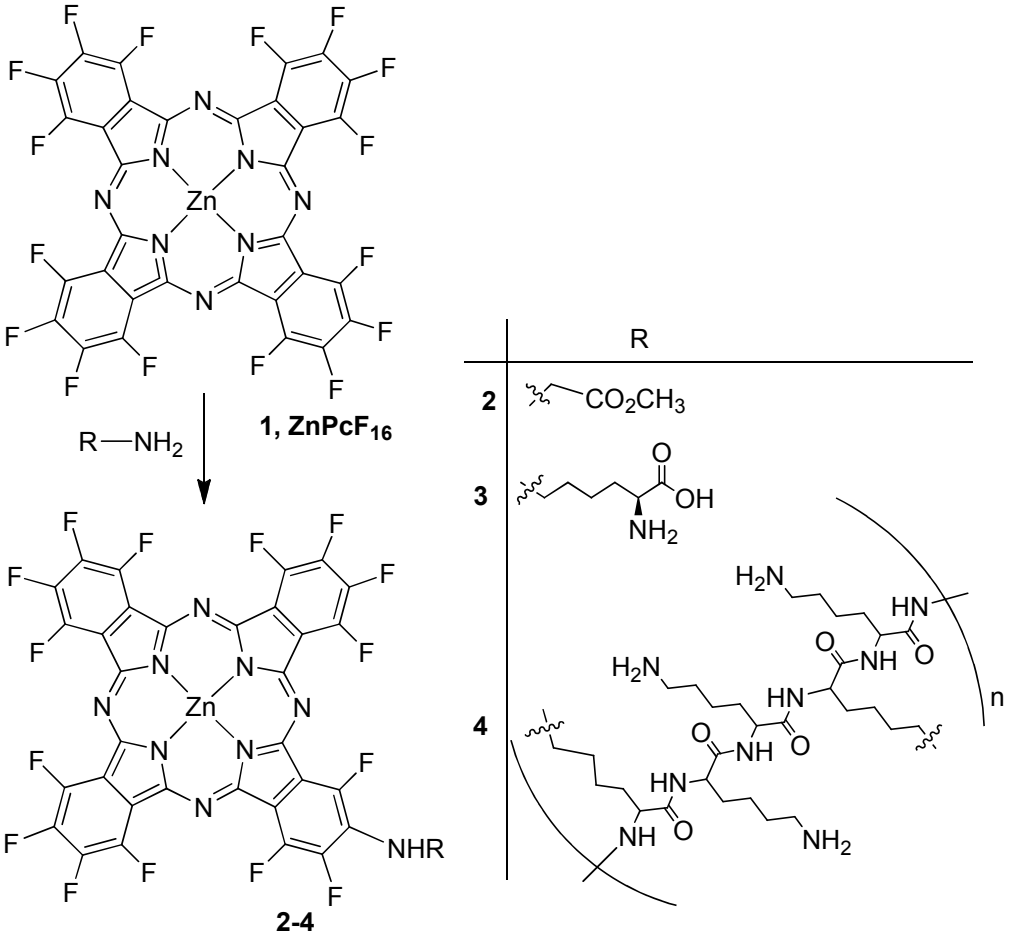

Scheme 2.2

Following the failed attempt to couple glycine methyl ester to **$ZnPcF_{16}$**, we tried the coupling reaction with the amino acid lysine (Scheme 2.2). Several approaches were made through classic and microwave assisted reactions, altering the several parameters, such as lysine equivalents, temperature, time, pressure, potency which could influence the reaction coupling and obtain compound **3**.The reaction conditions used in these classic and microwave synthesis are summarized in tables 2.1 and 2.2, respectively.

Table 2.1 - Classic synthesis conditions.

$ZnPcF_{16}$ (mg, mol)	Lysine eq.	Base	Solvent	T (°C)
10, 1.15×10^{-5}	1	NEt_3 (50 µl)	DMF	40
20, 2.31×10^{-6}	5	K_2CO_3 (15 mg)	DMF	40
25, 2.89×10^{-6}	1.1	NEt_3 (100 µl)	DMF	60
10, 1.15×10^{-5}	15	NEt_3 (100 µl)	NMP	60

Table 2.2 - Microwave synthesis conditions.

Lysine eq.	T (°C)	Time (min.)	Pressure	µλ (W)	Repetitions
4	70	20	200	60	3x
1.2	150	5	250	150	6x
4	120	20	200	250	5x

The purification of these reaction mixtures through column chromatography was very difficult, and several attempts had to be made. The isolated fractions were analyzed through ^{1}H NMR, ^{19}F NMR and mass spectrometry. Once again, the results indicated that the predominant fraction corresponded to **$ZnPcF_{16}$**, while the minor fractions were inconclusive.

The final coupling attempt was made using polylysine, in order to obtain the desired compound **4**. For that, to a DMF solution of polylysine was added NEt_3, however a complete dissolution of the polylysine did not occur. The mixture suffered ultrasound action and hot DMSO was added, but the complete dissolution was not achieved. Nevertheless, **$ZnPcF_{16}$** was added and the reaction mixture was kept stirring for 27 hours at 40 °C, under nitrogen atmosphere. After this time an insoluble material was obtained. In order to attempt their dissolution a methylation reaction was done, but the material/product remained insoluble and was discarded.

After all the unsuccessful attempts, the coupling reaction of **$ZnPcF_{16}$** to polylysine was set aside, and we moved to the preparation of the designed thio-pyridyl cationic phthalocyanines type **1a**. Thiols are efficient nucleophiles that usually allow nucleophilic substitution reactions in high yields. The cationization of the pyridyl groups will allow water solubility, affinity for Gram-negative bacteria and consequently we expected an efficient photoinactivation. Using the same strategy, **$ZnPcF_{16}$** reacted with different equivalents of 4-mercaptopyridine, knowing, however, that when used in ratios below 8 eq. a complex mixture, with several substitutions degrees in any of the eight beta-fluors of the **$ZnPcF_{16}$** periphery, would be obtained.

Later, a second approach involving cyclotetramerization of thiopyridyl-phthalonitriles generate two new pyridyl Pcs derivatives without fluorine atoms.

2.3 SYNTHESIS OF THIOPYRIDYL PHTHALOCYANINE DERIVATES – direct substitution

2.3.1 Reaction between $ZnPcF_{16}$ and mercaptopyridine

In this first synthesis, the commercial template **$ZnPcF_{16}$** reacted with 4 equivalents of 4-mercaptopyridine through direct nucleophilic substitution of 4 fluorine atoms. To do so, a DMF suspension of, **$ZnPcF_{16}$**, 4-mercaptopyridine (4 eq.) and NEt_3 were stirred at room temperature for 24 hours, under nitrogen atmosphere (Scheme 2.3). After this time a change in color to a darker blue was observed and the TLC showed the formation of a new product. Following solvent evaporation, the crude was subjected to column chromatography.

The major fraction obtained was characterized by ^{19}F and ^{1}H NMR. While ^{1}H NRM spectrum showed the resonance correspondingto the pyridyl groups on the new Pcs, the ^{19}F NMR confirmed the substitution of some fluorine atoms of the **$ZnPcF_{16}$**, proving the formation of several degrees of substitution. The presence of a mixture was also confirmed by mass spectrometry, but were not fully characterized.

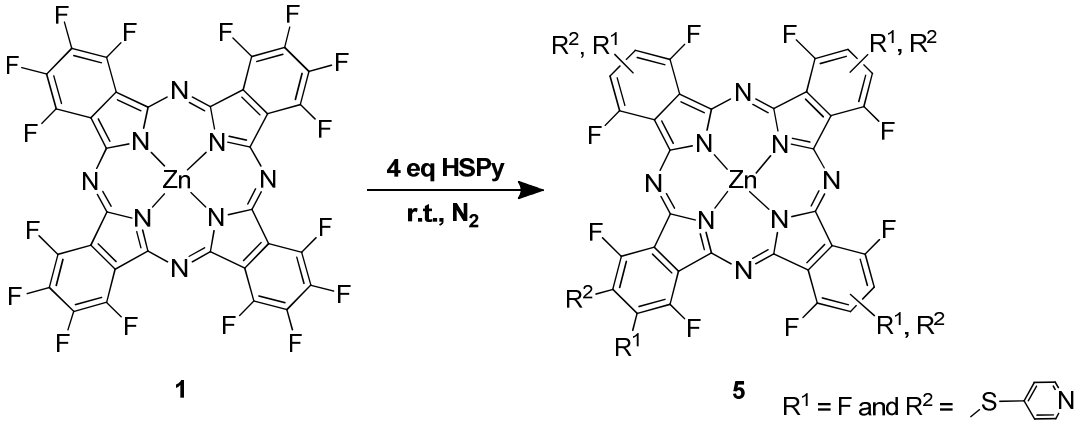

Scheme 2.3

2.3.2 Synthesis of Hepta-thiopyridylfluorophthalocyanine

Following the initial working plan, an attempt to synthesize a hepta-substituted phthalocyanine from **$ZnPcF_{16}$** was made. A mixture of the template and 4-mercaptopyridine (7 eq.) in DMF with DEA, remained overnight at room temperature under nitrogen atmosphere (Scheme 2.4). The reaction TLC indicated the formation of a new product.The crude reaction was submitted to column chromatography using H_2O/MeOH/Et_3N as eluent (5:2:2). ^{1}H and ^{19}F NMR showed that we get the octasubstituted compound, instead of the expected heptasubstituted one.

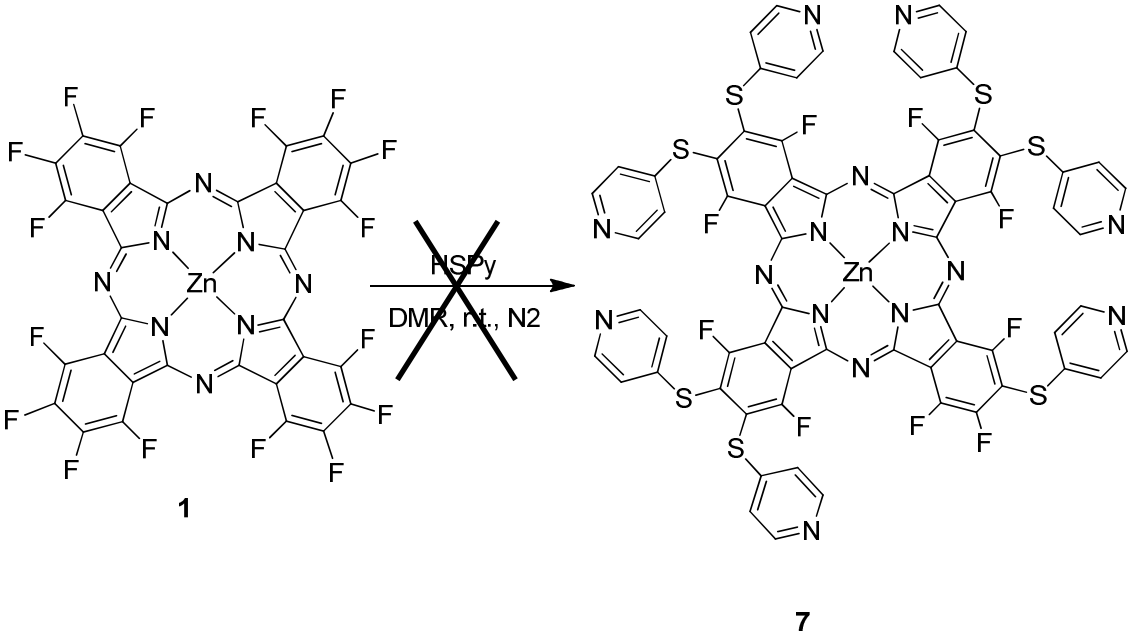

Scheme 2.4

2.3.3 Synthesis of Pc 8

Although the synthesis of the former tetra-substituted Pc, by direct substitution of a template, led to isomers formation, synthesis of an octa-substituted compound through the same methodology would be simpler and clear. The attempt to synthesize an hepta-substituted Pc also led to the conclusion that there is a preferential formation of a symmetric compound, with substitution of all beta fluorine atoms. So, $ZnPcF_8(SPy)_8$ (**8**) was obtained by derivatization of **$ZnPcF_{16}$** with 4-mercaptopyridine (8 eq.) in DMF and DEA (Scheme 2.5). The simple reaction was conducted at room temperature, under nitrogen atmosphere, for 24 hours. Subsequently, the solvent was evaporated under vacuum and compound **8** (89% yield) was washed with acetone. ^{1}H and ^{19}F NMR spectra confirmed the nucleophilic substitution of the **8** beta fluorine atoms.

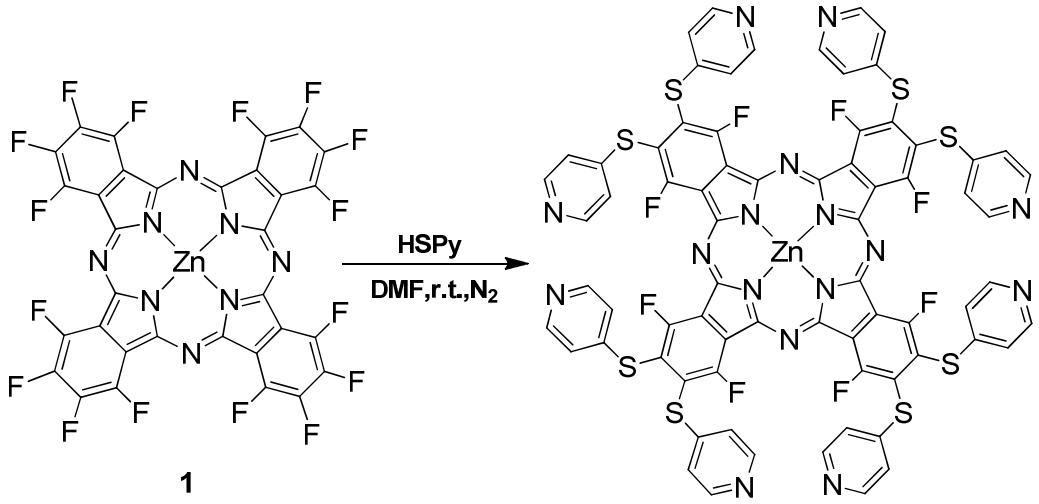

Scheme 2.5

^{1}H NMR spectrum (Fig. 2.1) specifies two singlets corresponding to the resonances of the 32 *orto*- and *meta*-proton atoms of the peripheral pyridyl groups at δ 7.28 and 8.19 ppm, respectively. ^{19}F NMR spectrum (Fig. 2.2) displays the fluorine resonances as two singlets at δ -126.7 and -127.2 ppm, agreeing with the 8 alpha fluorine Pc atoms.

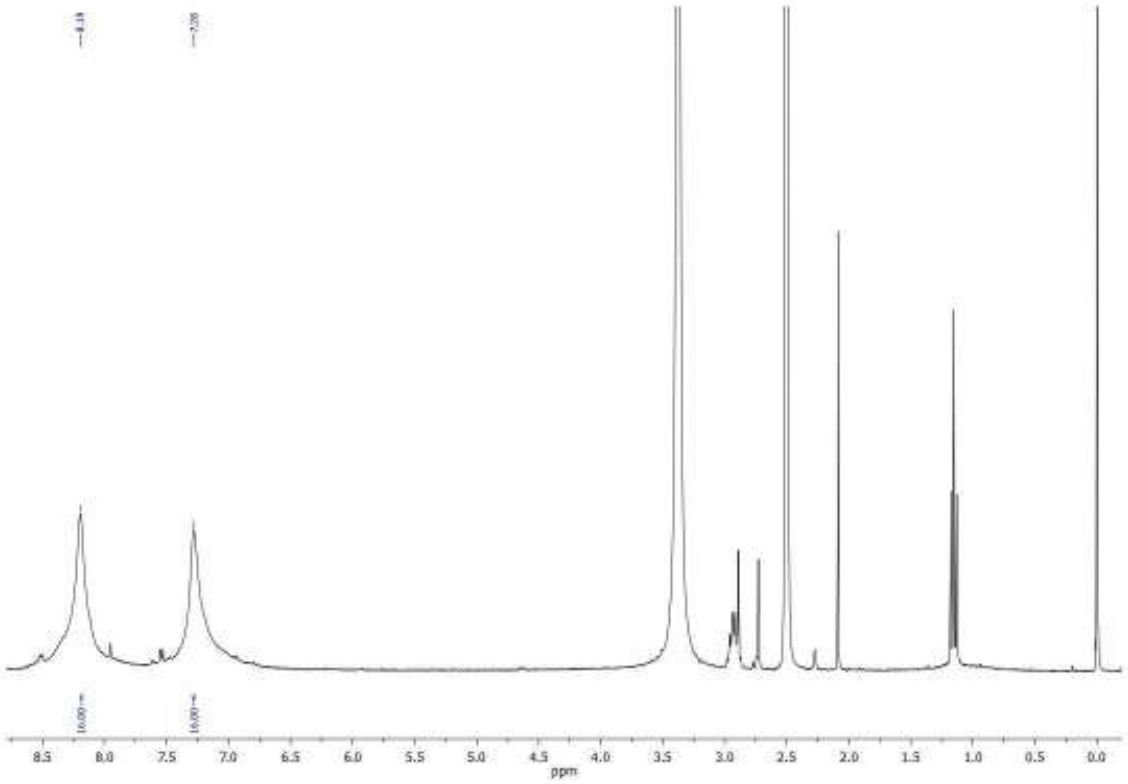

Figure 2.1 - ^{1}H-NMR spectrum of Pc **8**.

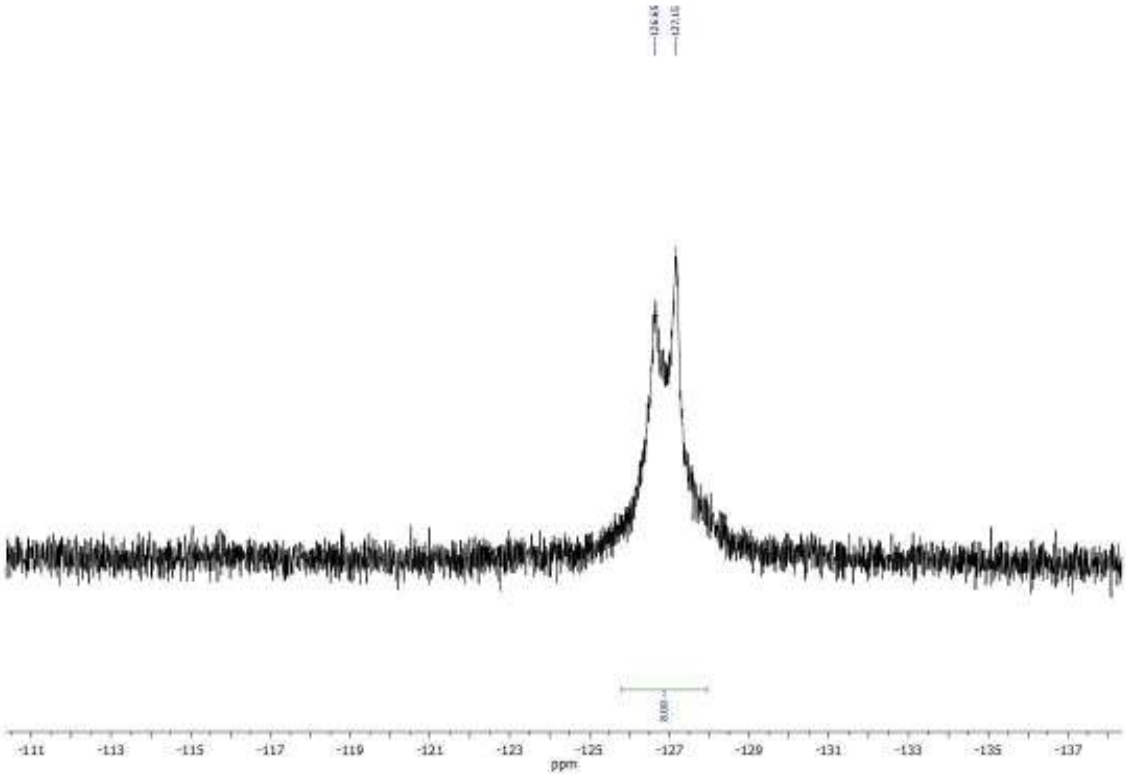

Figure 5 – ^{19}F-NMR spectrum of Pc **8**.

2.4 SYNTHESIS OF THIOPYRIDIL-PHTHALONITRILES

2.4.1 Derivatization of 3,4,5,6-tetrafluorophthalonitrile

Although the derivatization of the commercial **$ZnPcF_{16}$** proved to be relatively easy and fast, clear tetra-substituted compounds/mixtures are not easy to obtain. Cyclotetramerization of derivatized phthalonitriles, offers a more controlled phthalocyanine synthesis, so to pursue this option it was used the commercial 3,4,5,6-tetrafluorophthalonitrile, prospecting a single substitution of one of the 4 available fluorine atoms, with 4-mercaptopyridine (Scheme 2.6).

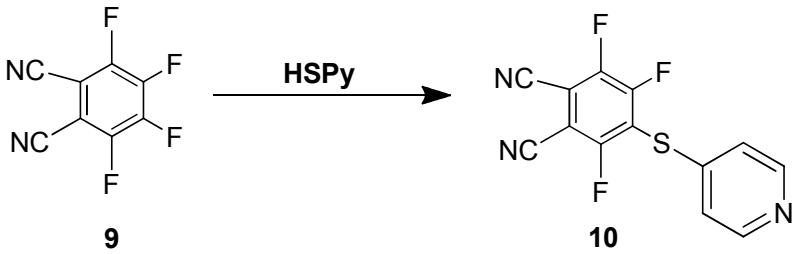

9 **10**

Scheme 2.6

The several efforts to obtain the mono-substitution of 3,4,5,6-tetrafluorophthalonitrile by mercaptopyridine are resumed in table 2.3.. Different procedures were employed to optimize the reaction, however without success. In all reaction a preferential di-substitution of the phthalonitrile was verified, possibly due to the high reactivity of fluorine atoms. It was also observed that the few mono-substituted phthalonitrile obtained, degraded readily.

Table 2.3 - Conditions used for the mono-substitution of 3,4,5,6-tetrafluorophthalonitrile.

HSPy Eq.	Base	Solvent (2 ml)	T (°C)	Observations
2	K_2CO_3	DMF	60	
0.9	K_2CO_3	DMF	r.t.	

0.9	K_2CO_3	Toluene	r.t.	
0.9	K_2CO_3	DEA	r.t.	
1	K_2CO_3	DMF	0	HSPy added in 2 portions
1	NEt_3	DMF	0	HSPy added dropwise
1	K_2CO_3	DMF	-80	HSPy added to frozen DMF, melting gradually

2.4.2 Reaction of 4-nitrophthalonitrile with 4-mercaptopyridine

The mono substitution of 3,4,5,6-tetrafluorophthalonitrile revealed to be fruitless, still the objective of obtaining a tetra-substituted phthalocyanine from a phthalonitrile remained. Attending this purpose, 4-nitrophthalonitrile is a preferential option as precursor of other phthalonitriles. In this direction, compound **12** was prepared by the addition of 4-mercaptopyridine to 4-nitrophthalonitrile (1:1), (Scheme 2.7). After the addition of dry K_2CO_3 the mixture was heated at 50 °C for 5 h. TLC showed formation of a new product so an extraction with water and ethyl acetate was made and compound **12** was purified by recrystallization with dichloromethane in 70% yield.

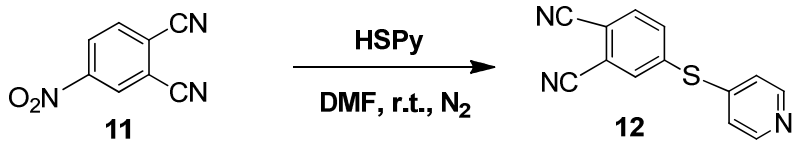

Scheme 2.7

^{1}H NMR spectrum (Fig. 2.3) indicates, the pyridyl *orto*- and *meta*-protons as two double doublets, positioned at δ 7.35 and 8.54 ppm, respectively. This is due to their difference of shield influenced by the sulphur atoms. The three remaining protons distributed on the two aromatic rings are localized at δ 7.91, 8.15 and 8.28 ppm. ^{13}C NMR spectrum (Fig. 2.4) displays the 8 asymmetric carbon atoms of the phthalonitrile ring and 5 carbon atoms as three signals due to the symmetry of the pyridyl moiety.

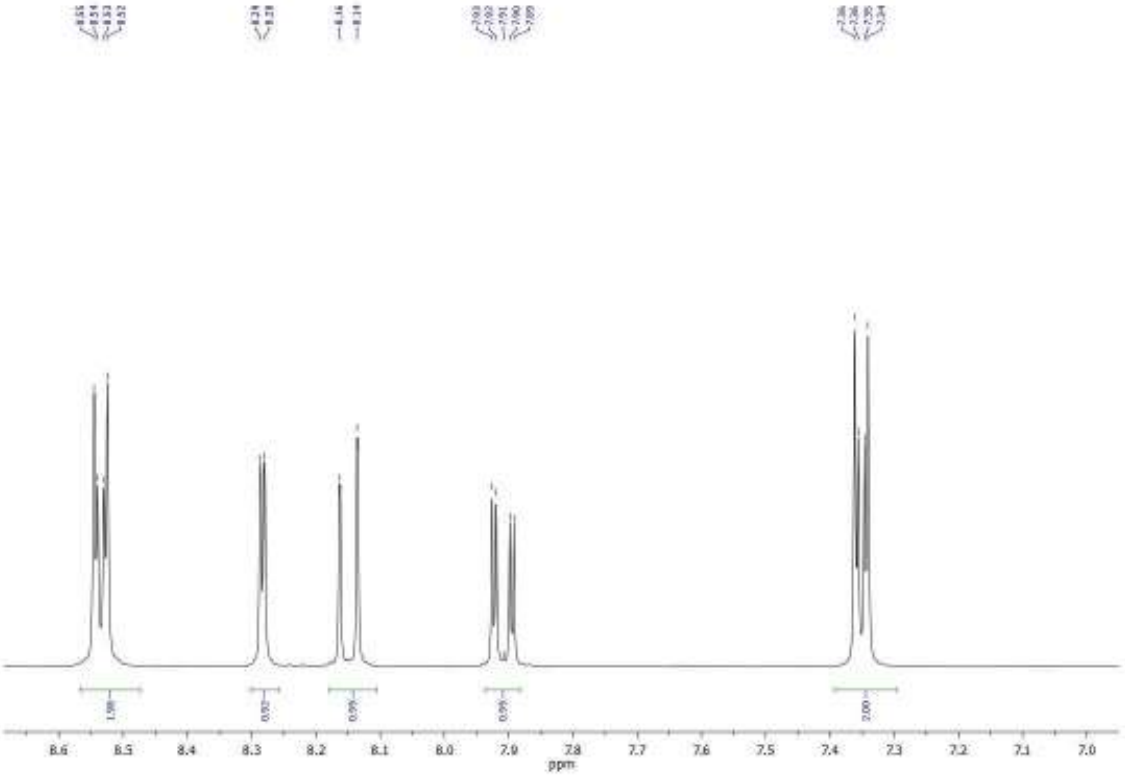

Figure 2.3 - ^{1}H-NMR spectrum of compound **12**.

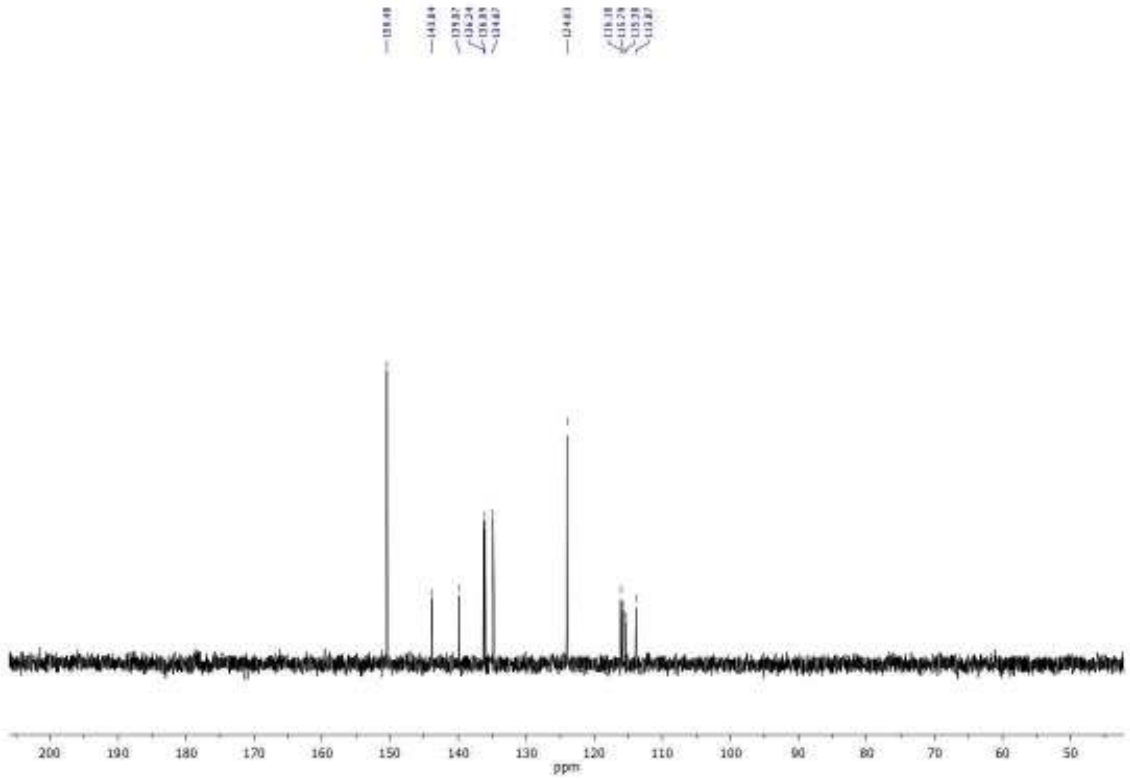

Figure 2.4 - ^{13}C-NMR spectrum of compound **12**.

2.4.3 Reaction of 4,5-dichlorophthalonitrile with 4-mercaptopyridine

Although an octa-substituted Pc **8** was formerly synthesized, it would be interesting to synthesize a different one, however similar. For that, phthalonitrile **14** was prepared by reacting 4,5-dichlorophthalonitrile with 4-mercaptopyridine in presence of K_2CO_3 (Scheme 2.8). Two hours later the reaction was complete and distilled water was added to precipitate the formed produts. The crude was filtered and submitted to column chromatography. The main fraction was recrystallized from CH_2Cl_2, yielding **14** in 50%.

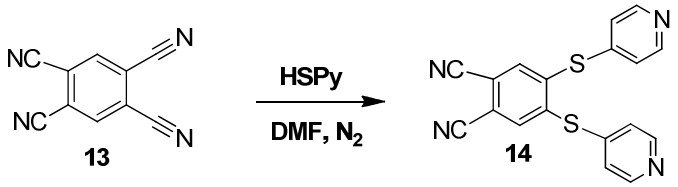

Scheme 2.8

^{1}H NMR spectrum (Fig. 2.5) of **14** show two double doublets at δ 7.25 and 8.67 ppm, referring to the pyridyl *orto*- and *meta*-protons, and one singlet at δ 7.57 ppm, related to the phthalonitrile protons. Due to the symmetric structure of the molecule, ^{13}C spectrum (Fig. 2.6) reveals 7 signals, each one corresponding to 2 carbon atoms, from a total of 14 carbon atoms.

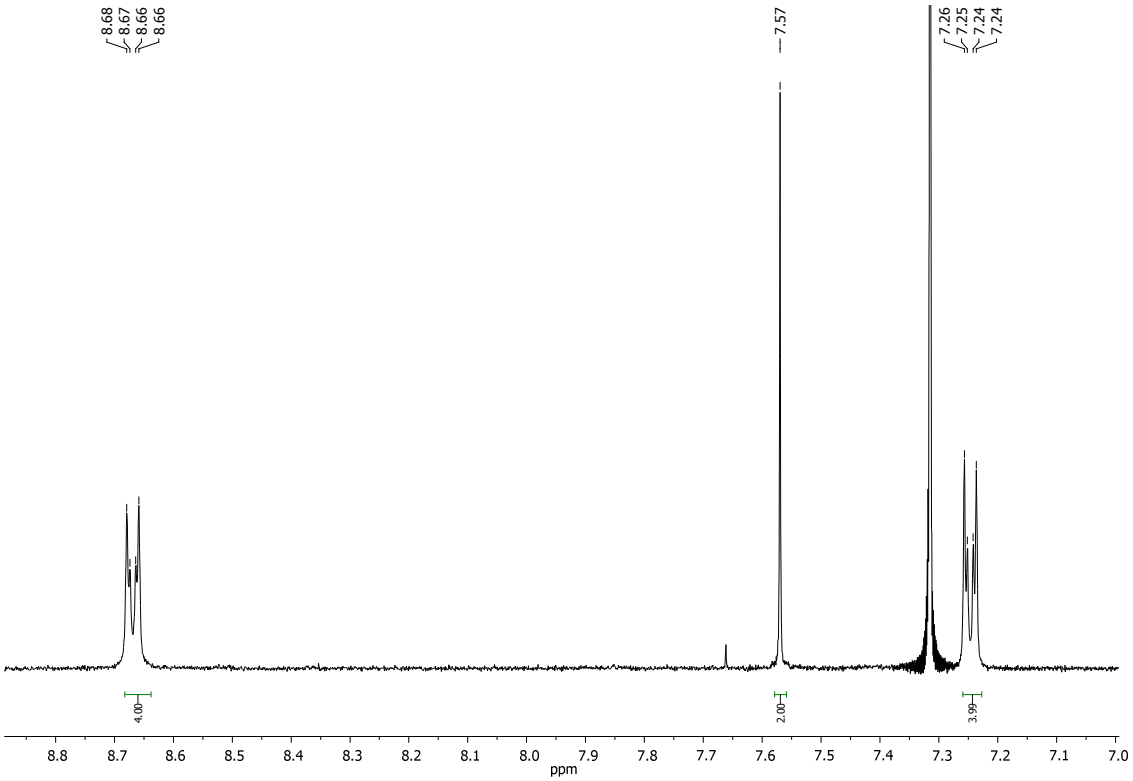

Figure 6 - ^{1}H-NMR spectrum of compound **14**.

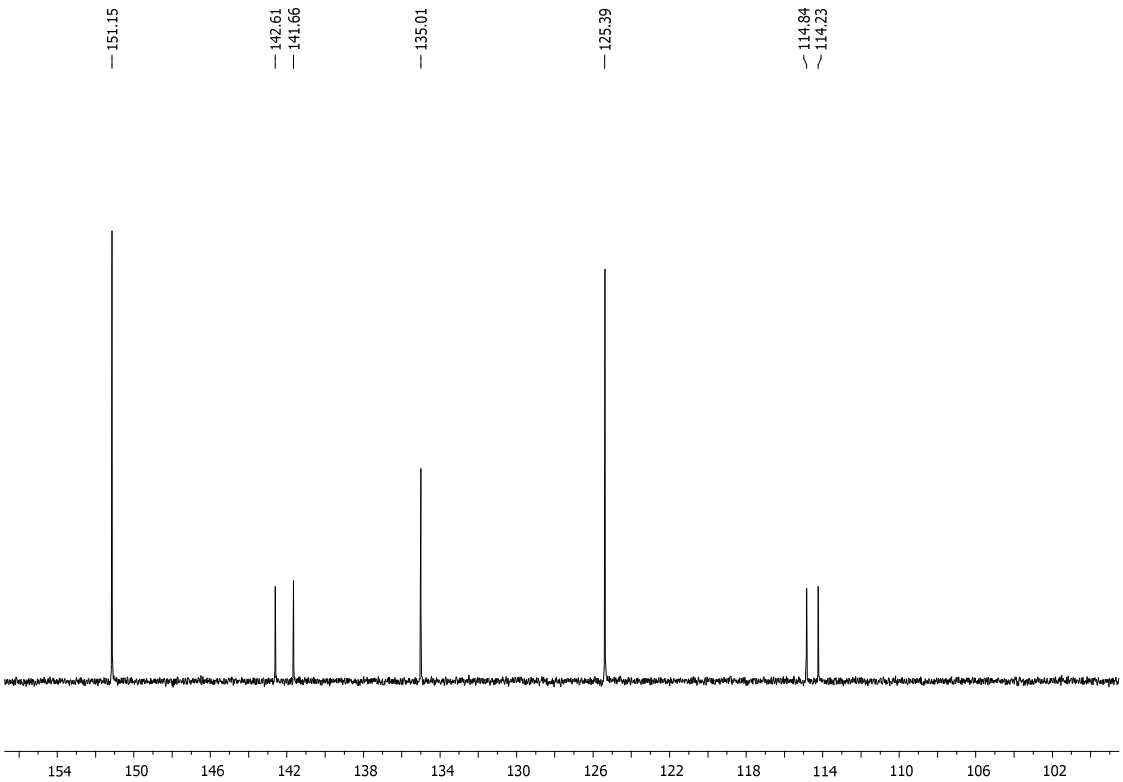

Figure 7 - ^{13}C-NMR spectrum of compound **14**.

2.5 SYNTHESIS OF THIOPYRIDIL PHTHALOCYANINE DERIVATIVES – cyclotetramerization of phthalonitrile precursors

2.5.1 Synthesis of 2,9(10),16(17),23(24)-tetrakis(4-pyridylsulfanyl)phthalocyaninatozinc (II)

Following the synthesis of the precursor, Pc **15** was synthesized by cyclotetramerization of four equivalents of phthalonitrile **12** with anhydrous zinc chloride. The reaction was conducted in DMAE for 15 hour under reflux (140 °C, Scheme 2.9). Following precipitation with MeOH/H_2O, the reaction crude was filtered and washed with MeOH to remove the remaining $ZnCl_2$. Metallophthalocyanine **15** was obtained in 82% yield.

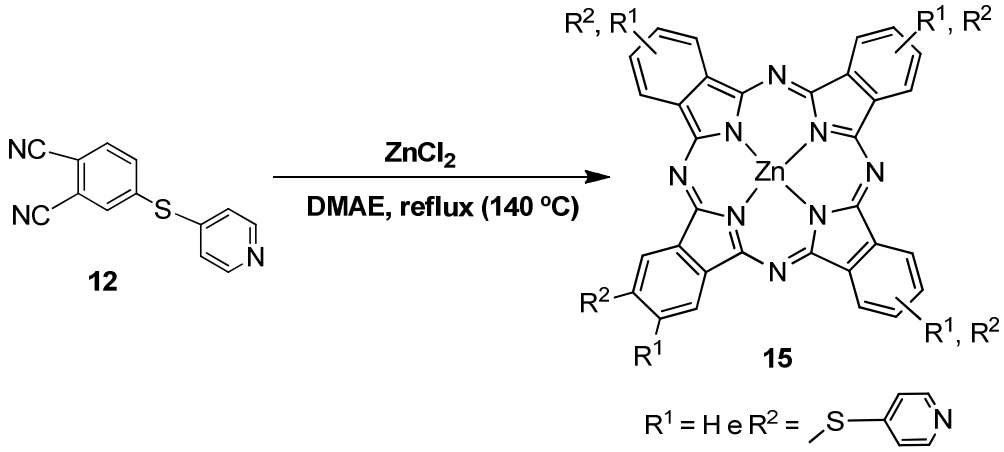

Scheme 2.9

^{1}H NMR spectrum (Fig. 2.7) show two multiplets between δ 8.90-9.45 and 8.29-8.45 ppm corresponding, respectively, to the 8 symmetrical α-proton atoms and four β-protons of the macrocycle . The *ortho*- and *meta*-protons corresponding to the mercaptopyridyl moieties appear also as multiplets at δ 7.79-7.92 and 8.65-8.70 ppm, respectively. MALDI-TOF-MS spectrum also confirmed the proposed structure of **15** showing the molecular ion peak *m/z* 1013.07 $[M+H]^+$.

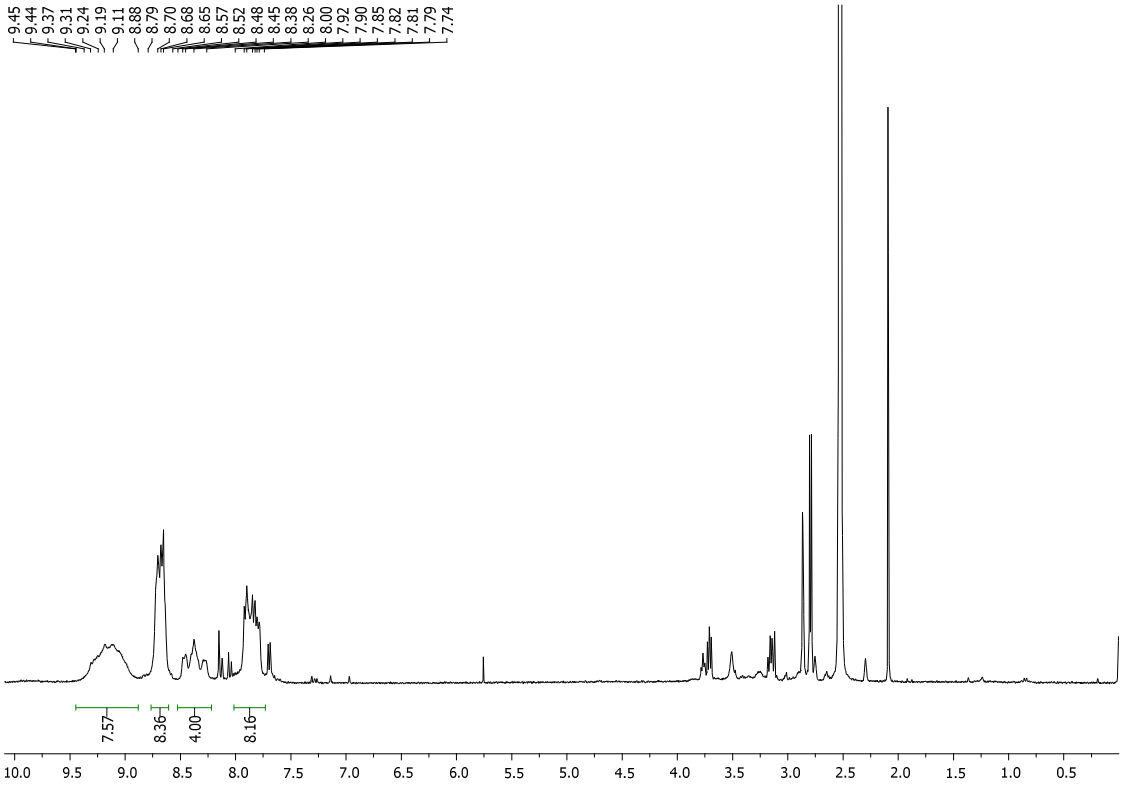

Figure 2.7 - ^{1}H-NMR spectrum of compound 15.

2.5.2 Synthesis of 2,3,9,10,16,17,23,24-Octakis(4-pyridylsulfanyl)phthalocyaninatozinc(II)

The synthesis and purification of Pc **16**, was similar to the one of Pc **15**, except the precursor employed, that was the phthalonitrile **14** instead of **12** (Scheme 2.10).

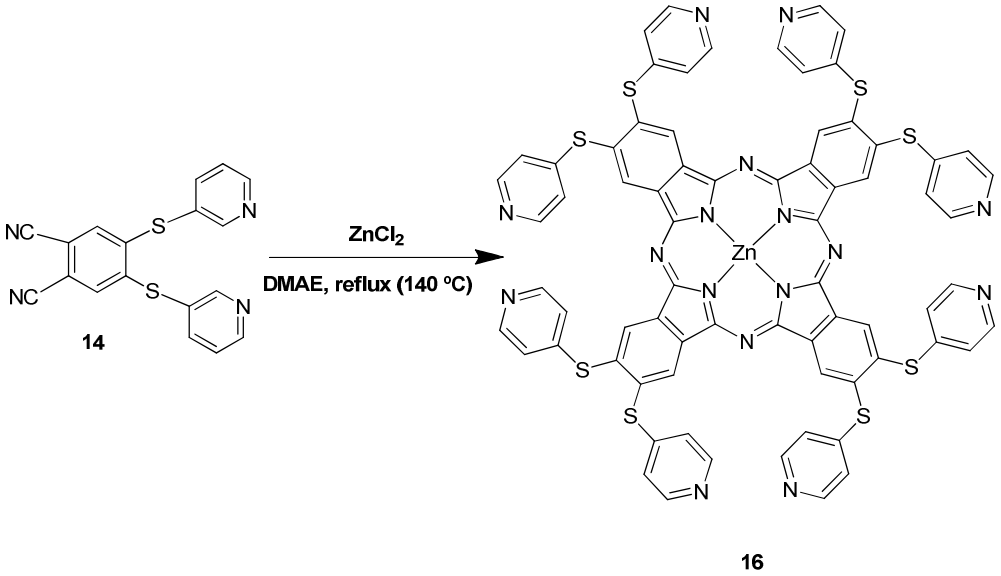

Scheme 2.10

From ^{1}H NMR spectrum (Fig. 2.8) it can be perceived the resonance of the 16 *orto*- and 16 *meta*-proton atoms of the mercaptopyridines, as duplets, respectively at δ 8.03 and 8.71 ppm. The signal of the 8 α-proton atoms can be perceived as a singlet at δ 10.15 ppm. Through MALDI-TOF-MS a molecular ion peak at *m/z* 1448.07 $[M+H]^{+}$ was obtained confirming once again the expected metallophthalocyanine.

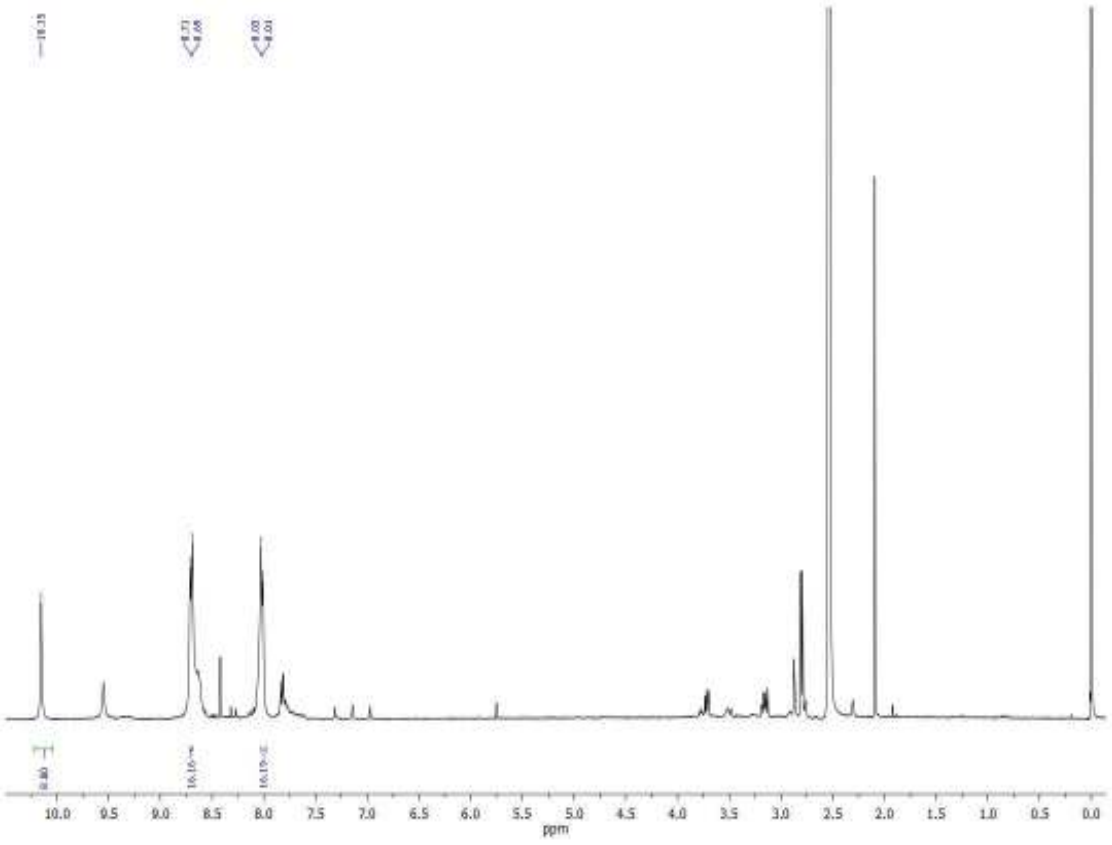

Figure 2.8 - ^{1}H-NMR spectrum of compound **16**.

2.6 METHYLATION OF METALLOPHTHALOCYANINES 8, 15 and 16

The final step of the photosensitizer synthesis was the cationization of the neutral compounds. In this process a stirred DMF solution (or suspension) of metallophthalocyanines **8**, **15** and **16** with a large excess of methyl iodide (CH_3I), reacted overnight in a sealed tube at 40 °C (Scheme 2.11). Following reaction completion, the crude was precipitated with diethyl ether, filtered and washed several times with diethyl ether. After dissolution in acetone/H_2O (1:1), the desired compounds were reprecipitated with acetone. Compounds **17**, **18** and **19** were dried under reduced pressure and obtained in quantitative yields.

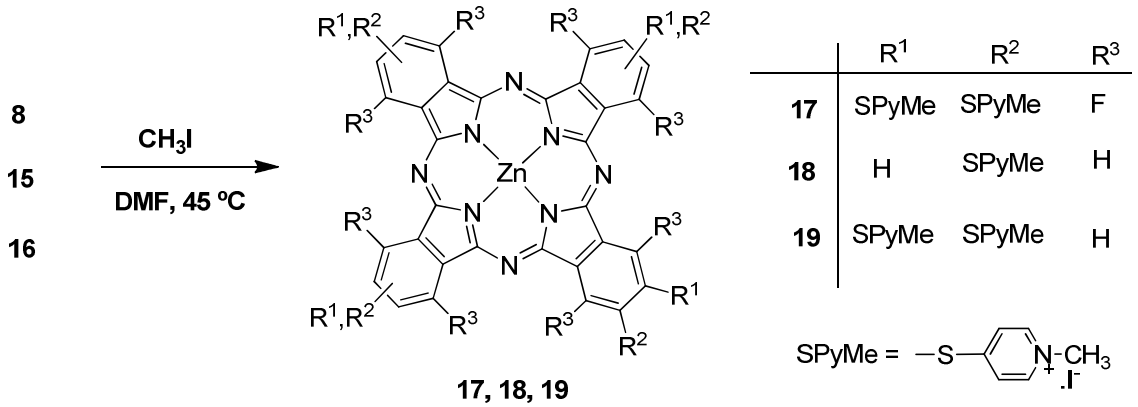

	R^1	R^2	R^3
17	SPyMe	SPyMe	F
18	H	SPyMe	H
19	SPyMe	SPyMe	H

Scheme 2.11

^{1}H NMR spectra of these cationic Pcs were similar to the neutral ones with the exception of a new signal generated by resonance of the new three methyl groups, characterized as a singlet at δ 4.2 ppm for All three compounds were also confirmed by MS MALDI-TOF, showing *m/z* of 1608.9, 1027.1 and 1463.0 corresponding to [**17**-7CH_3]$^+$, [**18**-3CH_3]$^+$and [**19**-7CH_3]$^+$ peaks, respectively.

2.7 EXPERIMENTAL PROCEDURES

Reagents, solvents and equipment:

- ^{1}H, ^{13}C, and ^{19}F NMR spectra were analysed on a Bruker Avance-300 spectrometer at 300.13, 75.47 and 282.38 MHz, respectively.
- $CDCl_3$ and DMSO-d_6 were used as solvents and TMS as internal reference; the chemical shifts are expressed in δ (ppm) and the coupling constants (*J*) in Hertz (Hz).
- Mass spectra were recorded on a MALDI-TOF/TOF 4800 Applied Biosystems.
- UV–Vis spectra were obtained on a Shimadzu UV-2501PC spectrophotometer.
- Column chromatography was carried out using silica gel (Merck, 35-70 mesh).
- All chemicals were supplied by Sigma–Aldrich. Solvents were purified or dried according to the literature procedures (126).

PC 8: DEA (5.0 mL) was added to a DMF (50 mL) solution of **$ZnPcF_{16}$** (200 mg, 0.23 mmol) and

4-mercaptopyridine (205 mg, 1.85 mmol) and the reaction mixture was kept under stirring at room temperature for 24 h under N_2 atmosphere. After this period, the DMF was evaporated under vacuum and the resulting product was washed with acetone. The desired derivative **8** was obtained in 89% (328 mg) yield after crystallization from water/acetone. mp: > 300 °C. ^{1}H NMR (DMSO-d_6): δ 7.28 (br s, 16H, Py-*o*-H), 8.19 (br s, 16H, Py-*m*-H). ^{19}F NMR (DMSO-d_6): δ -126.7 and -127.2 (2s, 8F, Pc-α-F). UV-vis (DMSO) λ_{max} (log ε): 384 (4.82), 690 (5.04), 720 (5.09) nm. HRMS (MALDI-TOF) *m/z*: calcd for $C_{72}H_{33}F_8N_{16}S_8Zn$ 1592.9998 ($[M+H]^+$), found 1592.9927.

4-Thiopyridylphthalonitrile (12): A DMF (5 mL) solution of 4-nitrophthalonitrile (1.00 g, 5.78 mmol) and 4-mercaptopyridine (1.62 g, 1.44 mmol) was stirred at room temperature under a nitrogen atmosphere for 10 min. Dry potassium carbonate (214 mg, 1.5 mmol) was added and the mixture was heated at 50 °C for 5 h. The residue was ressuspended in water (80 mL) and extracted with ethyl acetate (three portions of 50 mL). The fraction containing the 4-thiopyridylphthalonitrile **12** was purified by recrystallization from dichloromethane, yielding 0.96 g (70%). mp: 146-148 °C. ^{1}H NMR ($CDCl_3$): δ 7.35 (dd, *J* = 1.6 and 4.5, 2H, Py-*o*-H), 7.91 (dd, *J* = 1.8 and 8.2, 1H, H-5), 8.15 (d, *J* = 8.2, 1H, H-6), 8.28 (d, *J* = 1.8, 1H, H-3), 8.54 (dd, *J* = 1.6 and 4.5, 2H, Py-*m*-H). ^{13}C NMR ($CDCl_3$): δ 113.9, 115.4, 115.8, 116.1, 124.0, 134.9, 136.1, 136.2, 139.9, 143.8, 150.5.

4,5-Dithiopyridylphthalonitrile (14)*:* Dry potassium carbonate (0.5 g, 3.6 mmol) was added to a solution of 4-mercaptopyridine (0.677 g, 6.09 mmol) and 4,5-dichlorophthalonitrile (0.5 g, 2.5 mmol) in DMF (3 mL) in an ice bath and under a nitrogen atmosphere. The reaction was left at room temperature and more 9 portions of dry potassium carbonate (50 mg each portion) were sequentially added every 10 min. After the last addition, the reaction was kept under stirring for 2 h more. Distilled water was added and the precipitate formed was filtered and purified by chromatography over a silica gel column using a mixture of CH_2Cl_2/MeOH (9:1) as eluent. The resulting product was recrystallized from CH_2Cl_2, yielding 0.60 g of **14** (50%). mp: 238-240 °C. ^{1}H NMR ($CDCl_3$): δ 7.25 (dd, *J* = 1.5 and 4.5, 4H, Py-*o*-H), 7.57 (s, 2H, H-3,6), 8.67 (dd, *J* = 1.5 and 4.5, 4H, Py-*m*-H). ^{13}C NMR ($CDCl_3$): δ 114.2, 114.8, 125.4, 135.0, 141.7, 142.6, 151.2. MS

(ESI-TOF) *m/z*: 347 $[M+H]^+$.

2,9(10),16(17),23(24)tetrakis(*4-pyridylsulfanyl*)phthalocyaninatozinc(II) (15): A mixture of phthalonitrile **12** (400 mg, 1.69 mmol) and zinc acetate (276 mg, 2.02 mmol) in dimethylaminoethanol (DMAE, 1.5 mL) were placed under reflux (140 °C) for 15 h. After cooling to room temperature, the reaction mixture was washed with MeOH/H_2O (9:1) and the residue was filtered and washed with methanol. Metallophthalocyanine **15** was obtained in 82% yield (351 mg) after vacuum drying. mp: > 300 °C. ^{1}H NMR (DMSO-d_6 + TFA): δ 7.79-7.92 (m, 8H, Py-*o*-H), 8.29-8.45 (m, 4H, Pc-β-H), 8.65-8.70 (m, 8H, Py-*m*-H), 8.90-9.45 (m, 8H, Pc-α-H). UV-vis (DMSO) λ_{max} (log ε): 347 (4.98), 617 (4.55), 684 (5.37) nm. MS (MALDI-TOF) *m/z*: 1013.07 $[M+H]^+$.

2,3,9,10,16,17,23,24- Octakis(*4-pyridylsulfanyl*)phthalocyaninatozinc(II) (16)*:* A mixture of phthalonitrile **14** (285 mg, 0.82 mmol) and zinc acetate (138 mg, 1.01 mmol) in DMAE (1 mL) were placed under reflux (140 °C) for 15 h. After cooling to room temperature, the reaction mixture was washed with MeOH/H_2O (9:1) and the residue was filtered and washed with methanol. The product **16** was dried under vacuum, yielding 254 mg (85%). mp: > 300 °C. ^{1}H NMR (DMSO-d_6 + TFA): δ 8.02 (d, *J* = 6.0, 16H, Py-*o*-H), 8.70 (d, *J* = 6.0, 16H, Py-*m*-H), 10.15 (s, 8H, Pc-α-H). UV-vis (DMSO-d_6) λ_{max} (log ε): 371 (4.59), 632 (4.47), 663 (4.68), 702 (5.03) nm. HRMS (MALDI-TOF) *m/z*: calcd for $C_{72}H_{40}N_{16}S_8Zn$ ($[M]^{+\cdot}$) 1448.0673, found 1448.0643.

Methylation of metallophthalocyanines 8, 15, 16: A large excess of methyl iodide (4 mL) was added to a stirred solution (or suspension) of metallophthalocyanines **8**, **15** or **16** (100 mg) in dry DMF (20 mL). The reaction mixture was heated at 40 °C overnight in a sealed tube. After complete reaction, the cationic phthalocyanines were precipitated with diethyl ether, filtered and washed several times with diethyl ether. The solid was dissolved in acetone/H_2O (1:1) and reprecipitated with acetone. The products were dried under reduced pressure and obtained in quantitative yields.

(17) - mp > 300 °C. ^{1}H NMR (DMSO-d_6): δ 4.22 (s, 24H, CH_3), 8.25 (d, *J* = 7.0, 16H, Py-*o*-H), 8.77 (d, *J* = 7.0, 16H, Py-*m*-H). ^{19}F NMR (DMSO-d_6): δ -127.24 (s, 8F, Pc-α-F). UV-vis (DMSO) λ_{max} (log ε): 407 (4.46), 647 (4.29), 722 (4.84) nm. MS (MALDI-TOF) *m/z*: 1608.9 $[M\text{-}7CH_3]^+$.

(18)- mp > 300 °C. ^{1}H NMR (DMSO-d_6): δ 4.21 (4s, 12H, CH_3), 7.87-7.99 (m, 8H, Py-*o*-H), 8.35-8.51 (m, 4H, Pc-β-H), 8.67-8.74 (m, 8H, Py-*m*-H), 9.30 (br s, 8H, Pc-α-H). UV-vis (DMSO): λ_{max} (log ε): 352 (4.60), 616 (4.39), 685 (5.20) nm. MS (MALDI-TOF) *m/z*: 1027.10 $[M\text{-}3CH_3]^+$.

(19) - mp > 300 °C. ^{1}H NMR (DMSO-d_6): δ 4.23 (s, 24H, CH_3), 8.10 (d, *J* = 7.1, 16H, Py-*o*-H), 8.72 (d, *J* = 7.1, 16H, Py-*m*-H), 10.15 (s, 8H, Pc-α-H). ^{13}C NMR (DMSO-d_6): δ 46.9, 122.9, 133.1, 133.5, 141.2, 144.5, 153.4, 160.8. UV-vis (DMSO) λ_{max} (log ε): 383 (4.55), 630 (4.38), 702 (5.03) nm. MS (MALDI-TOF) *m/z*: 1463.0 $[M\text{-}7CH_3]^+$.

Chapter III

Photodynamic Studies

3.1 GENERAL CONSIDERATIONS

PDT is already considered an important and very promising alternative to control microbial infections. As stated in chapter I, Gram-positive bacteria are efficiently photoinactivated by a wide range of photosensitizers, however Gram-negative bacteria presents resistance to negatively charged or neutral PSs, at least without addition of chemical or biological agents to increase artificially membrane permeability (64). On the other hand, cationic photosensitizers have proved to photoinduce direct inactivation of Gram-negative bacteria, even devoid of the presence of additives (65,66). This is due to the tight electrostatic interaction with negatively charged sites at the outer surface of bacteria cells, promoted by the positive charge of the photosensitizer (68). Cationic zinc phthalocyanines have been studied as efficient drugs in microbial photodynamic inactivation (109,116)

To achieve an efficient sterilizing effect regarding the treatment of microbial infections, it should be obtained a reduction in the number of pathogenic cells comparable to at least 4-5 logs (127). This process (Figure 3.1) can be summarized in three steps (128):

i) Incubation – In this first step occurs the binding between the positively charge moieties of the PS and the negatively charged groups at the surface of microbial cells. The period of time required for electrostatic interaction to happen, can vary between 1 minute to at least 30 minutes, depending on the microorganism. This step is the main prerequisite for photoinactivation. The objective is to achieve endocellular photosensitizer concentrations which can be photochemically active. In bacteria, the uptake of the PS in the cell strongly depends on its physiological state, being higher in the exponential growth phase than in the lag phase (128).

ii) Primary targets of the photosensitized process - The initial and most frequent target by phthalocyanine derivatives in microbial cell inactivation appears to be represented by the cytoplasmic membrane. This conclusion is supported by several findings such as inactivation by irradiation in the presence of positively charged Pcs, of enzymes associated with the cytoplasmic membrane of bacterial cells (NADH, succinic and lactic dehydrogenase), at a rate faster that observed for the photoinduced cell death.

Also, loss of membrane barrier properties of bacterial cells induced by photosensitization process, led to collapse of K^+ and ionic balance (128).

iii) Later stages of photosensitization process - Although photosensitizer uptake into cells is an important factor, subcellular localization may play a major role in photodynamic efficiency (115). Following incubation in the dark, the PS is initially positioned in the cytoplasmic membrane, the primary site of attack by the photogenerated reactive oxygen species. Following alteration of membrane permeability, and as the irradiation progresses, there is a gradual diffusion of the PS to inner cellular areas. So, it could be legitimate to suppose that several non-membranous sites, including DNA, are involved in photooxidative reactions at later stages of the global photoprocess (128).

Globally, this photoinactivation process is of multi-target nature, making development of protection strategies extremely difficult for microbial cells, avoiding treatment resistance. This is one major advantageous characteristic of PDT. This process is not completely understood, so more in-depth studies are necessary to shed a light on this issue (128).

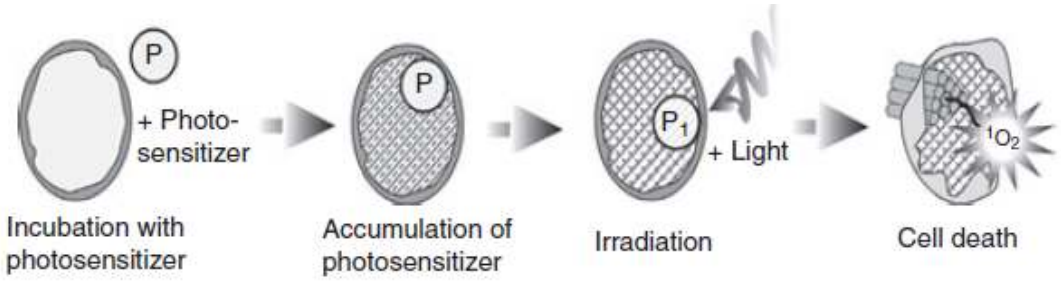

Figure 3.1 – Photosensitization process in cell: P. photosensitizer; P_1, excited state of P after light absorption; $^1O_2$, reactive singlet oxygen. (Luksiene and Zukauskas, 2009)

Besides PS interaction with the cell, it should be taken in consideration that efficient PS activation by light also affects the photoinactivation process outcome. The wavelength of light necessary for induction of lethal reactions in cells depends on the structure an electron absorption spectrum of the PS. The higher overlap of the Q-bands

with the emission spectrum of light, more efficient PS excitation. Wavelength also determines the penetration depth of light into tissue: 400-500 nm relates to a penetration of 300-400 μm (surface treatment), while 600-700 nm penetrates about 50-200% profounder (deeper treatment) (129).

E. coli caused numerous diseases outbreaks and deaths associated with contaminated food and water (130). In this study, the photoinactivation efficiency of three cationic phthalocyanine derivatives was evaluated, in real time, using a bioluminescent *E. coli* strain as a model of Gram-negative pathogenic bacteria.

3.2 EXPERIMENTAL PROCEDURES

3.2.1 Photosensitizers

All photodynamic related studies were carried out using three cationic phthalocyanines, whose syntheses were described in chapter II: Pc **17**, **18** and **19** (Fig. 3.2). A stock solution for each compound was prepared at a concentration of 500 μM in DMSO.

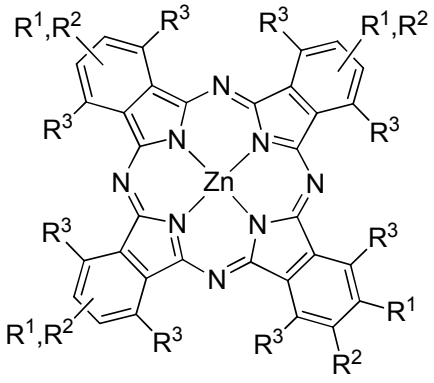

	R^1	R^2	R^3
17	SPyMe	SPyMe	F
18	H	SPyMe	H
19	SPyMe	SPyMe	H

SPyMe = —S— N^+-CH_3 $.I^-$

Figure 3.2 - Structures of the photosensitizers used on the photodynamic studies.

3.2.2 Bacterial culture

The bioluminescent *E. coli* strain used in this work was obtained in a previous work (131) and stored at - 80 °C in 10% glycerol. Before each photoinactivation assay, *E. coli* was aseptically spread-plated on TSA with antibiotics: ampicillin (100 mg mL^{-1}) and

chloramphenicol (25 mg mL^{-1}) and grown for one day at 26 °C. One isolated colony was aseptically inoculated on Luria Broth (LB, Merck) with both the antibiotics and grown overnight at 26 °C under stirring (130 rpm). An aliquot (240 µL) of this culture was subcultured in LB (30 mL) with antibiotics and grown overnight under stirring (130 rpm) at 26 °C.

3.2.3 Correlation between bioluminescence and colony-forming units

To assess the correlation between the bioluminescent signal (in relative light units, RLU) of *E. coli* and the colony-forming units number, two independent assays were carried out in dark conditions. A bioluminescent *E. coli* overnight culture (≈ 10^7 CFU mL^{-1}) was serially diluted (10^{-1} to 10^{-7}) in PBS. The non-diluted and diluted aliquots were read on a luminometer (Turner Designs – 20/20) and pour plated in TSA medium. After 24 h of incubation at 37 °C, the number of colonies was counted in the most convenient dilution series.

3.2.4 Photoinactivation procedure

Experimental setup

Bacterial cultures grown overnight were diluted tenfold in PBS to a final concentration of ≈ 10^6 colony forming units per milliliter (CFU mL^{-1}). This bacterial suspension was equally distributed in 100 mL sterilized and acid-washed glass beakers. Then, appropriate quantities of the three stock solution of the phthalocyanines derivatives **17**-**19** under study (500 µmol L^{-1} DMSO) were added to achieve final concentrations of 20 µmol L^{-1} (test sample) in a total volume of 10 mL per beaker. The samples were protected from light with aluminium foil and incubated during 10 min under 100 rpm stirring, at 25-30 °C, to promote PS binding to *E. coli* cells. Light and dark controls were included in the experiments. The light control was irradiated without phthalocyanine. The dark control contained 20 µmol L^{-1} of phthalocyanine but was protected from light with aluminium foil. Two independent assays were conducted for each condition.

Irradiation conditions

Following the pre-incubation period, the samples were irradiated with white light (400-800 nm) or red light (620-750 nm) delivered by an illumination system (LC-122 LumaCare, London) equipped with a halogen/quartz 250 W lamp coupled to two different interchangeable optic fiber probes (400–800 nm and 620-750 nm). The lights were delivered at a fluence rate of 150 mW cm^{-2}, measured with an energy meter Coherent FieldMaxII-Top combined with a Coherent PowerSens PS19Q energy sensor. All samples were irradiated during 30 min under 100 rpm stirring, on a water bath at 25 °C.

Bioluminescence monitoring

In all experiments, aliquots of treated and control samples were collected at time 0 and after 2.5, 5, 10, 15, 20, 25 and 30 min of irradiation for bioluminescence measurement in a luminometer (TD-20/20 Luminometer, Turner Designs, Inc., USA).

Statistical Analysis

Statistical analysis was performed with SPSS package (SPSS 15.0 for Windows, SPSS Inc., USA). Normal distributions were assessed by the Kolmogorov-Smirnov test. The significance of both irradiation time and type of PS on bacterial inactivation was assessed by two-way univariate analysis of variance (ANOVA) model with the Bonferroni post-hoc test. A value of $p < 0.05$ was considered significant.

3.2.5 Phthalocyanine solubility studies

The solubility of cationic phthalocyanines **17**-**19** in DMSO and PBS was assessed by UV-Visible spectroscopy. Concentrations, between 0.625 and 25 µmol L^{-1}, obtained by the addition of aliquots of each phthalocyanine stock solution, were analyzed. The intensity of the Q band versus phthalocyanine concentration was plotted in a graphic for linear regression, in order to determine if these concentrations follow the Beer-Lambert law.

3.2.6 Photostability studies

The photobleaching rates of compounds **17**-**19** were determined by irradiating 2 mL of a diluted solution of each phthalocyanine in PBS (Abs ≈1) under the same conditions used in the biological assays (150 mW cm^{-2}). During the irradiation the solutions were magnetically stirred and kept at room temperature. The concentration of the phthalocyanine derivative was quantified by visible absorption spectroscopy at regular time intervals. UV–visible spectroscopy assessed the intensity of the Q band at different intervals of time and the photostability was expressed as I_t/I_0 (%) (I_t = intensity of the band at given time of irradiation, I_0 = intensity of the band before irradiation). Similar assays were performed in the dark to account for the effect of aggregation as a source of light-independent decay.

3.2.7 Singlet oxygen generation

The ability of the PSs to generate singlet oxygen were qualitatively evaluated following the photooxidation of 3-diphenylisobenzofuran (DPBF), a singlet oxygen quencher (132). Stock solutions of each cationic phthalocyanine at 0.1 mmol L^{-1} in DMF and a stock solution of DPBF at 10 mmol L^{-1} in DMF/H_2O (9:1) were prepared. The reaction mixtures of 50 µmol L^{-1} of DPBF and 0.5 µmol L^{-1} of each phthalocyanine derivative in DMF/H_2O (9:1) were irradiated, in a glass cuvette at room temperature and under gentle magnetic stirring, with white light filtered through a cut-off filter for wavelengths <550 nm, at a fluence rate of 9.0 mW cm^{-2}. The absorption decay of DPBF at 415 nm was measured at irradiation intervals of 1 up to 10 min. The percentage of the DPBF absorption decay, proportional to the production of $^1O_2$, was assessed by the difference between the initial absorbance and the absorbance of DPBF after a given period of irradiation.

3.2.8 Fluorescence quantum yield

The fluorescence quantum yields (Φ_F) of the phthalocyanine derivatives in DMF were measured in 1 cm x 1 cm quartz optical cells under normal air conditions on a

spectrofluorimeter Fluoromax 3 (Horiba Jovin Yvon). The Φ_F of the phthalocyanine derivatives were calculated by comparison of the area below the corrected emission spectrum (600-800 nm) with that of phthalocyaninatozinc(II) (ZnPc). ZnPc was used as fluorescence standard (λ_{exc} = 410 nm) with Φ_F = 0.28 in DMF (116). In all cases, the absorbance of the sample and reference solutions was kept at 0.02 at 410 nm, the excitation wavelength. Fluorescence quantum yield was calculated according equation 1:

$$\Phi_F^{sample} = \Phi_F^{ref} \frac{AUC^{sample}(1-10^{-Abs_{ref}})}{AUC^{ref}(1-10^{-Abs_{sample}})}$$

Equation 1

Where AUC is the integrated area under the fluorescence curves of each phthalocyanine and the standard and Abs is the absorbance of the samples and the standard at the excitation wavelength, respectively.

3.2.9 Cellular uptake of the phthalocyanines

A bacterial suspension (10^7 to 10^8 cells mL^{-1}) was incubated for 10 min in the dark at room temperature in the presence of the same PS concentration used in the inactivation studies (20 µmol L^{-1}). The unbound PS was removed out of the suspension by centrifugation at 13,000 g for 10 min (Eppendorf Microcentrifuge 5414). For the digestion, the pellets were resuspended in 1 mL of a digestion solution containing 0.5 mL of 2% aqueous SDS (Merck) and incubated at room temperature for at least 24 h. The concentration of the phthalocyanine derivatives in the digested extracts was analyzed by fluorimetry with a Fluoromax 3 (Horiba Jovin Yvon). The samples were excited at 425 nm and the fluorescence emission of the PS was monitored in the 440–900 nm range. The measured fluorescence intensity allowed the determination of the corresponding concentration by interpolation with a calibration plot built with known concentrations of each PS using the digestion solution as solvent. Parallel aliquots of the bacteria incubated in the presence of the PS were serially diluted and spread plated in TSA for the determination of the concentration of viable *E. coli* (CFU mL^{-1}). The adsorption value (PS CFU^{-1}) was calculated according to the literature (133). For each PS three independent assays were done.

3.2.10 Cellular localization of phthalocyanines

Bacterial cells (≈10^8 CFU mL^{-1}) were incubated with each PS, as described in cellular uptake. After the incubation period, samples were centrifuged (12,000 g, 6 min), and bacterial cells were washed twice with 1 mL of PBS, in order to remove unbound PS. Cells were fixed with 4% paraformaldehyde in PBS for 30 min at room temperature. Cells were washed twice with 1 mL of PBS and permeabilized for 10 min in 500 µL of 0.1% Triton X-100 (Merck) in PBS, pH 7.4 at 50 ºC. The cells were washed twice with 1 mL of PBS, stained with the membrane marker FM1-43 (25 µmol L^{-1}, Molecular Probes, Invitrogen) during 15 min at room temperature in the dark, washed twice with 1 mL of PBS and then 10 µL of glycerol were added to the pellet. Images of PS and FM1-43 fluorescence were acquired with a confocal microscope (Zeiss LSM 710). The preparation was excited at 488 nm and light emitted above 493 nm was collected for analysis of FM1-43. For analysis of the PS, each preparation was excited at 633 nm and emitted light was collected above 650 nm.

3.3 RESULTS

3.3.1 Bioluminescence versus CFU of an overnight culture

The bioluminescence results reflect the bacterial abundance of the bioluminescent *E. coli* strain (Figure 3.3). A significant linear correlation (R^2 = 0.980) was observed between bioluminescence units and colony counts.

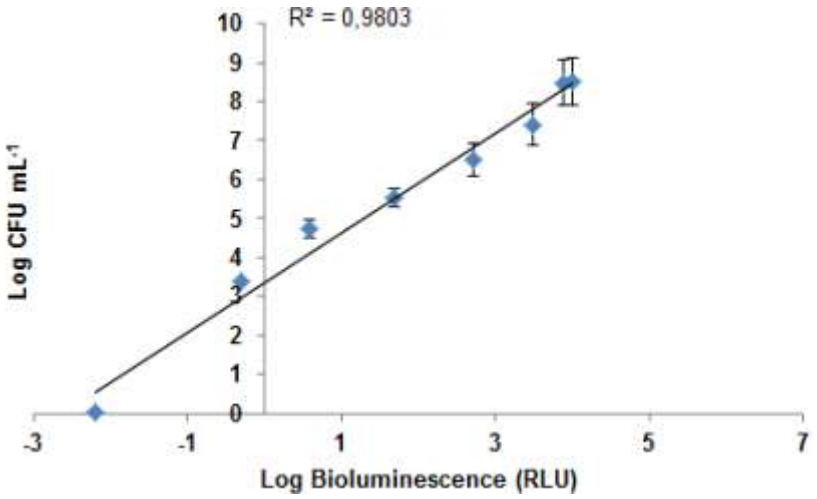

Figure 3.3 - Linear correlation between the bioluminescence signal and viable counts of overnight cultures of recombinant bioluminescent E. coli. Viable counts are expressed in CFU mL^{-1} and bioluminescence in relative light units (RLU). Each value represents average ± standard deviation of two independent experiments.

3.3.2 Photoinactivation efficiency

The inactivation kinetics, in real time, of transformed bioluminescent *E. coli* are represented in Figure 3.4.

Comparing the bioluminescence values obtained in the experiments carried out under white light (Figure 3.4a), a clear difference in the photoinactivation patterns of the three phthalocyanines was observed. Compounds **18** and **19** were more efficient than **17** ($p < 0.05$, ANOVA). The first two caused a 5 log (99.999% of reduction) decrease of bioluminescence after 30 min of irradiation, while the last one caused only 2.1 log reduction (≈ 99.33% of reduction).

The experiments carried out under red light also showed different patterns of inactivation with the three PSs (Figure 3.4b). The photodynamic inactivation efficiency of **18** was not very different from that obtained with white light (> 5 log decrease of bioluminescence) after 30 min of irradiation. However, the photodynamic inactivation with red light in the presence of compound **19** was lower than that observed under white light (3.5 log decrease after 30 min of irradiation). In these conditions, compound **17** was

even less effective than under white light, causing 1 log decrease in bacterial bioluminescence.

The results of the photoinactivation experiments show that the viability of the recombinant bioluminescent *E. coli* was not affected neither by light alone (light control) nor by the direct effect of any of the tested PS (dark controls) (Figure 3.4). Significant differences (ANOVA, p> 0.05) between the independent assays conducted for each phthalocyanine were not found.

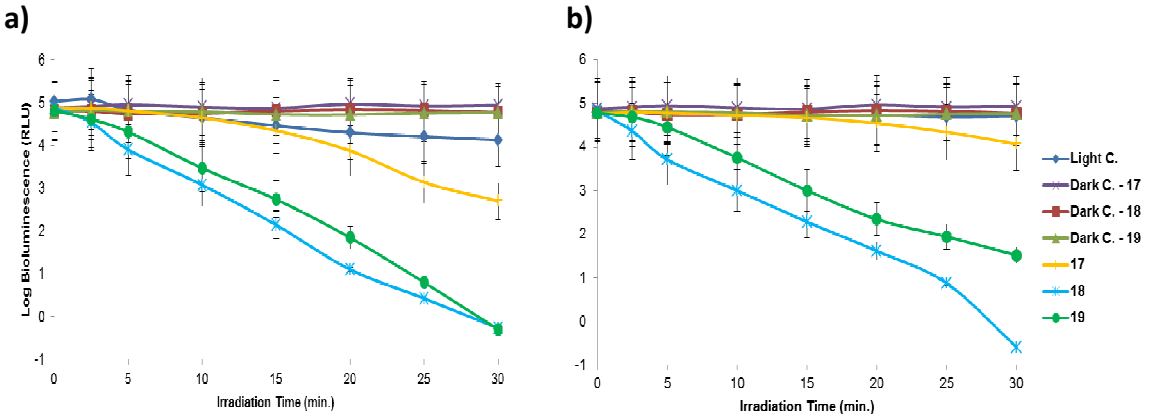

Figure 3.4 - Photoinactivation bioluminescent *E. coli* in the presence of 20 µM of each PS under white light (a) or red light (b) at 150 mW cm^{-2}. Each value represents the average ± standard deviation of two independent experiments.

3.3.3 Phthalocyanine solubility studies

The phthalocyanines solubility in DMSO and PBS were measured by UV-visible spectroscopy in concentrations between 0.625 and 25 µmol L^{-1} in order to determine if the phthalocyanines, at this concentration range, follows the Beer-Lambert law. The graphics obtained from the plotting of the Q band intensity *versus* phthalocyanine concentration in DMSO (Figure 3.5) show a non-linear regression for all the cationic phthalocyanines under study confirming that aggregation processes are occurring. A different situation occurs in PBS for compounds **18** and **19** at concentrations below 25 µmol L^{-1} where the Beer-Lambert law is followed for both derivatives (Figure 3.6). However, the behavior of phthalocyanine **17** did not improve in PBS maintaining its high tendency to aggregate such as in DMSO.

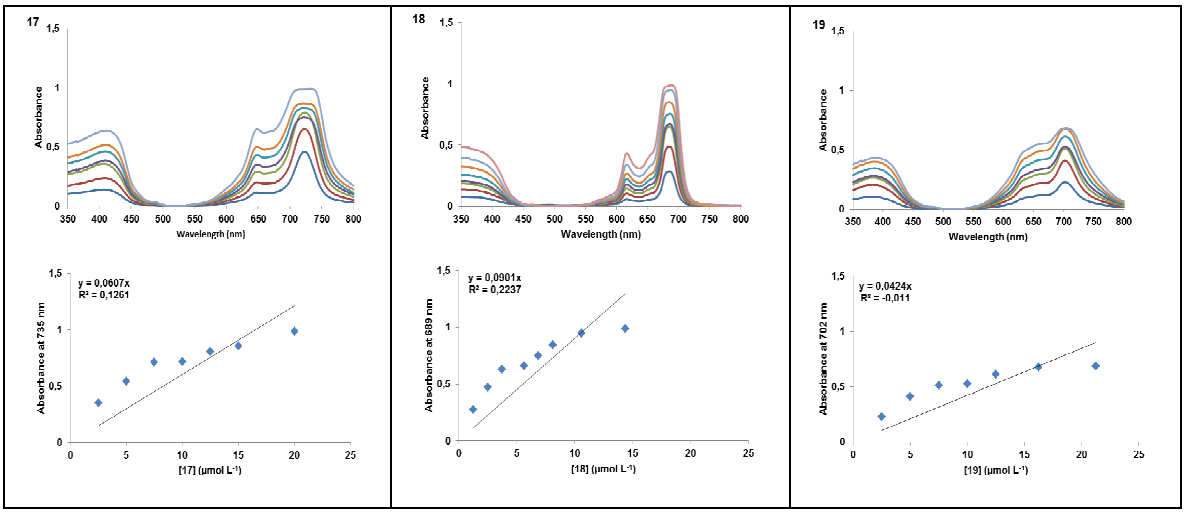

Figure 3.5 - UV-Vis spectra of compounds **17**, **18** and **19** in DMSO at different concentrations. The linear regression graphics plotted the Q-band absorbances at 725 nm (**17**), 689 nm (**18**) and 702 nm (**19**) and versus the concentrations in DMSO.

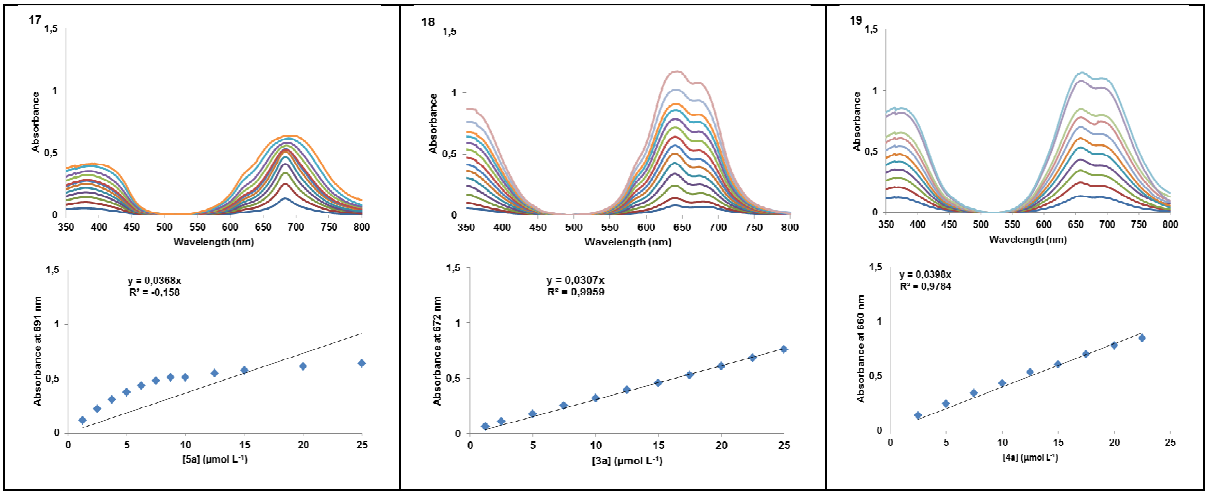

Figure 3.6 - UV-Vis spectra of **17**, **18** and **19** at different concentrations in PBS. The linear regression graphics plotted the Q-band absorbances at 691 nm (**17**), 672 nm (**18**) and 660 nm (**19**) and versus the concentrations in PBS.

3.3.4 Photostability, singlet oxygen generation and fluorescence quantum yield

The photostability studies showed that the three cationic compounds **17**-**19** when irradiated with white light or red light in PBS, under the same conditions used in the biological assays (30 min at a fluence rate of 150 mW cm^{-2}), do not suffer pronounced

changes in the residual absorbance (Table 3.1), indicating that the new derivatives are photostable in the used conditions.

The results of the photooxidation of DPBF in the presence of the cationic phthalocyanines show that they are able to generate singlet oxygen, causing the photodegradation of DPBF when irradiated with light at a fluence rate of 9 mW cm^{-2} (Table 3.1). However, the decay caused by tetra-substituted phthalocyanine **18** was much higher (90% of DPBF decay after 5 min of irradiation) than those caused by the octa-substituted compounds (**17**, **19**), indicating a higher singlet oxygen rate production by this PS.

All new cationic derivatives were able to show fluorescence emission after excitation with visible light. In Table 3.1 are summarized the fluorescence quantum yields obtained for the derivatives **17**-**19** in DMF. According to the results obtained, compound **18** (0.43) showed higher fluorescence quantum yield followed by compounds **19** (0.25) and **17** (0.16).

Table 3.1 – Photostability, fluorescence quantum yield and relative photooxidation of DPBF by singlet oxygen generated by the cationic phthalocyanine derivatives.

Compounds	Photostability (%)		DPBF Decay††† (%)	$\Phi_F{}^{\dagger\dagger\dagger\dagger}$
	White light†	Red light††		
17	97	99	11	0.16
18	90	90	90	0.43
19	99	100	13	0.25

†upon 30 min of irradiation in PBS with white light (400-800 nm) at a fluence rate of 150 mW cm^{-2}; ††upon 30 min of irradiation in PBS with red light (620-750 nm) at a fluence rate of 150 mW cm^{-2}; ††† upon 5 min of irradiation in DMF/H_2O (9:1) with white light filtered through a cut-off filter for wavelengths < 550 nm, at a fluence rate of 9.0 mW cm^{-2}; ††††reference ZnPc in DMF.

3.3.5 Cellular uptake of phthalocyanines

The uptake values of cationic phthalocyanines by the *E. coli*, obtained after 10 min of incubation in the dark at a concentration of 20 μmol L^{-1}, and after two washings are summarized in Figure 3.7. Compound **17** showed the highest amount of phthalocyanine retention in *E. coli* cells, with an average value of 9.99 x 10^{21} molecules CFU^{-1}. The tetra-

substituted phthalocyanine **18** and the octa-substituted **19** presented a similar uptake, with 5.24 x 10^{21} and 5.11 x 10^{21} molecules CFU^{-1}, respectively. The amount of phthalocyanine taken up by the bacterial cells decreased after, each washing, and this decrease was more evident for **17** (Fig. 3.7).

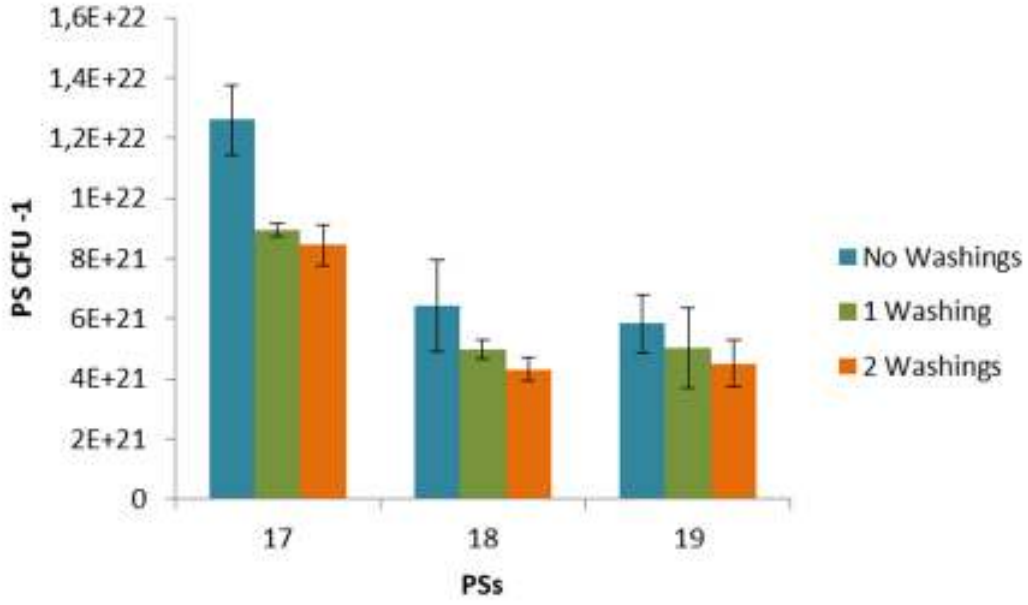

Figure 3.7 - Adsorption of phthalocyanines **17** – **19** to *E. coli* in the presence of 20 μmol L^{-1} of each PS, after 10 min incubation in the dark. Error bars represent the standard deviation of three independent experiments.

3.3.6 Cellular localization of phthalocyanines

The confocal immunofluorescence microscopy with FM1-43 as a membrane cell marker showed that all the compounds, even **17** with a much higher uptake than **18** and **19**, have a similar behavior, with a uniform redistribution within the cell (Fig. 3.8).

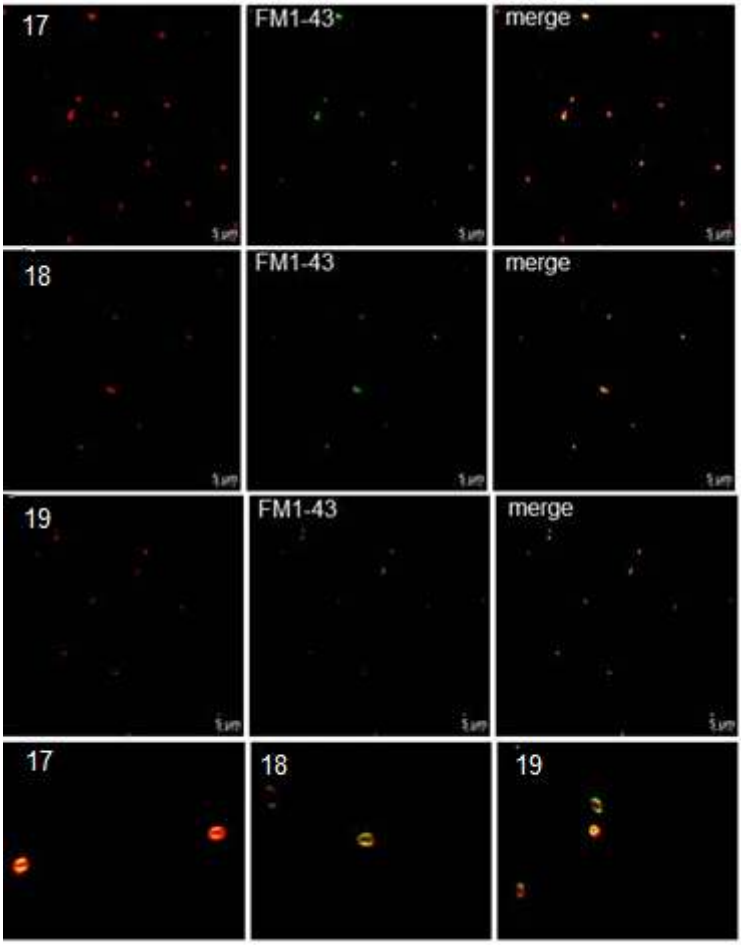

Figure 3.8 - Confocal fluorescence microscopy images of *E. coli*, double stained with the PS (**17**, **18** and **19**) and with the cell membrane marker, FM1-43. Right panels show the superimposed images from PS (red) and FM1-43 (green). The last row shows representative bacteria amplified from the merged images.

3.4 DISCUSSION

The possibility of designing an enormous variety of structurally different phthalocyanines with high absorption in the red region of the electromagnetic spectrum, places this class of second generation PSs among the most promising for the inactivation of pathogenic microorganisms in the clinic area. The results of this study show that: i) the three new cationic thio-pyridinium phthalocyanines with different physico-chemical properties have different photoinactivation efficiencies to inactivate a gram-negative bacterium; ii) two of them, **18** and **19**, have high potential to be used as antimicrobial photosensitizers under white light (5 log reduction in *E. coli* bioluminescence) and iii)

phthalocyanine **18** is the most promising of the three PSs under red light (5.5 log reduction in bioluminescence).

The better performance of the tetra- and octa-substituted phthalocyanines **18** and **19** when compared with the octa-substituted one **17** in the photoinactivation of gram-negative bacteria, can be explained by the tendency of **17** to aggregate accompanied by its low $^1O_2$ production. The production of $^1O_2$ by phthalocyanine **18** is approximately 9 times higher than the octa-substituted **19** and **17**, probably due to the lower substitution of the Pc core by thiol groups. It is well known that $^1O_2$ can be quenched by thiols (134). According to the literature, $^1O_2$ is the main ROS through which the PS exerts their photodynamic action (135-138). Although the overall production of $^1O_2$ by **19** is also reduced, the photoinactivation results show that it is still enough to photoinactivate efficiently the bacteria under white light. The low tendency of **18** to aggregate, perhaps due to the simultaneous presence of symmetric and asymmetric isomers that can assign them higher solubility, can justify the different profile of the two eight-positive charge PS. The presence of one or more positively charged groups plays an essential role in driving the PS toward sites which are critical for the stability of cell organization and/or the cell functions (65,139,140). In fact, several studies demonstrate a high rate of bacterial inactivation with tri- and tetra-cationic porphyrinic PS compared with di- and mono-cationic molecules (140,141). However, other studies report on contradicting results (64,141) and it was even suggested that a high number of positive charges can decrease the PS efficiency (Jori, personal communication). In this study, under white light, the tetra- (**18**) and octa-substituted (**19**) Pcs show similar photoinactivation effect suggesting that the high number of positive charges does not affect PS efficiency.

All cationic compounds show higher photoinactivation efficiency under white light (400-800 nm) comparatively to red light (620-750 nm), most probably due to the higher overlap of the Q-bands with the emission spectrum of the white light used (fig. 3.9). The light wavelength necessary to induce microorganism photoinactivation depends on the electronic absorption spectrum of the PS, and the emission spectrum of the light source must cover all the PS absorption spectrum or at least some of the absorption bands (142). Under red-light irradiation, the most preferable for treatment of microbial infections,

because it penetrates deeper into infected human tissues, the photoinactivation efficiency of PS **19** was significantly lower ($p<0.05$) than the one observed for **18**. In this case, although, the overlap of the **18** Q-band with the red light emission is lower than the corresponding **19** Q-band overlap (fig. 3.9), the lower molar extinction coefficients of **19** Q-band in that region, can be responsible by a much lower production of $^1O_2$ due to less photons to be absorbed.

Compound **17** unexpectedly displayed the highest values of cellular uptake. The compounds **18** and **19** showed similar uptake, although lower than **17**. However, it has been shown that antibacterial photoinactivation is generally not dependent on surface-bound PS, but on the permeabilization of the cell membrane by reactive species produced by unbound PS molecules (143). Localization of the compounds may point out the sites of direct photodamage. Confocal microscopy images show that after 10 min incubation all compounds have an identical cellular localization.

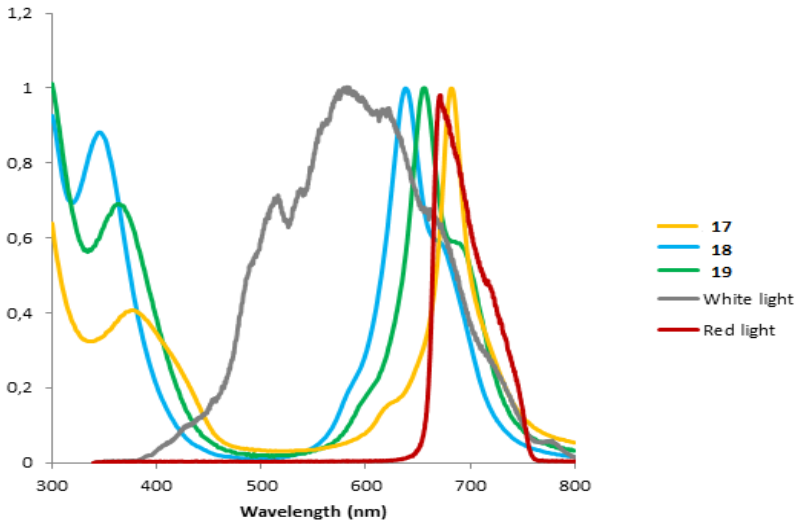

Figure 3.9 - Normalized UV-Vis spectra of **17**-**19** in PBS and white and red light source emission.

Chapter IV

Conclusions

Phthalocyanines **18** and **19** were prepared from pyridylphthalonitriles in very good yields (82 and 85%). Similar tetra- and octa-substituted compounds bearing 2-thiopyridyl groups were already described in previous works in very low yields (12%) (144,145).

Phthalocyanine **17** was also obtained, in high yield (89%), via nucleophilic substitution of the alfa fluor atoms of the hexadecafluorophthalocyaninatozinc(II) by mercaptopyridine, followed by cationization.

The tetra-cationic phthalocyanine **18** generates high amounts of singlet oxygen making it an effective PS against *E. coli* by reaching a 5 log reduction in bioluminescence emission after 30 min of irradiation with white light and 5.5 log under red light. Phthalocyanines with high amounts of thio-pyridinium groups showed a significant reduction in singlet oxygen generation; however Pc **19** under white light showed similar photoinactivation efficiency than the tetra-cationic Pc **18**. Compound **17** was the least efficient photosensitizer, under both red and white lights, with only a slight decrease of cell survival rate. These findings demonstrate that several factors such as solubility and Q-band overlap with wavelength emission also influence significantly the photoinactivation process efficacy.

Confocal immunofluorescence microscopy showed that phthalocyanines are uniformly distributed in the cell wall and within the cells. Under the studied conditions, compound **17** did not show photoinactivation activity, however, its direct synthesis from the commercial perfluorinated $ZnPcF_{16}$, can still justify the use of this template to prepare novel cationic PSs, if a different disposition/number from the combination used here, or if other cationic groups, rather than the pyridinium ones, were considered.

References

1. Allison R.R., H. C. Mota and C. H. Sibata (2004) Clinical PD/PDT in North America: An historical review. *Photodiagnosis Photodyn Ther*. **1**: 263—277.

2. Fitzpatrick T.B. and M. A. Pathak (1959) Historical aspects of methoxsalen and other furocoumarins. *J. Invest. Dermatol.* **32**: 229–31.

3. Moan J. and Q. Peng (2003) An outline of the hundred-year history of PDT. *Anticancer Res.* **23**: 3591-3600.

4. Mitton, D. and R. Ackroyd (2008) A brief overview of photodynamic therapy in Europe. *Photodiagn Photodyn.* **5**: 103-111.

5. Dougherty T., B. W. Henderson, C. J. Gomer, G. Jori, D. Kessel, M. Korbelik, J. Moan and Q. Peng (1998) Photodynamic therapy. *J Natl Cancer Inst*. **90**: 889–905.

6. Sibata C. H., V.C., Colussi, N. L. Oleinick and T. J. Kinsella (2000) Photodynamic therapy: a new concept in medical treatment. *Braz J Med Biol Res.* **33**: 869-880.

7. Detty M., S. Gibson and S.Wagner (2004) Current clinical and preclinical photosensitizers for use in photodynamic therapy. *J. Med. Chem*. **47**: 3897–3915.

8. Allison R.R., G.H. Downie, R. Cuenca, X-H. Hu, C. J. Childs and C.H. Sibata (2004) Photosensitizers in clinical PDT. *Photodiag Photodynam Ther*. **1**: 27–42.

9. Wainwright M. (2009) Photosensitisers in biomedicine, John Wiley & Sons Ltd, West Sussex, UK.

10. Juzeniene A. and J. Moan (2007) The history of PDT in Norway Part one: Identification of basic mechanisms of general PDT. *Photodiagnosis Photodyn Ther.* **4**: 3—11.

11. Spikes J. D. (1990) Chlorins as photosensitizers in biology and medicine. *J Photochem Photobiol B: Biol*. **6**: 259—74.

12. Hader D. and Jori G. (2003) Photodynamic Therapy. In Comprehensive series in photochemistry & photobiology, Vol2, European Society for Photobiology, Cambridge, UK.

13. Josefsen L.B. and W. Boyle (2008) Photodynamic therapy: novel third-generation photosensitizers one step closer? *Br J Pharmacol.* **154**: 1–3.

14. Moan J. (1984) The photochemical yield of singlet oxygen from porphyrins in different states of aggregation. *Photochem Photobiol.* **39**: 445—9.

15. Moan J. and S. Sommer (1985) Oxygen dependence of the photosensitizing effect of hematoporphyrin derivative in NHIK 3025 cells. *Cancer Res*. **45**: 1608—1610.

16. Boye E. and J. Moan (1980) The photodynamic effect of hematoporphyrin on DNA. *Photochem Photobiol*. **31**: 223—228.

17. Moan J. and E. Boye (1981) Photodynamic effect on DNA and cell survival of human cells sensitized by hematoporphyrin. *Photobiochem Photobiophys*. **2**: 301—307.

18. Moan J. (1990) On the diffusion length of singlet oxygen in cells and tissues. *J Photochem Photobiol B: Biol*. **6**: 343—344.

19. Mang T. S. (2004) Lasers and light sources for PDT: past, present and future. *Photodiagnosis Photodyn Ther*. **1**: 43—48.

20. Wardle B. (2009) Principles and Applications of Photochemistry, John Wiley & Sons Ltd, Cornwall,UK.

21. Chin W. W. L. and P. W. S. Heng (2008) Improved formulation of photosensitizer chlorin e6 polyvinylpyrrolidone for fluorescence diagnostic imaging and photodynamic therapy of human cancer. *Eur J Pharm Biopharm*. **69**: 1083–1093.

22. Uzdenskya A., V. Iani, L. Ma and J. Moan (2006) On hypericin application in fluorescence diagnosis and cancer treatment: Pharmacokinetics and photosensitizing efficiency in nude mice bearing WiDr carcinoma. *Medical Laser Application*. **21**: 271–276.

23. Melo C. A. S., C. Kurachi, C. Grecco, C. H. Sibata, O. Castro-e-Silva and V. S. Bagnato (2004) Pharmacokinetics of Photogem using fluorescence monitoring in Wistar rats. *J. Photochem. Photobiol. B: Biology*. **73**: 183–188.

24. Castano A. P., T. N. Demidova and M. R. Hamblin (2004) Mechanisms in photodynamic therapy: part one -photosensitizers, photochemistry and cellular localization. *Photodiag Photodyn Ther*. **1**:279–293.

25. Plaetzer K., B. Krammer, J. Berlanda, F. Berr and T. Kiesslich (2009) Photophysics and photochemistry of photodynamic therapy: fundamental aspects. *Lasers Med Sci.* 24: 259–268.

26. DeRosa M. and R. Crutchley (2002) Photosensitized singlet oxygen and its applications. *Coord Chem Rev.* **233**: 351-371.

27. Foote C. S. (1984) Mechanisms of photo-oxygenation. In Porphyrin localization and treatment of tumors. (Editors: Doiron D. R., Gomer C. J.), Alan R. Liss, New York, USA.

28. Quintero B. and M. A Miranda (2000) Mechanisms of photosensitization induced by drugs: a general survey. *Ars Pharmaceutica*. **41**: 27-46.

29. Zeitouni N. C., A. R. Oseroff and S. Shieh (2003) Photodynamic therapy for nonmelanoma skin cancers: Current review and update. *Mol Immunol.* **39**: 1133-1136.

30. MacCormack M. A. (2008) Photodynamic therapy in dermatology: an update on applications and outcomes. *Semin Cutan Med Surg*. **27**: 52-62.

31. Haddad R., E.Nesher, J. Weiss, Y. Skornick and H. Kashtan (2004) Photodynamic therapy for Bowen's disease and squamous cell carcinoma of the skin. *Photodiagns Photodyn.* **1**: 225-230.

32. Allison R. R., C. H. Sibata, G. H. Downie and R. E. Cuenca (2006) A clinical review of PDT for cutaneous malignancies. *Photodiagnosis Photodyn Ther*. **3**: 214-226.

33. Foroulis C. N., J. A. C. Thorpe (2006) Photodynamic therapy (PDT) in Barrett's esophagus with dysplasia or early cancer. *Eur J Cardiothorac Surg*. **29**: 30-34.

34. Moghissi K., K. Dixon, J.A.C.Thorpe, C.Oxtoby and M.R.Stringer (2004) Photodynamic therapy (PDT) for lung cancer: the Yorkshire Laser Centre experience. *Photodiagnosis Photodyn Ther*. **1**: 253-262.

35. Kelly J. F., M. E. Snell and M. C. Berenbaum (1975) Photodynamic destruction of human bladder carcinoma. *Br J Cancer*. **31**: 237—44.

36. Moore C. M., T. R. Nathan, W.R. Lees, C. A. Mosse, A. Freeman, M. Emberton and S. G. Brown (2006) Photodynamic therapy using meso tetra hydroxy phenyl chlorin (mTHPC) in early prostate cancer. *Lasers Surg Med*. **38**: 356–363.

37. Stylli S. S., M. Howes, L. MacGregor, P. Rajendra, A. H. Kaye (2004) Photodynamic therapy of brain tumours: evaluation of porphyrin uptake versus clinical outcome. *J Clin Neurosci*. **11**: 584-596.

38. Grebeňová D., K. Kuželová, K. Smetana, M. Pluskalová, H. Cajthamlová, I. Marinov , O. Fuchs, J. Souček, P. Jarolím and Z. Hrkal (2003) Mitochondrial and endoplasmic reticulum

stress-induced apoptotic pathways are activated by 5-aminolevulinic acid-based photodynamic therapy in HL60 leukemia cells. *J. Photochem. Photobiol. B: Biology*. **69**: 71-85.

39. Orenstein A., J. Haik, J. Tamir, E. Winkler, H. Trau, Z. Malik and G. Kostenich (2000) Photodynamic Therapy of Cutaneous Lymphoma Using 5-Aminolevulinic Acid Topical Application. *Dermatol Surg*. **26**: 765-770.

40. Jori, G., C. Fabris, M. Soncin, S. Ferro, O. Coppellotti, D. Dei, L. Fantetti, G. Chiti and G. Roncucci (2006) Photodynamic therapy in the treatment of microbial infections: basic principles and perspective applications. *Lasers Surg Med*. **38**: 468-481.

41. Hamblin M.R. and T. Hasan (2004) Photodynamic therapy: a new antimicrobial approach to infectious disease? *Photochem Photobiol Sci*. **3**: 436-450.

42. Pelletier J.P., S. Transue and E.L. Snyder (2006) Pathogen inactivation techniques. *Best Pract Res Clin Haematol*. **19**: 205-242.

43. McClaskey J., M. Xu, E. L. Snyder and C. A. Tormey (2009) Clinical trials for pathogen reduction in transfusion medicine: a review. *Transfus Apher Sci*. **41**: 217-225.

44. Wu Y. Y. and E. L. Snyder (2003) Safety of the blood supply: role of pathogen reduction. *Blood Rev*. **17**: 111-22.

45. Itoh Y., Y. Ninomiya, S. Tajima and A. Ishibashi (2001) Photodynamic therapy of acne vulgaris with topical delta-aminolevulinic acid and incoherent light in Japanese patients. *Br J Dermatol*. **144**: 575–579.

46. Carvalho, C., A. Gomes, S. Fernandes, A. Prata, M. Almeida, M. Cunha, J. Tomé, M. Faustino, M. Neves, A. Tomé, J. Cavaleiro, Z. Lin, J. Rainho and J. Rocha (2007) Photoinactivation of bacteria in wastewater by porphyrins: Bacterial β-galactosidase activity and leucine-uptake as methods to monitor the process. *J Photochem Photobiol B*. **88**: 112–118.

47. Rebeiz C., J. Juvik and C. Rebeiz (1988) Porphyric insecticides, Concept and phenomenology. *Pestic Biochem Phys*. **30**: 11–27.

48. Bressler N.M. (2001) Photodynamic therapy of subfoveal choroidal neovascularization in age-related macular degeneration with verteporfin: two-year results of 2 randomized clinical trials-tap report 2. *Arch Ophthalmol*. **119**: 198-207.

49. Ratkay L.G., J.D. Waterfield and D.W. Hunt (2000) Photodynamic Therapy in Immune (Non-Oncological) Disorders: Focus on Benzoporphyrin Derivatives. *BioDrugs*. **14**: 127-135.

50. Pai M., W. Jamal, A. Mosse , C.Bishop, S.Bown and J.McEwan (2005) Inhibition of In-stent Restenosis in Rabbit Iliac Arteries with Photodynamic Therapy. *Eur J Vasc Endovasc*. **30**: 573-581.

51. Sessler J.L. and R.A. Miller (2000) Texaphyrins: new drugs with diverse clinical applications in radiation and photodynamic therapy. *Biochem Pharmacol*. **59**: 733-739.

52. Malik E., A. Meyhofer-Malik, C. Berg, W. Böhm, K. Kunzi-Rapp, K. Diedrich and A. Rück (2000) Fluorescence diagnosis of endometriosis on the chorioallantoic membrane using 5-aminolaevulinic acid. *Hum Reprod*. **15**: 584-588.

53. Shum P., J.M. K im and D.H. Thompson (2001) Phototriggering of liposomal drug delivery systems. *Adv Drug Deliv Rev*. **53**: 273-84.

54. Tenover F. C. (2006) Mechanisms of antimicrobial resistance in bacteria. *Am J Med*. **119(6 A)**:S3-10.

55. Maisch T., R. M. Szeimies, G. Jori and C. Abelsa (2004) Antibacterial photodynamic therapy in dermatology . *Photochem. Photobiol. Scl*. **3**: 907-917.

56. Konopka K. and T. Goslinski (2007) Photodynamic Therapy in Dentistry. *J DENT RES*. **86**: 694-1126.

57. Hamblin M., J. Viveiros, C. Yang, A. Ahmadi, R.A. Ganz and M. J. Tolkoff (2005) Helicobacter pylori Accumulates Photoactive Porphyrins and Is Killed by Visible Light .*Antimicrob. Agents Chemother*. **49**: 2822-2827.

58. Dai T., Y. Huang and M. Hamblin (2009) Photodynamic therapy for localized infections – state of the art. *Photodiagn photodyn ther*.**6**: 170-188.

59. Grellier P., J. Benach, M. Labaied, S. Charneau, H. Gil, G. Monsalve, R. Alfonso, L. Sawyer, L. Lin, M. Steiert and K. Dupuis (2008) Photochemical inactivation with amotosalen and long-wavelength ultraviolet light of Plasmodium and Babesia in platelet and plasma components. *Transfusion.* **48**: 1676–1684.

60. Asilian, A. and M. Davami (2006) Comparison between the efficacy of photodynamic therapy and topical paromomycin in the treatment of Old World cutaneous leishmaniasis: a placebo-controlled, randomized clinical trial. *Clin Exp Dermatol*. **31**:634-637.

61. Tardivo J. P., A. Del Giglio, C. Santos de Oliveira, D. S. Gabrielli, H. C. Junqueira, D. B. Tada, D. Severino, R. F. Turchiello and M. S. Baptista (2005) Methylene blue in photodynamic therapy: From basic mechanisms to clinical applications. *Photodiagn. Photodyn. Ther*. **2**: 175-191.

62. Wainwright M. (1998) Photodynamic antimicrobial chemotherapy (PACT). *J. Antimicrob. Chemother*. **42**: 13-28.

63. Beveridge T. (1999) Structures of Gram-Negative Cell Walls and Their Derived Membrane Vesicles. *J. Bacteriol*. **181**: 4725-4733.

64. Banfi S., E. Caruso, L. Buccafurni, V. Battini, S. Zazzaron, P. Barbieri and V. Orlandi (2006) Antibacterial activity of tetraaryl-porphyrin photosensitizers: An in vitro study on Gram negative and Gram positive bacteria. *J Photochem Photobiol B*. **85**: 28-38.

65. Merchat M., G. Bertolini, P. Giacomini, A. Villanueva, and G. Jori (1996) Meso-substituted cationic porphyrins as efficient photosensitizers of gram-positive and gram-negative bacteria*. J. Photochem. Photobiol. B.* **32**: 153-157.

66. Minnock A., D. I. Vernon, J. Schofield, J. Griffiths, J. H. Parish and S. B. Brown (2000) Mechanism of uptake of a cationic water-soluble pyridinium zinc phthalocyanine across the outer membrane of Escherichia coli. *Antimicrob Agents Chemother*. **44**: 522-527.

67. Jori G. and S. Brown (2004) Photosensitized inactivation of microorganisms. *Photochem. Photobiol. Scl.* **3**: 403-405.

68. Hancock R. (1997) The bacterial outer membrane as a drug barrier. *Trends microbiol*. **5**: 37-42.

69. MacDonald I. and T Dougherty (2001) Basic principles of photodynamic therapy. *J. Porphyrins Phthalocyanines*. **5**: 105-129.

70. Valduga G., B. Breda, G. M. Giacometti, G. Jori and E. Reddi (1999) Photosensitization of wild and mutant strains of Escherichia coli by meso-tetra (N-methyl-4-pyridyl)porphine. *Biochem. Biophys. Res. Commun*. **256**: 84–88.

71. Bertoloni G., F. Rossi, G. Valduga, G. Jori and J. van Lier (1990) Photosensitizing activity of water- and lipid-soluble phthalocyanines on Escherichia coli. *FEMS Microbiol. Lett*. **59**: 149–155.

72. Nitzan Y., A. Balzam-Sudakevitz and H. Ashkenazi (1998)Eradication of Acinetobacter baumannii by photosensitized agents in vitro*. J. Photochem. Photobiol. B*. **42**: 211–8.

73. Hamblin M., D. A. O'Donnell, N. Murthy, C. H. Contag and T. Hasan (2002) Rapid control of wound infections by targeted photodynamic therapy monitored by in vivo bioluminescence imaging. *Photochem. Photobiol*. **75**: 51-57.

74. Francis K. P., J. Yu, C. Bellinger-Kawahara, D. J oh, M. J.Hawkinson, G.Xiao, T. F. Purchio, M. G.Caparon, M. Lipsitch and P. R. Contag (2000) Visualizing pneumococcal infections in the lungs of live mice using bioluminescent Streptococcus pneumoniae transformed with a novel gram-positive lux transposon. *Infect Immun*. **69**:3350-3358.

75. Rocchetta H. L., C. J. Boylan, J. W. Foley, P. W. Iversen, D. L. LeTourneau, C. L. McMillian, P. R. Contag, D. E. Jenkins and T. R. Parr Jr. (2001) Validation of a noninvasive, real-time imaging technology using bioluminescent Escherichia coli in the neutropenic mouse thigh model of infection. *Antimicrob Agents Chemother*. **45**: 129-37.

76. Meighen E. A. (1991) Molecular biology of bacterial bioluminescence. *Microbiol. Mol. Biol. Rev*. **55**: 123-142.

77. Vesterlund S., J. Paltta, A. Lauková , M. Karp and A. Ouwehand (2004) Rapid screening method for the detection of antimicrobial substances. *J. Microbiol. Meth*. **57**: 23-31.

78. Harveyi E. (1952) Bioluminescence., Academic Press, Inc., New York, USA.

79. Rodriguez A., I. Nabi and E. Meighen (1985) ATP turnover by the fatty acid reductase complex of Photobacterium phosphoreum. *Can. J. Biochem. Cell Biol*. **63**: 1106-1111.

80. Meighen E. A. (1993) Bacterial bioluminescence: organization, regulation, and application of the lux genes. *FASEB J*. **7**: 1016-1022.

81. Demidova T. N., F. Gad, T. Zahra, K. P. Francis and M. R. Hamblin (2005) Monitoring photodynamic therapy of localized infections by bioluminescence imaging of genetically engineered bacteria. *J Photochem Photobiol B*. **81**:15-25.

82. Hill P., C. Rees, M. K. Winson and G. S. Stewart (1993) The application of lux genes. *Biotechnol. Appl. Biochem*.**17**: 3-14.

83. Beard S., V. Salisbury, R. J. Lewis, J. A. Sharpe and A. P. MacGowan (2002) Expression of lux genes in a clinical isolate of Streptococcus pneumoniae: using bioluminescence to monitor gemifloxacin activity. *Antimicrob. Agents Chemother*. **46**: 538-542.

84. Salisbury V., A. Pfoestl, H. Wiesinger-Mayr, R. Lewis, K. E. Bowker, A. P. MacGowan (1999) Use of a clinical Escherichia coli isolate expressing lux genes to study the antimicrobial pharmacodynamics of moxifloxacin. *J. Antimicrob. Chemother.* **43**: 829-832.

85. Marincs F. (2000) On-line monitoring of growth of Escherichia coli in batch cultures by bioluminescence. *Appl. Microbiol. Biotechnol*. **53**: 536-541.

86. Stewart G.S.A.B. and P. Williams (1992) lux genes and the applications of bacterial bioluminescence: a review. *J. Gener. Microbiol*. **138**:1289-1300.

87. Moser F. H. and A. L. Thomas (1963) Phthalocyanine Compounds. *J. Chem. Educ.* **41**: 245-249.

88. Christie R. M. (2001) Colour Chemistry. The Royal Society of Chemistry, Cambridge, UK.

89. McKeown N. B. (1998) Phthalocyanine materials: synthesis, structure, and function. University Press, Cambridge, UK.

90. Torre G., C. G. Claessens and T. Torres (2007) Phthalocyanines: old dyes, new materials. Putting color in nanotechnology. *Chem. Commun*. **20**: 2000-2015

91. Torre G., M. Nicolau and T. Torres (2001) Supramolecular Photosensitive and Electroactive Materials. Academic Press, New York, USA.

92. The porphyrin handbook (2001) (Edited by K. M. Kadish, K. M. Smith and R. Guilard) Vol.15, Academic Press, San Diego, USA.

93. Christie R. M. (2001) Colour Chemistry. The Royal Society of Chemistry, UK.

94. Functional phthalocyanine molecular materials. In Structure and bonding. (Editor D. M. P. Mingos) Springer, London, UK.

95. The porphyrin handbook (2001) (Edited by K. M. Kadish, K. M. Smith and R. Guilard) Vol. 17, Academic Press, San Diego, USA.

96. Nemykin V. N. and E. A. Lukyanets (2010) Synthesis of substituted phthalocyanines. *ARKIVOC* . **i**: 136–208.

97. Tau P. and T. Nyokong (2007) Electrochemical characterisation of tetra- and octa-substituted oxo(phthalocyaninato)titanium(IV) complexes. *Electrochim Acta*. **52**: 3641-3650.

98. Gregory P. (2000) Industrial applications of phthalocyanines. *J. Porphyrins Phthalocyanines*. **4**: 432–437.

99. Sorokin A.B. and E.V. Kudrik (2011)Phthalocyanine metal complexes: Versatile catalysts for selective oxidation and bleaching. *Catal Today*. **159**: 37-46.

100. Fitzsimmons V. G., R. L. Merker and C. R. Singleterry (1952) Phthalocyanine Lubricating Greases. *Ind. Eng. Chem. Res*. **44**: 556-563.

101. Calvete M., G. Y. Yang and M. Hanack (2004) Porphyrins and phthalocyanines as materials for optical limiting. *Synthetic Met*. **141**: 231-243.

102. Moreira L. M., F. V. Santos, J. P. Lyon, M. Maftoum-Costa, C. Pacheco-Soares, and N. S. Silva (2008) Photodynamic Therapy: Porphyrins and Phthalocyanines as Photosensitizers . *Aust. J. Chem*. **61**: 741–754.

103. Ben-Hur E. and I. Rosenthal (1985)The Phthalocyanines: A New Class of Mammalian Cells Photosensitizers with a Potential for Cancer Phototherapy. *Int. J. Radiat. Biol*. **47**: 145-147.

104. Wainwright M. (2008) Photodynamic therapy: the development of new photosensitisers*. Anti Canc Agents Med Chem*. **8**: 280-91.

105. Phthalocyanines - Properties and Applications (1989) (Edited by C. C. Leznoff and A. B. P. Lever) Vol. VCH Publishers, Inc.Cambridge, UK.

106. Josefsen L. B. and R. W. Boyle (2008) Photodynamic Therapy and the Development of Metal-Based Photosensitisers. *Met Based Drugs*. **2008**: 1-24.

107. Zmudzka B. Z., A. G. Strickland, J. Z. Beer and E. Ben-Hur (1997)Photosensitized decontamination of blood with the silicon phthalocyanine Pc 4: no activation of the human immunodeficiency virus promoter. *Photochem Photobiol*. **65**: 461-4.

108. Zhao X. J., S. Lustigman, M. E. Kenney and E. Ben-Hur (1997) Structure-Activity and Mechanism Studies on Silicon Phthalocyanines with *Plasmodium falciparum* in the Dark and Under Red Light. *Photochem Photobiol*. **66**: 282–287.

109. Segalla A., C. D. Borsarelli, S. E. Braslavsky, J. D. Spikes, G. Roncucci, D. Dei, G. Chiti, G. Jori and E. Reddi (2002) Photophysical, photochemical and antibacterial photosensitizing properties of a novel octacationic Zn(II)-phthalocyanine. *Photochem. Photobiol. Sci.* **1**: 641–648.

110. Lustigman S. and E. Ben-Hur (1996) Photosensitized inactivation of Plasmodium falciparum in human red cells by phthalocyanines. *Transfusion*.**36**: 543-6.

111. Gottlieb P., L.G.Shen, E. Chimezie, S. Bahng, M. E. Kenney, B. Horowitz and E. Ben-Hur (1995) Inactivation of *Trypanosoma cruzi* trypomastigote forms in blood components by photodynamic treatment with phthalocyanines. *Photochem Photobiol*. **62**: 869–874.

112. Soncin M., C. Fabris, A. Busetti, D. Dei, D. Nistri, G. Roncucci and G. Jori (2002) Approaches to selectivity in the Zn(II)–phthalocyanine-photosensitized inactivation of wild-type and antibiotic-resistant Staphylococcus aureus. *Photochem. Photobiol. Sci*. **1**: 815-819.

113. Mantareva V., V., Kussovski, I., Angelov, E., Borisova, L., Avramov, G., Schnurpfeil and D. Wohrle (2007) Photodynamic activity of water-soluble phthalocyanine zinc(II) complexes against pathogenic microorganisms. *Bioorg. Med. Chem*. **15**: 4829-4835.

114. Chen J., Z. Chen, Y. Zheng, S. Zhou, J. Wang, N. Chen, J. Huang, F. Yan and M. Huang (2011) Substituted zinc phthalocyanine as an antimicrobial photosensitizer for periodontitis treatment. *J Photochem Photobiol*. **15**: 293-299.

115. Minnock A., D. I. Vernon, J. Schofield, J. Griffiths, J. H. Parish and S. B. Brown (1996) Photoinactivation of bacteria – use of a cationic water soluble zinc phthalocyanine to photoinactivate both Gram negative and Gram positive bacteria. *J. Photochem. Photobiol. B: Biol*. **32**: 159–164.

116. Scalise I. and E.N. Durantini (2005) Synthesis, properties, and photodynamic inactivation of Escherichia coli using a cationic and a noncharged Zn(II) pyridyloxyphthalocyanine derivatives. *Bioorg. Med. Chem*. **13**: 3037-3045.

117. Tabata K., K. Fukushima, K. Oda and I. Okura (2000)Selective aggregation of zinc phthalocyanines in the skin. *J. Porphyrins Phthalocyan*. **4**: 278-284.

118. Nyokong T. (2007) Effects of substituents on the photochemical and photophysical properties of main group metal phthalocyanines. *Coordin Chem Rev*. **251**: 1707–1722.

119. Filippis M. P., D. Dei, L .Fantetti and G. Roncucci (2000) Synthesis of a new water-soluble octa-cationic phthalocyanine derivative for PDT. *Tetrahedron Lett*. **41**: 9143-9147.

120. Liao M., J. D. Watts, M. Huang, S. M. Gorun, T. Kar and S. Scheiner (2005) Effects of Peripheral Substituents on the Electronic Structure and Properties of Unligated and Ligated Metal Phthalocyanines, Metal = Fe, Co, Zn. *J. Chem. Theory Comput*. **1**: 1201–1210.

121. Peng Q. (2001) Correlation of intracellular and intratumoral photosensitizer distribution with photodynamic effect. in Photodynamic Therapy and Fluorescence Diagnosis in Dermatology, Elsevier Science, Amsterdam, The Netherlands.

122. Ozoemena K. I. and T. Nyokong (2003) Synthesis, spectroscopy and photochemistry of octasubstituted thiol-derivatized phthalocyaninatozinc(II) complexes. *Inorg. Chem. Commun*. **6**: 1192–1195.

123. Gureka A. G. and Ö. Bekaroğlu (1994) Octakis(alkylthio)-su bstituted Phthalocyanines and their Interactions with Silver(I) and Palladium(II). *Ions J. Chem. Soc. Dalton Trans*. 1419-1423.

124. Tomé J., M. G. P. M. S. Neves, A. C. Tomé, J. A. S. Cavaleiro, M. Soncin, M. Magaraggia, S. Ferro and G. Jori (2004) Synthesis and antibacterial activity of new poly-L-lysine-porphyrin conjugates. *J Med Chem*. **47**:6649–6652.

125. Polo L., A. Segalla, G. Bertoloni, G. Jori, K. Schaffner and E. Reddi (2000) Polylysine-porphycene conjugates as efficient photosensitisers for the inactivation of microbial pathogens. *J Photochem Photobiol B: Biol*. **59**:152–158.

126. Armarego W. L. F. and D. D. Perrin (1996) In: Purification of Laboratory Chemicals, 4th Edt. Butterworth-Heinemann, Oxford, New York, U.S.A.

127. Jori G. (2006) Photodynamic Therapy of Microbial Infections: state of the art and perspectives. *J*. *Environ*. *Pathol*. Toxicol. *Oncol*. **25**: 505-519.

128. Jori, G., M. Camerin, M. Soncin, L. Guidolin and Coppellotti, O. (2011) Antimicrobial photodynamic therapy: basic principles. In: Photodynamic Inactivation of Microbial

Pathogens: Medical and Environmental Applications. (M. R: Hamblin and G. Jori), pp 1-18. Royal Society of Chemistry, Cambridge, U.K.

129. Luksiene Z. and A. Zukauskas (2009) Prospects of photosensitization in controlo f pathogenic and harmful micro-organisms. *J App Microbiol*. **107**: 1415-1424.

130. Cassell G. and J. Mckalanos (2001) Development of antimicrobial agents in the era of new and reemerging infectious diseases and increasing antiniotic resistance. JAMA. 285: 601-603.

131. Alves E., C. Carvalho, J. Tomé, M. Faustino, M. Neves, A. Tomé, J. Cavaleiro, A. Cunha, S. Mendo and A. Almeida (2008) Photodynamic inactivation of recombinant bioluminescent Escherichia coli by cationic porphyrins under artificial and solar irradiation. *J Ind Microbiol Biotechnol.* **35**: 1447–1454.

132. Mitzel F., S. FitzGerald, A. Beeby and R. Faust (2004) The synthesis of arylalkyne-Substituted tetrapyrazinoporphyrazines and an evaluation of their potential as photosensitisers for photodynamic therapy. *Eur. J. Org. Chem.* **5**: 1136–1142.

133. Demidova T. N. and M. R. Hamblin (2005) Photodynamic Inactivation of Bacillus spores, mediated by phenothiazinium dyes. *Appl Environ. Microbiol.* **71**: 6918-6925.

134. Devasagayam T. P., A. R. Sundquist, P. Di Mascio, S. Kaiser and H. Sies (1991) Activity of thiols as singlet molecular oxygen quenchers. *J Photochem Photobiol B.* **9**: 105-16.

135. Müller-Breitkreutz K., H. Mohr, K. Briviba and H. Sies (1995) Inactivation of viruses by chemically and photochemically generated singlet molecular oxygen. *J. Photochem. Photobiol. B. Biol.* **30**: 63-70.

136. Ragàs X., M. Agut, and S. Nonell (2010) Singlet oxygen in *Escherichia coli*: New insights for antimicrobial photodynamic therapy. *Free Radical Bio. Med.* **49**: 770-776.

137. Nitzan Y., B. Shainberg, and Z. Malik (1989) The mechanism of photodynamic inactivation of Staphylococcus aureus by deuteroporphyrin. *Curr. Microbiol.* **19**: 265- 269.

138. Maisch T., R. M. Szeimies, N. Lehn and C. Abels (2005) Antibacterial photodynamic therapy. A new treatment for bacterial skin diseases? *Hautarzt*, **56**: 1048- 1055.

139. Lazzeri D., M. Rovera, L. Pascual and E. N. Durantini (2004) Photodynamic studies and photoinactivation of Escherichia coli using meso-substituted cationic porphyrin derivatives with asymmetric charge distribution. *Photochem. Photobiol.* **80**: 286- 293.

140. Caminos D.A., M. B. Spesia and E. N. Durantini (2006) Photodynamic inactivation of *Escherichia coli* by novel meso-substituted porphyrins by 4-(3-N,N,N-trimethylammoniumpropoxy)phenyl and 4-(trifluoromethyl)phenyl groups. *Photochem Photobiol Sci.* **5**: 56-65.

141. Merchat M., J. D. Spikes, G. Bertoloni and G. Jori (1996) Studies on the mechanism of bacteria photosensitization by meso-substituted cationic porphyrins*. J. Photochem. Photobiol. B.* **35**: 149-157.

142. Costa L., C. M. B. Carvalho, M. A. F. Faustino, M. G. P. M. S. Neves, J. P. C. Tomé, A. C. Tomé, J. A. S. Cavaleiro, A Cunha, and A. Almeida (2010) Sewage bacteriophage inactivation by cationic porphyrins: influence of light parameters. *Photochem. Photobiol. Sci.* **9**: 1126–1133.

143. Merchat M., J. D. Spikes, G. Bertoloni and G. Jori (1996) Studies on the mechanism of bacteria photosensitization by meso-substituted cationic porphyrins*. J. Photochem. Photobiol. B.* **35**: 149-157.

144. Saydan, N., M. Durmuş, M. G.. Dizge, H. Yaman, A. G. Gürek, E. Antunes, T. Nyokong and V. Ahsen (2009) Water-soluble phthalocyanines mediated photodynamic effect on mesothelioma cells. *J. Porphyrins Phthalocyanines* **13**, 681-690.

145. Durmuş¸ M., H. Yaman, C. Göl, V. Ahsen, and T. Nyokong, (2011) Water-soluble quaternized mercaptopyridine-substituted zinc-phthalocyanines: Synthesis, photophysical, photochemical and bovine serum albumin binding properties. *Dyes Pigments.* **91**, 153-163